Epigenetic inheritance of a phenotypically plastic epimutation

Inauguraldissertation

zur

Erlangung der Würde eines Doktors der Philosophie

vorgelegt der

Philosophisch-Naturwissenschaftlichen Fakultät

der Universität Basel

von

Lea Duempelmann

Schweiz

2021

Genehmigt von der Philosophisch-Naturwissenschaftlichen Fakultät

auf Antrag von

Prof. Dr. Marc Bühler

Prof. Dr. Helge Grosshans

Dr. Vincent Colot

Basel, den 17.03.2020

Prof. Dr. Martin Spiess

Dekan

SUMMARY

Organisms constantly have to adapt to changing environments in order to survive, thrive and successfully multiply. Phenotypic changes can be acquired by alterations of the deoxyribonucleic acid (DNA) sequence. If beneficial under natural selection, the DNA variation can become fixed permanently in a population and thereby drive its evolution. In addition to DNA sequence changes, a concept emerged that a soft, reversible layer could also potentially contribute to heritable adaptation. Epigenetic changes were shown to affect the development and complex phenotypic traits of almost isogenic organisms. Such changes can be inherited over many generations by strong self-reinforcing feedback loops without the initial trigger. Evidence for such a 'soft' inheritance is only just emerging and whether such phenomena are of physiological relevance in heritable adaptation though remains to be unraveled.

Gene expression is regulated through several mechanisms. DNA does not exist as bare molecule, but is packaged into a highly complex structure called chromatin. Besides serving structural functions, chromatin also impacts gene expression. Chromatin can be broadly divided into transcriptionally active, gene-rich euchromatin and gene-poor, condensed heterochromatin, which serves as repressive structure for repetitive elements, such as transposons, and makes up most of the euchromatic genome. In some organisms, nuclear small ribonucleic acid (RNA) pathways are essential to initiate and maintain constitutive heterochromatin. The centerpiece of such pathways is a small RNA-bound Argonaute protein, which binds by complementary base-pairing to nascent transcripts and subsequently recruits effector complexes that mediate silencing. Given the appropriate small RNA, this pathway can theoretically target any expressed locus, thereby making it a versatile silencing strategy. In nematodes, small RNAs were shown to induce stable silencing of some protein coding genes that can be epigenetically maintained over tens of generations.

During my PhD, I studied RNA interference (RNAi)-mediated epigenetic phenomena in the fission yeast *Schizosaccharomyces pombe* (*S. pombe*). In *S. pombe*, RNAi-mediated silencing is under strong negative control and can only be initiated in the presence of an enabling mutation, such as in genes encoding subunits of the RNA polymerase-associated factor 1 complex (Paf1C). On one hand, such mutations can have a detrimental effect on viability. On the other hand, the silencing phenotype observed in Paf1C mutants cannot be inherited to wild-type cells, suggesting that also all marks of the silencing event were erased. If RNAi-mediated epigenetic phenomena also exist in wild-type cells was not known.

SUMMARY

My main achievement during PhD was to discover that wild-type *S. pombe* cells remember a parental silencing event through acquiring a phenotypically neutral epimutation. I could show that such epimutation does not cause gene silencing when inherited by wild type cells. Yet, upon repeated mutation of Paf1C, the silencing phenotype was reinstated in subsequent generations. I could further show that the phenotypically neutral epimutation entails high levels of small interfering RNA (siRNA) and histone 3 lysine 9 tri-methylation (H3K9me3), and that its transgenerational inheritance depends on RNAi and H3K9 methylation. This finding is astounding, because H3K9me3 has commonly been associated with gene repression. That we have not observed silencing, despite high enrichments of this mark, was therefore highly unexpected. Based on my findings, I conclude that H3K9me3 is not repressive *per se*, but rather functions as stable epigenetic mark that can retain information of a previous gene-silencing event. Upon deposition of H3K9me3, the silencing phenotype is dependent on the modulation of Paf1C function. The discovery of this distinct form of epigenetic memory lets me speculate that it may have evolved to allow population adaptation to dynamic environments.

TABLE OF CONTENTS

LIST OF FIGURES

ABBREVIATIONS

A. thaliana	*Arabidopsis thaliana*
3'-/5'-UTR	3'-/5'-untranslated region
ade6-hp	RNA hairpin complementary to *ade6+*
ARC	Argonaute siRNA chaperone
A^{vy}	Agouti viable yellow allele
$Axin^{Fu}$	Axin fused allele
C. elegans	*Caenorhabditis elegans*
ChIP-seq	Chromatin immunoprecipitation sequencing
cKO	conditional knockout
CLRC	Clr4-Rik1-Cul4 complex
cnt	central core (of the centromere)
CPF	Cleavage and polyadenylation factor
CTD	C-terminal domain (of RNA polymerase II)
CTGS	Co-transcriptional gene silencing
DCL3	DICER-LIKE 3
DNA	Deoxyribonucleic acid
dsRNA	double-stranded RNA
ERV	Endogenous retrovirus
FACT	Facilitates chromatin transcription
H3K4/9/14/27/36	H3 lysine 4/9/14/27/36
HP1	Heterochromatin protein 1
HRDE-1	Heritable RNAi Deficient 1
IAP	Intracisternal A particle
imr	innermost repeats
kb	kilobase
lncRNA	long non-coding RNA
LTR	Long terminal repeats
me	methylated residue
me1/2/3	mono-/di-/tri-methylated residue
miRNA	micro RNA

MOTEK	modified transgenerational epigenetic kinetics
mRNA	messenger RNA
NET-Seq	Native elongating transcript-sequencing
otr	outermost repeats
Paf1C	RNA polymerase-associated factor 1 complex
PTGS	Post-transcriptional gene silencing
PTM	Post-translational modification
RdDM	RNA-directed DNA methylation
RDR2	DEPENDENT RNA POLYMERASE 2
RDRC	RNA-directed RNA polymerase complex
RdRP	RNA-dependent RNA polymerase
REIII	Repressor element III
RITS	RNA-induced transcriptional silencing
RNA	Ribonucleic acid
RNA Pol II	RNA polymerase II
RNAe	RNA-induced epigenetic silencing
RNAi	RNA interference
S. cerevisiae	*Saccharomyces cerevisiae*
S. pombe	*Schizosaccharomyces pombe*
Ser2/5/7P	phosphorylated Serine 2/5/7 (of CTD)
SHREC	Snf2/Hdac-containing repressor complex
siRNA	small interfering RNA
SNP	Single nucleotide polymorphism
TGS	Transcriptional gene silencing
tRNA	transfer RNA
ura4-hp	RNA hairpin complementary to *ura4+*
WAGO	Worm-specific Argonaute protein

INTRODUCTION

"The only constant is change" *Heraclitus, ~500 BC*

Populations constantly have to adapt to a changing environment in order to survive and flourish. Phenotypic changes can be induced by alteration of the DNA sequence, driving the evolution of a population in the new environment. A concept emerged that, in addition to DNA changes, also epigenetic changes could potentially contribute to heritable adaptation. However, evidence for such a 'soft' inheritance is only just emerging and we are far away from tangible implications in physiological relevance. This thesis focuses on the fascinating observation of multigenerational epigenetic inheritance of self-enforcing feedback loops. I chose to study such phenomenon in the fission yeast *S. pombe* due to its well-studied RNAi-mediated silencing mechanism that can induce facultative heterochromatin. This introduction covers observed epigenetic phenomena, with a special focus on small RNA-mediated silencing.

1. Epigenetics as a driver of phenotypic variation

1.1. The origins of 'epigenetics'

The term epigenetics is rooted in developmental biology and changed its meaning over time to nowadays describe heritable gene expression changes that do not originate from DNA mutations.

Early theories about embryology and inheritance can already be found in the fourth century B.C. in writings from Aristotle, who is often seen as the first philosopher to define epigenesis (Aristotle, *On the Generation of Animals;* Nicoglou and Wolfe, 2018). He proposed that an embryo is formed by different parts that gradually and orderly develop ('Epigenesis'), contrary to the back then common theory that all embryonic parts already would pre-exist in the semen ('Preformation') (Nicoglou and Wolfe, 2018; Aristotle, *On the Generation of Animals*). Furthermore, Aristotle proclaimed that offspring resemble their parents and that heredity results from the parental seed (Henry, 2006).

Several centuries later, and after the discovery of cells (Vasil, 2008; Robert Hooke, 1665), the idea of the environment shaping acquired characteristics was famously proposed by the botanist and evolutionist Lamarck, though the idea rather reflects the general thinking of that time and was not originally conceived by him (Noble, 2015). Darwin's theory of natural selection (Darwin, *The Origin of Species*) is often seen as the opposing theory to Lamarck's writings. Interestingly, Darwin widely agreed with the theory that the environment could shape inheritance (Penny, 2015). He himself proposed that so-called gemmules would arise during environmental stress in the soma and be transmitted from parent to offspring, thereby conferring some advantage (Darwin, *Variation of Animals and Plants under Domestication*; Heard and Martienssen, 2014; Liu and Chen, 2018).

After the first isolation of DNA (Miescher, 1869; Dahm, 2005), the developmental biologist and embryologist Waddington speculated that genes form networks that could change during development (Van Speybroeck, 2002). He linked the formation of new features during development (epigenesis) to the inheritance of genes (related to preformation), and thus saw both as being complementarily involved in embryonic development, rather than exclusively (Van Speybroeck, 2002). Waddington originally coined the term '**Epigenetics**' to describe the relation between phenotype and genotype during development (epigenesis + genetics = epigenetics) (Waddington, 2012).

Nowadays, epigenetics expands the view of gene-centric inheritance, and can be literally interpreted as "over" (Greek "epi-") genetics. Epigenetics is widely referred to as heritable changes in gene expression that do not originate from DNA mutations. In this thesis, I will follow a more strict definition of epigenetic phenomena as 'gene expression changes that are mutation independent and heritable in the *absence of the triggering event*' (Ptashne, 2013). Thus, it is important to distinguish between transgenerational inheritance and intergenerational inheritance (or 'parental effects') when studying the impact of epigenetic changes on subsequent generations (Figure 1). In oviparous animals, which lay eggs, an epigenetic change may be considered transgenerational from F2 onwards (reviewed in Heard and Martienssen, 2014). However, in viviparous animals, exposure of a pregnant animal to a stimulus that can trigger an epigenetic change in gene expression can potentially affect mother, fetus, and the fetus' developing germline simultaneously. Thus, epigenetic changes would be considered intergenerational up to F2 (grandchildren), and transgenerational from F3, in which no single cell was directly exposed to the initial trigger of the change (Ptashne, 2013; Rechavi and Lev, 2017) (Figure 1). One of the most widely used example given for epigenetics in humans, that of famines affecting the immediate offspring (Painter et al., 2008), therefore cannot be considered a truly epigenetic effect, but should rather be attributed to parental effects (Rechavi and Lev, 2017). (Adapted from Duempelmann et al., 2020)

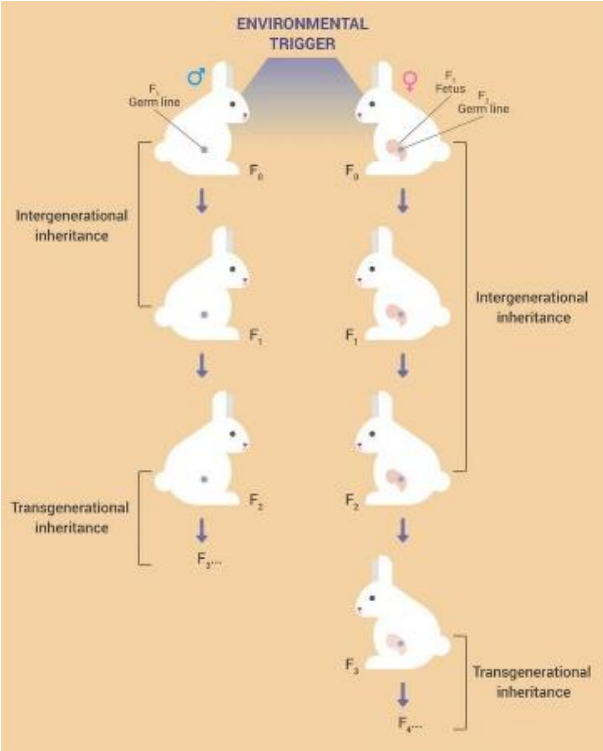

Figure 1. Intergenerational vs transgenerational inheritance in viviparous animals. *Figure re-used from Vaiserman et al., 2017 with permission (CC BY 4.0).*

1.2. Characteristics of epigenetics

Mechanistically, epigenetic phenomena can differ substantially, but they also share several common characteristics. Heritable responses would be quickly diluted and lost during cell divisions in the absence of the initial trigger. Active mechanisms are required to amplify the silencing signal and maintain the memory across generations. Epigenetic phenomena are commonly linked to changes in chromatin or DNA modifications, although other mechanisms are likely to exist, and gene expression must not necessarily be different. Positive feedback loops can include the following components:

- Chromatin marks: DNA methylation, histone modifications, histone variants
- RNA (coding and noncoding)
- prions

Those components and modifications are not self-perpetuating (except prions) and require multiple factors for their maintenance and amplification. The enzymes imposing chromatin modifications or small RNA generation mostly lack the requisite specificity and have to be continuously recruited to the target loci through specificity factors such as DNA-binding proteins (Ptashne, 2007), or small RNAs that specifically base-pair with the nascent transcript of the target locus. Once a self-sustaining feedback loop is established, epigenetic inheritance could in theory be maintained ad infinitum (Rechavi and Lev, 2017; Sapetschnig et al., 2015). However, opposing activities counteract indefinite inheritance, restricting the length of a silencing response (see INTRODUCTION chapter 5.3).

The heritability of epigenetic changes, in comparison to genetic changes, can vary significantly and generally does not follow Mendelian rules. Striking examples of non-Mendelian inheritance are prions and paramutation where any of the offspring can potentially inherit the epigenetic state of one parent (see INTRODUCTION chapter 1.3.1). Prions are infectious, proteinaceous agents that can transmit their distinct conformation to their native counterparts, causing heritable structural and functional changes (reviewed in Halfmann and Lindquist, 2010). (Adapted from Duempelmann et al., 2020)

In complex organisms, epigenetic marks have to pass several major barriers (Heard and Martienssen, 2014). First, heritable material has to be communicated to the germline and then escape germline and early embryo reprogramming. During this time, most histone modifications, as well as small RNAs and DNA methylation, are reset. In offspring, the heritable material has to be communicated back to the different tissue. Diffusible factors, in particular RNA, rather than DNA methylation or chromatin, are good candidates for transgenerational inheritance in complex organisms because they could potentially be transported between soma and germline (Heard and Martienssen, 2014; Posner et al., 2019).

1.3. Epigenetic inheritance of phenotypic variation

Epigenetic changes can affect development and influence complex traits, even of closely related members of a species that share essentially identical DNA sequence (Daxinger and Whitelaw, 2012; Heard and Martienssen, 2014). Examples can be found across kingdoms.

1.3.1. Paramutations

Paramutation is a classic example of epigenetics, discovered long before the terms "transgenerational" and "epigenetic" were in widespread use (Arteaga-Vazquez and Chandler, 2010; Coe, 1959; Heard and Martienssen, 2014). First characterized in maize, paramutation describes a trans-interaction between two alleles, causing heritable gene expression changes in a non-Mendelian pattern (Figure **2**, reviewed in Chandler, 2007). During paramutation, a so-called paramutagenic allele imposes its silent chromatin state on a paramutable allele, which is sensitive to paramutation. The second paramutated allele thereby becomes paramutagenic, and is in turn capable of inducing paramutation, even in the absence of the original paramutagenic allele or any DNA sequence change. This creates a non-Mendelian inheritance pattern (Arteaga-Vazquez and Chandler, 2010). While it is still unclear exactly how the alleles interact, several lines of evidence suggest the involvement of RNA, not least because mutants deficient in RNAi-directed transcriptional silencing are unable to undergo paramutation (Arteaga-Vazquez and Chandler, 2010). Additionally, transcribed noncoding tandem repeats can mediate paramutation, and the strength of paramutation correlates with the number of repeats (Chandler, 2010). Nonetheless, small RNAs are not sufficient to induce a paramutagenic

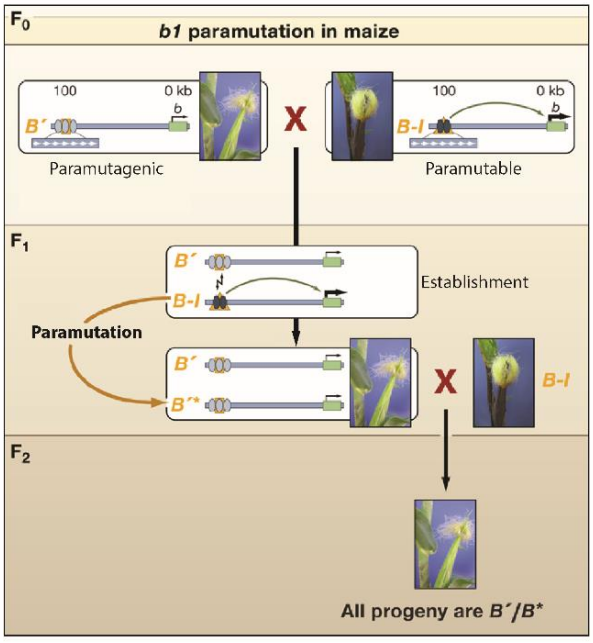

Figure 2. Paramutation in maize. *The b1 locus encodes a transcription factor that promotes the biosynthesis of purple pigments. Expression of the b1 locus depends on DNA methylation and the chromatin structure of upstream tandem repeats (white arrows). The weakly transcribed B' allele produces green plants, the highly transcribed B-I allele dark purple plants. The B' allele is extremely stable and is paramutagenic. All progeny from B' crossed with B-I are B'. Figure adapted from Chandler, 2007 with permission.*

allele. Thus, different models have been suggested, such as protein-DNA interaction, DNA pairing, or a combination of such mechanisms (Chandler, 2010). Paramutation phenomena involving RNA-directed DNA methylation (RdDM) and/or small RNAs were also found in tomato, *Drosophila*, *Caenorhabditis elegans* (*C. elegans)* and mouse (Heard and Martienssen, 2014; Sapetschnig et al., 2015).

1.3.2. Epigenetic inheritance of complex traits in Arabidopsis

Epigenetics was found to impact beside simple traits, such as the before mentioned quantity of pigment in maize, also complex traits, such as flowering time and pathogen resistance. Natural accessions of the flowering plant *Arabidopsis thaliana* (*A. thaliana*) can substantially differ in their traits, as well as DNA methylation profile (Vaughn et al., 2007). Unfortunately, no direct correlation could have been made between trait variation and DNA methylation due to the differences in their DNA sequence. Thus, a high number of almost isogenic epigenetic recombinant inbred lines (epiRILs) were generated to study the direct impact of epigenetic variation on complex traits (Figure 3) (Johannes et al., 2009).

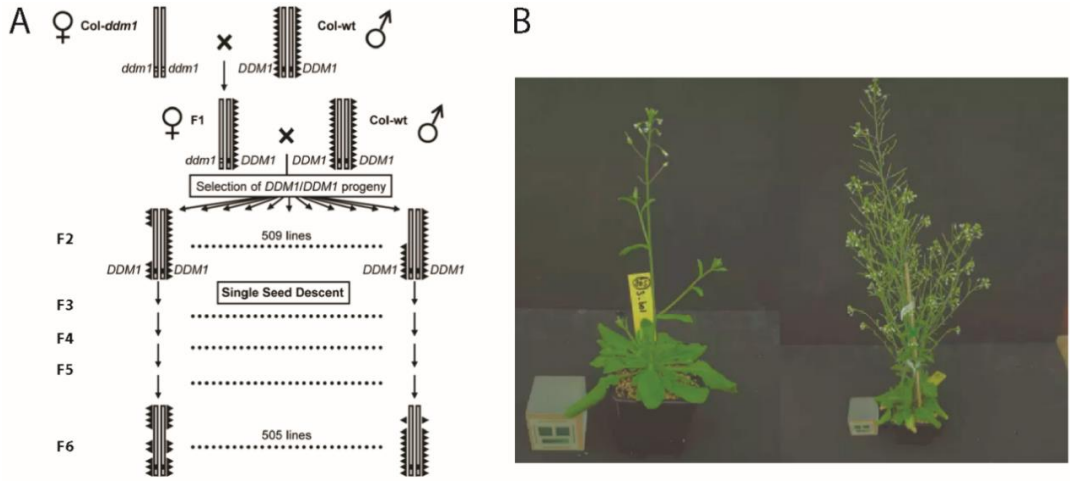

Figure 3. Epigenetic recombinant inbred lines (epiRILs) display high variation in DNA methylation and complex traits. *(A) Crossing scheme to derive epiRILs. Deletion of the ATPase chromatin remodeler DDM1 leads to severe reduction of DNA methylation (triangles). Hypomethylated ddm1/ ddm1 A. thaliana plants (Col-ddm1) were back-crossed to otherwise almost isogenic wild-type plants (Col-DDM1), to remove the ddm1 mutation. Over 500 homozygous DDM1/ DDM1 individuals were propagated for six generations by single seed descent to generate the epigenetic recombinant inbred lines. Despite being almost isogenic, those lines displayed hundreds of differences in DNA methylation, as well as high variation in complex traits. (B) Exemplary images of epiRIL plants with great phenotypic differences in complex traits, such as flowering time. Figure (A) re-used from Johannes et al., 2009 with permission, Figure (B) image courtesy of Vincent Colot.*

Those experimentally induced DNA methylation changes are stably maintained and inherited through meiosis over at least eight generations and these lines have been well characterized by high-throughput phenotyping, quantitative genetics, and epigenetic profiling (Colome-Tatche et al., 2012; Cortijo et al., 2014; Johannes et al., 2009). This allowed several studies to correlate epigenetic variation with physiological consequences, such as flowering time, nutrient plasticity, drought tolerance and even pathogenic clubroot resistance (Cortijo et al., 2014; Johannes et al., 2009; Liegard et al., 2019; Zhang et al., 2013). Various quantitative Loci under epigenetic control (QTLepi) were found to highly correlate with such heritable complex traits, some of which overlapped with e.g. previously identified clubroot resistance genes (Cortijo et al., 2014; Kooke et al., 2015; Liegard et al., 2019).

1.3.3. Epigenetic inheritance of fur color and tail kinks in mice

In contrast to non-mammalian model organisms, epigenetic inheritance appears not very prominent in mammals, probably due to the extensive genome-wide epigenetic reprogramming that occurs during pre-implantation embryogenesis and early germ cell lineage specification (Bertozzi and Ferguson-Smith, 2020; Heard and Martienssen, 2014). Mammalian endogenous metastable epialleles have variable DNA methylation states within isogenic populations and were found to be inherited only in rare cases (Kazachenka et al., 2018). Classical examples thereof are the Agouti viable yellow (A^{vy}) and Axin fused ($Axin^{Fu}$) alleles (Duhl et al., 1994; Vasicek et al., 1997). Both exhibit variable gene expression due to ectopic insertions of a Class II endogenous retrovirus (ERV) of the intracisternal A particle (IAP) class. Those repetitive elements are characterized by long terminal repeats (LTRs) at the 5' and 3' end. LTRs can act as promoters and enhancers of host genes, leading to ectopic gene expression, as observed for the A^{vy} and $Axin^{Fu}$ alleles (Bertozzi and Ferguson-Smith, 2020; Heard and Martienssen, 2014). Constitutive Agouti expression (A^{vy}) caused by these LTRs leads to a completely yellow coat, as well as adult-onset obesity and diabetes. DNA methylation at the IAPs inversely correlates with their promotion of transcriptional activity of those alleles. Mice with methylated, silenced IAP (pseudoagouti) have brown fur, as wild-type mice (Figure 4A and 4B). The parental phenotype is inherited with moderate penetrance, affecting the range of phenotypes observed in the offspring (Figure 4C), whereas grand-maternal effects result in a more severe phenotypic shift. Analogous, aberrant transcription of Axin, caused by IAP insertion, results in the heritable development of a kinked tail (Rakyan et al., 2003; Vasicek et al., 1997).

Interestingly, supplementation of the maternal diet with methyl donors and other co-factors was shown to also shift the coat colour of A^{vy}/a offspring towards pseudoagouti, possibly due to an increase in methylation at the A^{vy} IAP (Cropley et al., 2006; Waterland and Jirtle, 2003). Even though the epigenetic

phenotype of A^{vy} correlates with the methylation state of the corresponding allele, methylation is unlikely to be the agent transmitting the memory, due to its erasure from the locus during the pre-implantation stage. The mechanism causing epigenetic inheritance of metastable epialleles and its conservation remain to be investigated (Bertozzi and Ferguson-Smith, 2020; Heard and Martienssen, 2014).

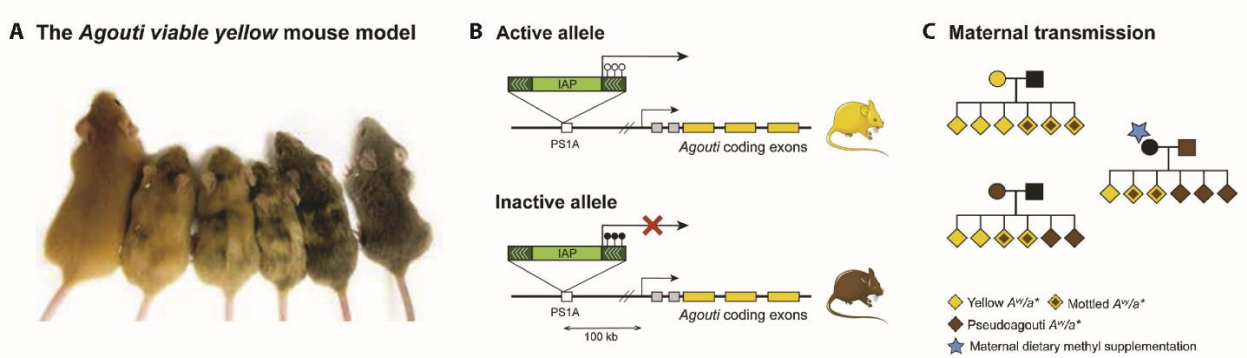

Figure 4. Expression of Agouti modulates epigenetic phenotype. *(A) The coat color phenotypes of isogenic A^{vy} mice can range from yellow to pseudoagouti (brown), even within the same litter. (B) The A^{vy} allele contains an IAP insertion 100 kilobases (kb) upstream of the Agouti coding exons. Methylation of the IAP inversely correlates with Agouti expression. High expression of Agouti results in yellow fur, low expression in pseudoagouti (brown) fur and intermediate expression in mottling. (C) The coat color distribution of offspring is influenced by the maternal coat color phenotype (originally adapted from Morgan et al., 1999), as well as the maternal diet. Figure re-used from Bertozzi and Ferguson-Smith, 2020 with permission.*

2. Overview of chromatin properties and function

The expression of genes is regulated at multiple levels. DNA does not exist as a mere fiber, but is packaged together with histone proteins into a highly complex, more compact structure called chromatin. Besides its structural role in genome stability and proper chromosome segregation, chromatin also plays a role in gene expression. Chromatin can be broadly divided into gene-rich, transcriptionally more active euchromatin and gene-poor, condensed heterochromatin, which keeps repetitive elements, such as transposons, in a repressed state and makes up most of the eukaryotic genome. Gene expression is further modulated by covalent chromatin modifications, which serve as binding sites for various effector proteins with repressing or activating function. This chapter will cover the general structure of chromatin and end with a description of the main heterochromatic regions of *S. pombe*, which are partially regulated by RNAi.

2.1. Chromatin structure

The entire genetic information of a human cell is encoded in about 2-meters of DNA, yet is packaged into a cell nucleus of only 5 to 20 micrometers as a highly complex structure called chromatin (Figure 5). The basic building block of chromatin is the nucleosome, which consists of 147 base pairs negatively charged DNA wrapped around a histone octamer core, itself composed of two highly positive charged H2A, H2B, H3 and H4 proteins (Kornberg and Thomas, 1974; Luger et al., 1997). Each histone protein has a relatively unstructured histone tail that protrudes from the nucleosome surface and can be subjected to post-translational modifications (PTMs) (Zhao and Garcia, 2015). The nucleosomes are linked by short stretches of highly accessible DNA. This first level of chromatin organization leads to a 6-7 fold compaction of DNA and is visible as nucleosome 'beads on a string' of DNA under an electron microscope (Olins and Olins, 1974). This structure is further compacted to chromatin fibers and ultimately to chromosomes (Jansen and Verstrepen, 2011). Nucleosomes play crucial roles not only in packaging, but also in many regulatory roles of cellular processes, such as gene expression, chromosome segregation, genome stability, DNA

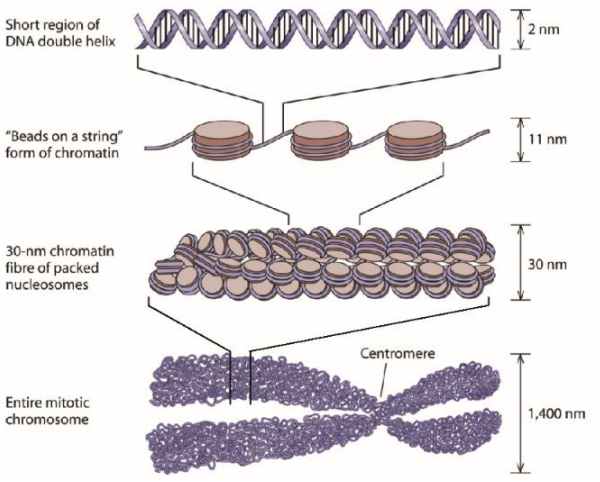

Figure 5. Chromatin structure. *DNA wrapped around a histone octamer core forms a nucleosome, the basic unit of chromatin. Nucleosomes form upon compaction a 30-nm chromatin and ultimately higher-order structures. Figure adapted from Jansen and Verstrepen, 2011 with permission.*

replication and recombination by controlling DNA accessibility (Jansen and Verstrepen, 2011). These processes are regulated by chromatin through several mechanisms: 1) Tight compaction of broad chromatin regions makes DNA less accessible (see INTRODUCTION chapter 2.2). 2) DNA tightly wrapped around nucleosomes is less accessible than linker regions. The chromatin structure is dynamic and accessibility can be actively altered by remodeling or eviction of nucleosomes. 3) Differential histone variant usage. 4) The histone tails can be post-translationally modified, changing the physical properties of the nucleosome and creating binding sites for different effector complexes with repressing or activating function (Jansen and Verstrepen, 2011).

Many gene expression programs have to be reversibly changed, especially during development from a zygote to an organism (Waddington, 2012). Histone PTMs are thought to play a role during this process, in maintaining as well as reversibly changing gene expression levels (Greer and Shi, 2012). To date, around 500 PTMs were found on more than 200 sites of the different histone variants, for most of which the physiological function remains to be uncovered (Zhao and Garcia, 2015). In general, PTMs influence gene expression through two modes. First, chromatin compaction is directly affected by PTMs that change the overall charge of histones. For example acetylation of lysines neutralizes and thereby reduces the electrostatic interaction between the positively charged histones and the negatively charged DNA, thereby making chromatin more accessible (Shogren-Knaak et al., 2006). Second, PTMs function as specific binding sites for chromatin binding proteins that in return recruit effector complexes. The same chemical modification can play a different role depending on the histone residue it is placed on. Furthermore, also the degree of e.g. methylation (mono/di/tri) affects the affinity for a binding partner (Jih et al., 2017; Schalch et al., 2009). In general, methylation of histone H3 on K4, K36, and K79 and hyper-acetylation have been associated with gene expression and euchromatin, whereas methylation of H3 on K9 and K27 as well as of histone H4 on K20 and hypo-acetylation are associated with gene repression and heterochromatin (Strahl and Allis, 2000).

2.2. Euchromatin and Heterochromatin

Cytological observations in the early 20th century gave rise to the concept that chromatin can be broadly divided into two classes (Heitz, 1928). While euchromatin is often gene rich, transcriptionally active and dynamic, heterochromatin is highly condensed, gene poor, contains many silenced repetitive elements and often localizes to the nuclear periphery (Buchwalter et al., 2019; Towbin et al., 2013; van Steensel and Belmont, 2017). Heterochromatin can be further divided into two classes. Constitutive heterochromatin is found at highly repetitive DNA elements, at the centromeres and telomeres. It is

important for genome stability and proper chromosome segregation as well as having a repressive activity on transposable elements and repetitive sequences (Buhler and Gasser, 2009). Facultative heterochromatin forms within a euchromatic environment and can effect gene expression, in some cases stably over multiple generations (Sapetschnig et al., 2015; Trojer and Reinberg, 2007). Heterochromatin formation commonly co-occurs with several changes of chromatin, including H3K9 methylation, histone deacetylation, increased compaction and recruitment of heterochromatin protein 1 (HP1) family members (Grewal and Jia, 2007). Unexpectedly, a substantial fraction of heterochromatin is transcribed, and silencing does not occur exclusively at the transcriptional level (Buhler et al., 2006; Chow et al., 2010; Keller et al., 2012; Volpe et al., 2002; Wilhelm et al., 2008; Zhao et al., 2008). In several eukaryotes, also small RNA pathways play a role in heterochromatin formation.

2.2.1. Constitutive heterochromatin in S. pombe

In *S. pombe*, constitutive heterochromatin is found at repetitive DNA elements at the centromeres, the telomeres and the mating-type locus, and contributes to proper chromosome segregation and genome stability (Verdel and Moazed, 2005). Heterochromatin formation includes a number of activities such as histone deacetylation, H3K9 methylation by Clr4 and recruitment of histone binding proteins such as the HP1 homologs Swi6 and Chp2, and Chp1, which bind with their chromodomain specifically to H3K9me2 and H3K9me3 (Buhler and Gasser, 2009; Schalch et al., 2009). After initiation, heterochromatin is thought to spread to adjacent nucleosomes by cycles of Clr4-catalyzed H3K9 methylation and binding, as well as dimerization of chromatin associated factors (Grewal and Moazed, 2003).

All three *S. pombe* chromosomes contain one centromere that spans 35-110 kb of DNA (Verdel and Moazed, 2005). Each centromere consists of a central region (*cnt*) with a unique DNA sequence and is flanked by the innermost (*imr*) and outermost (*otr*) repeats (Figure 6) (Martienssen and Moazed, 2015). The *imr* region is composed of large inverted repeats that contain transfer RNA (tRNA) genes. The *otr* region comprises tandem alternating copies of *dg* and *dh* repeats (Steiner et al., 1993). The centromeric repeat regions are marked with high levels of H3K9 methylation and complementary siRNAs (Buhler et al., 2008; Cam et al., 2005; Nakayama et al., 2001). Impairment of the RNAi pathway leads to a strong reduction of H3K9 methylation and Swi6 recruitment, as well as the accumulation of sense and anti-sense transcripts, originating from the *dg* and *dh* repeats (Volpe et al., 2002). Thus, the RNAi pathway was first suggested to initiate and/or maintain centromeric heterochromatin formation by recruiting Clr4 and Swi6 (Hall et al., 2002; Volpe et al., 2002) (see INTRODUCTION chapter 3.2.1. for more details).

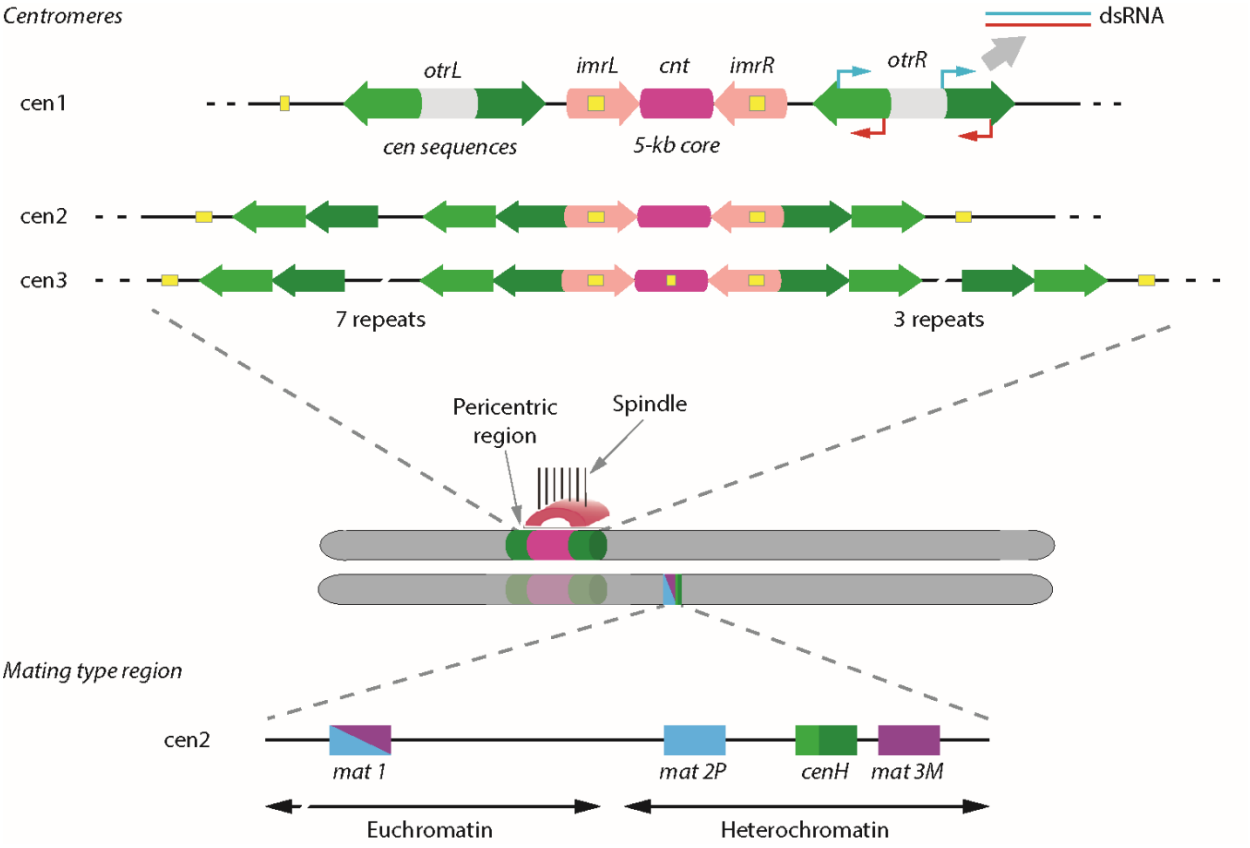

Figure 6. Organization of the three centromeres and mating-type locus in S. pombe. *The centromeres of each chromosome (cen1, cen2 and cen3) consist of a central core (cnt), flanked by innermost (imrL and imrR) and outermost (otrL and otrR) repeats. The pericentric otr region is composed of conserved dg and dh sequences (green arrows), which are transcribed bidirectional, giving rise to dsRNA. tRNA gene regions are represented by yellow boxes. Below the represented whole chromosome, a diagram of the mating-type region consisting of the switchable mat1 locus and the silent mat 2P and mat3M donor loci. The mating-type is determined by the allele present at the expressed mat1 locus. Furthermore, the maiting-type locus contains the cenH domain that shares high sequence identity with a dh/dg centromeric repeat and serves as nucleation site for RNAi-dependent heterochromatin formation. Figure adapted from Martienssen and Moazed, 2015; Verdel and Moazed, 2005 and Volpe et al., 2002 with permission.*

At the mating-type locus, heterochromatin is important to control the cell type identity (Martienssen and Moazed, 2015). The heterochromatic domain spans over 10 kb, including mat2P, mat3M and a 3 kb DNA region called cenHomology (cenH). Nucleation of heterochromatin is mediated in parallel by RNAi and by the two transcription factors Atf1 and Pcr1 (Jia et al., 2004; Kim et al., 2004). Heterochromatin is nucleated at the cenH region in an RNAi-dependent manner and spreads to the entire silent domain (Hall et al., 2002; Noma et al., 2004). This region has a high sequence identity (96%) with a portion of the centromeric *dh* and *dg* repeats (Grewal and Klar, 1997). The cenH region, as the cen repeats, is transcribed divergently and produces sense and anti-sense transcripts that could potentially base-pair to double-stranded RNA (dsRNA) and serve as source for primary siRNA production (Noma et al., 2004). Furthermore, complementary siRNAs produced at the centromere could additionally guide silencing effector complexes to this nucleation site. Atf1 and Pcr1 bind to specific DNA sequences within the mating-type locus termed repressor element (REIII) and recruit the heterochromatin-machinery RNAi-independently (Jia et al., 2004). Once established, heterochromatin at the mating-type locus is stably maintained over many cell divisions, also without a functional RNAi pathway (Jia et al., 2004; Sadaie et al., 2004). Only combined impairment of those redundant RNAi-dependent and independent pathways leads to a loss of heterochromatin at the mating-type locus (Hall et al., 2002; Jia et al., 2004).

Heterochromatin at the subtelomeric DNA regions is also partially mediated by RNAi (Kanoh et al., 2005), but will not be further discussed here. In summary, all three main heterochromatic regions are partially regulated by RNAi. In contrast to the centromeres, the mating-type locus and telomeres maintain heterochromatin also after impairment of the RNAi pathway.

3. Small RNA-directed silencing pathways

3.1. Small RNA-directed gene silencing pathways

RNAi was originally defined as a gene silencing mechanism triggered by the introduction of complementary dsRNA in *C. elegans* (Fire et al., 1998). During the last two decades, this definition was broadened to gene silencing triggered by small RNAs bound by an Argonaute family protein (Martienssen and Moazed, 2015). RNAi is conserved from fungi to mammals and is important for host defense against viruses and repetitive DNA elements, as well as for the regulation of gene expression (Martienssen and Moazed, 2015). Furthermore, small RNAs are involved in or correlate with multiple cellular processes including regulation of development, differentiation, apoptosis, and cancer (Croce and Calin, 2005; Verdel and Moazed, 2005).

Small RNAs mostly derive from dsRNAs, originating from bidirectional transcription, dsRNA synthesis from single stranded RNA (ssRNA) or hairpin structures resulting from internal base-pairing of an RNA molecule (Martienssen and Moazed, 2015). Dicer, an RNAse III class ribonuclease, cleaves the dsRNA into small RNAs (Bernstein et al., 2001) that are processed into siRNAs and micro RNAs (miRNAs). The small RNAs act as specificity factors and play a central role in RNAi by targeting the effector complexes to complementary target sequences through base-pairing interactions (Fire et al., 1998; Hamilton and Baulcombe, 1999; Hammond et al., 2000; Verdel et al., 2004). Therefore, small RNAs form the centerpiece of all RNAi-mediated silencing mechanisms.

The Argonaute-associated small RNA can induce silencing through different mechanisms by targeting either messenger RNAs (mRNAs) post-transcriptionally (post-transcriptional gene silencing, PTGS), or chromatin regions (co-transcriptional gene silencing, CTGS or transcriptional gene silencing, TGS) (Martienssen and Moazed, 2015). In the cytoplasmic PTGS, siRNAs or miRNAs guide the RNA-induced silencing complex (RISC) to mRNA by complementary base-pairing. The Argonaute/PIWI subunit of RISC endonucleolytically cleaves with its RNase H domain the mRNA in the base-paired region to the siRNA, initiating the degradation of the target mRNA (Irvine et al., 2006; Liu et al., 2004; Song et al., 2004). Alternatively, RISC bound mRNAs can also be silenced by translational repression. In the nuclear CTGS or TGS, the RNA-induced transcriptional silencing (RITS) complex makes a direct link between RNAi and heterochromatin (Partridge et al., 2002), which will be discussed in more detail in the following chapter.

3.2. Nuclear small RNA-directed gene silencing pathways

RNA was initially suggested to direct TGS by studies in plants of homology-dependent silencing of viroids (Mette et al., 1999; Napoli et al., 1990; Wassenegger et al., 1994). The potato spindle tuber viroid (PSTVd) is composed of a small, circular and single-stranded RNA molecule which is replicated by the host's RNA polymerase II (RNA Pol II). Introduction of a PSTVd transgene into the tabacco genome resulted in methylation of the PSTVd sequence (Wassenegger et al., 1994), however only in plant hosts that supported viroid RNA replication. Thus, these experiments suggested that *de novo* methylation could be induced by RNA in a sequence specific manner (Wassenegger et al., 1994). Few years later, the silencing of viral genomes in plants was found to be accompanied by the accumulation of ~25 nt RNAs (Hamilton and Baulcombe, 1999), being the first example of small RNAs (Martienssen and Moazed, 2015).

Chromatin-regulatory processes directed by small RNAs have been extensively studied in yeasts, nematodes, plants, and fruit flies (reviewed in Holoch and Moazed, 2015a; Luteijn and Ketting, 2013; Matzke and Mosher, 2014). Mechanistically, they differ substantially between organisms, but they share important key features, suggesting that general concepts are conserved. At the core of each pathway is a small-RNA-bound Argonaute complex that targets nascent RNA via complementary base-pairing. Although base-pairing with DNA would in principle be possible, work in yeast and plants has shown that this is unlikely (Shimada et al., 2016; Wierzbicki et al., 2008). Upon nascent transcript binding, the small RNA-Argonaute complex recruits additional effector complexes that can induce changes in chromatin states and/ or inhibit elongation of the RNA polymerase, and amplify the siRNA pool, leading to self-reinforcing feedback loops. Nuclear siRNA-directed gene silencing has been intensively studied in *S. pombe*, *C. elegans*, and *A. thaliana* (Figure 7, reviewed in Holoch and Moazed, 2015a; Luteijn and Ketting, 2013; Matzke and Mosher, 2014). (Adapted from Duempelmann et al., 2020)

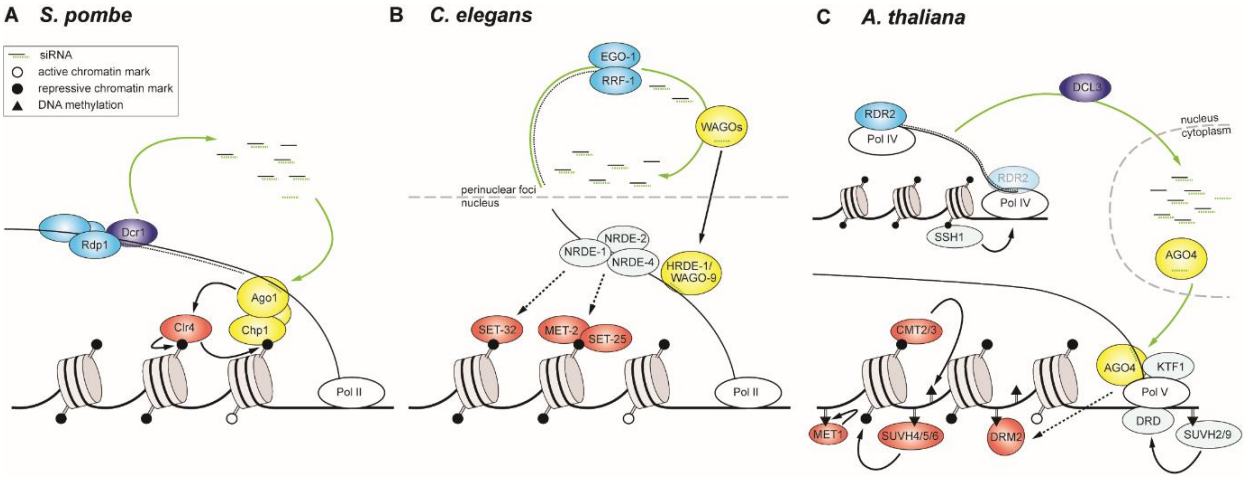

Figure 7. Positive Feedback Loops Maintain Chromatin Modifications. *Similarities of the small RNA silencing pathways in S. pombe (A), C. elegans (B), and A. thaliana (C) are highlighted by identical coloring of conserved effector proteins. (A) The S. pombe RNA-induced transcriptional silencing (RITS) complex (yellow) is guided to the nascent transcript by its small RNA-bound Ago1 subunit. Chp1 binds to methylated chromatin and RITS recruits the cryptic loci regulator complex (CLRC) (red) and the RNA-dependent RNA polymerase (RdRP) complex RDRC (light blue). The CLRC subunit Clr4 mediates H3K9me2/3 and the Rdp1 subunit of RDRC synthesizes dsRNA from the nascent transcript: dsRNA is processed by Dcr1 (dark blue) into secondary siRNAs channeled into new RITS complexes, creating a self-reinforcing feedback loop that stabilizes H3K9me2/3 heterochromatin. Clr4 creates a positive feedback loop by binding methylated histones through its chromo-domain and methylation of neighboring histones. (B) In C. elegans, 22G RNAs (siRNAs) are continuously amplified in perinuclear foci, which requires the RdRPs EGO-1 and RRF-1 (light blue). Mature 22G RNAs associate with different worm-specific Argonaute proteins (WAGOs), such as Heritable RNAi Deficient 1 (HRDE-1/ WAGO-9). The 22G RNA-HRDE-1 complex (yellow) re-enters the nucleus and targets nascent RNA Pol II transcripts. This interaction and the association with the NRDE factors NRDE-1/-2/-4 likely recruits H3K9 histone methyltransferases SET-25, SET-35, and MET-2, which ultimately repress transcription. (C) The RNA-dependent DNA methylation (RdDM) pathway in A. thaliana requires DNA-dependent RNA polymerases Pol IV and V. Pol IV produces short transcripts that are channeled into the associated RdRP RDR2 (light blue) (Singh et al., 2019). RDR2-synthesized dsRNA serves as substrate for DCL-3 (dark blue), which generates 24-nt siRNAs that load onto AGO4 (yellow). The siRNA-AGO4 complex then binds the nascent transcript of Pol V, Pol V itself, and the elongation factor KTF1. These interactions are thought to promote the recruitment of DRM2, which mediates de novo DNA methylation. Subsequently, histone methyltransferases (SUVH4/5/6) deposit H3K9me2. The repressive chromatin modifications are maintained via positive feedback loops, including DNA and H3K9 methyltransferases (red) (Law and Jacobsen, 2010; Wendte and Pikaard, 2017). Both modifications further promote positive feedback as H3K9me2-bound SHH1 recruits Pol IV, and DNA methylation-bound SUVH2 and SUVH9 recruit Pol V through the DRD complex (Wendte and Pikaard, 2017). Filled arrows indicate confirmed interactions, dashed arrows indicate putative recruitment of chromatin modifiers. Figure re-used from Duempelmann et al., 2020 with permission.*

3.2.1. RNAi-mediated heterochromatin assembly in *S. pombe*

In *S. pombe*, centromeric heterochromatin is mediated by a strong re-enforcing feedback loop that couples RNAi and H3K9me (Figure 8). *S. pombe* contains only single gene copies for Argonaute (*ago1+*), Dicer (*dcr1+)*, and RdRP (*rdp1+*), which are all essential for centromeric heterochromatin (Volpe et al., 2002), therefore making it a great model organism to study RNAi-mediated heterochromatin.

Assembly and targeting of the RITS complex

dsRNA from the centromeric *dg* and *dh* repeats are processed by the *S. pombe* Dicer homolog Dcr1 into a broad size range of small duplex RNA cleavage products with its RNase III domains (Colmenares et al., 2007). These small duplex RNAs are loaded by the Argonaute siRNA chaperone (ARC) complex onto Ago1. As long as Ago1 is part of the ARC complex, its endonucleolytic cleavage (slicer) activity is inhibited and the passenger-strand cannot be released (Buker et al., 2007; Holoch and Moazed, 2015b).

Upon loading, the RNA-bound Ago1 in conjunction with Tas3 and Chp1 forms the RITS complex (Verdel et al., 2004). Tas3 contains a glycine and tryptophan (GW) motif, links Ago1 to Chp1 (Debeauchamp et al., 2008) and can oligomerize, thus spread along nucleosomes (Li et al., 2009; Stunnenberg et al., 2015). Chp1 is a chromodomain-containing protein that interacts with H3K9me2/3 marked nucleosomes (Partridge et al., 2002; Schalch et al., 2009), a conserved mark of heterochromatin. The guide siRNA has a typical 5’ U bias, likely due to a loading preference of Ago1 (Buhler et al., 2008). Upon slicing and release of the passenger small RNA (Buker et al., 2007; Irvine et al., 2006), the guide siRNA is exonucleolytically trimmed to a length of 22-23 nucleotides (Colmenares et al., 2007; Halic and Moazed, 2010; Marasovic et al., 2013). RITS complexes are targeted by complementary base-pairing of their small guide RNA to nascent centromeric RNA transcripts from RNA Pol II (Shimada et al., 2016). In summary, RITS strongly localizes to the centromeric repeats by the interaction of siRNA-bound Ago1 with nascent transcripts, as well as the binding of Chp1 with H3K9 methylated nucleosomes. Subsequently, RITS recruits different effector complexes, leading to heterochromatin formation (Holoch and Moazed, 2015a).

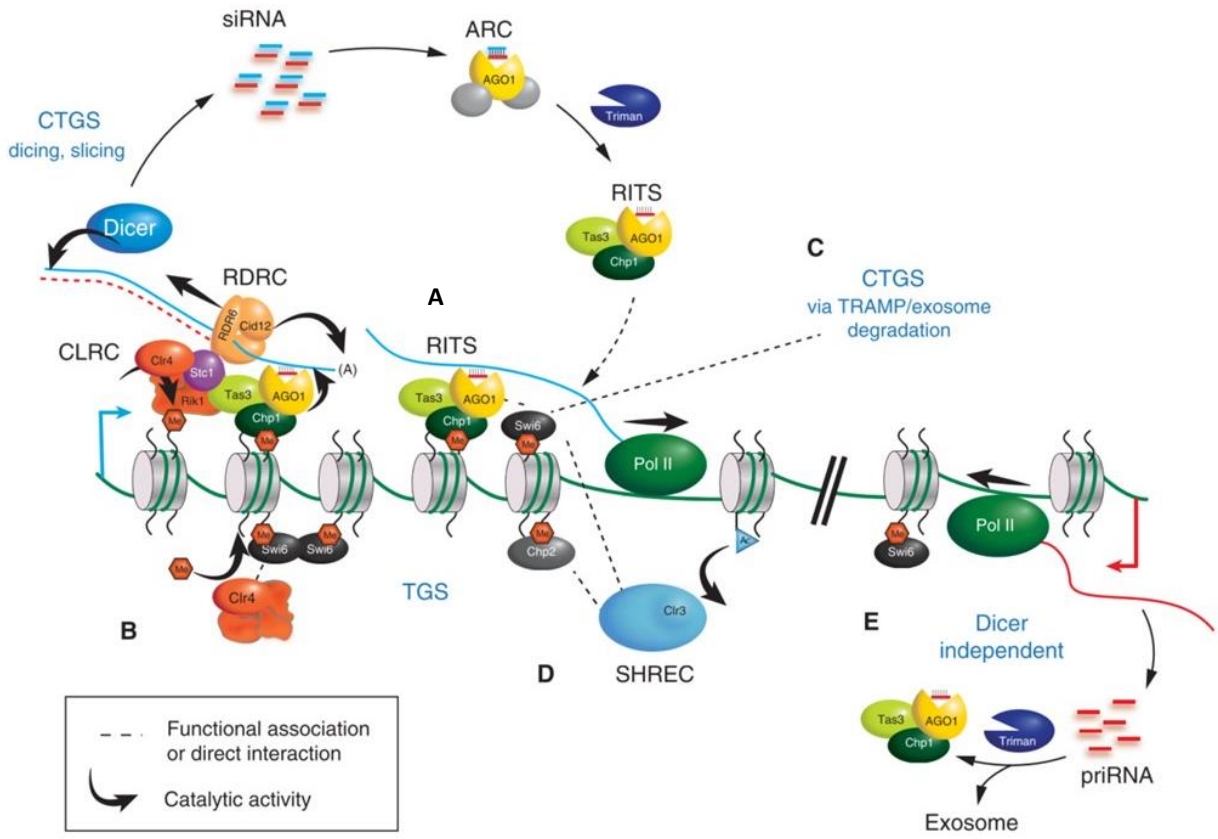

Figure 8. The 'nascent transcript' model for heterochromatin assembly*. In S. pombe, siRNA production is coupled to chromatin modifications through a self-sustaining feedback loop. (**A**) The RITS complex interacts through its siRNA-bound Ago1 subunit with nascent transcripts from centromeric long non-coding RNAs (lncRNAs). Furthermore, RITS also binds H3K9me with its chromo-domain containing subunit Chp1 and thereby establishes a physical connection between siRNAs and heterochromatin. The siRNA bound lncRNA becomes a template for the RDRC, which synthesizes dsRNA. Dicer 1 (Dcr1) generates from the dsRNA new siRNA, leading to further recruitment of RITS complexes to the nascent transcript. (**B**) Additionally, the RITS complexe recruits by physical interaction the Clr4 methyltransferases containing CLRC complex. Clr4 methylates H3K9, and thereby promotes RITS complex binding, leading to a self-reinforcing epigenetic loop. H3K9 methylation provides a binding site for HP1 proteins (Swi6 and Chp2). Swi6 promotes the recruitment of RDRC and the degradation of centromeric RNA by TRAMP/exosome. (**C**) Chp2 recruits the Snf2/Hdac-containing repressor complex (SHREC), which deacetylates H3K14 (**D**) and thereby promotes TGS. Figure re-used from Martienssen and Moazed, 2015 with permission.*

H3K9 methylation and recruitment of HP1 proteins

One of the key steps in initiating heterochromatin assembly is the recruitment of the H3K9 histone methyl transferase Clr4. At the centromere, RITS promotes H3K9 methylation by physical interaction with the cryptic loci regulator complex (CLRC) (Bayne et al., 2010; Buhler et al., 2006). The Clr4 subunit of CLRC is the only known H3K9 methyltransferase in *S. pombe* (Nakayam et al., 2001). It can deposit mono-, di-, and tri-methylation marks on H3K9 and automethylate Clr4, increasing the H3K9me deposition activity (Iglesias et al., 2018). Once methylated, H3K9 (H3K9me2/3) serves as a binding site for the four *S. pombe* chromo-domain proteins, Clr4 itself, the RITS complex subunit Chp1 and the HP1 homologs Swi6 and Chp2 (Bannister et al., 2001; Motamedi et al., 2008; Nakayam et al., 2001; Partridge et al., 2002; Sadaie et al., 2004; Thon and Verhein-Hansen, 2000; Zhang et al., 2008). The HP1 homolog Chp2 is primarily responsible for the recruitment of the Snf2/Hdac Repressive Complex (SHREC), which mediates chromatin remodeling and histone deacetylation (Job et al., 2016; Sugiyama et al., 2007). The SHREC subunit Clr3 deacetylates histone H3K14, which is an important step for heterochromatin formation, leading to reduced RNA Pol II transcription and promoting TGS (Sugiyama et al., 2007). Nevertheless, the centromeric repeats are still transcribed by RNA Pol II in intact heterochromatin, but the transcripts are rapidly turned over by multiple mechanisms (Buehler et al., 2007; Buhler et al., 2006; Keller et al., 2012; Volpe et al., 2002). The HP1 homolog Swi6 dynamically localizes to H3K9me marked nucleosomes, interacts with RITS and binds through a nonspecific affinity to heterochromatic RNAs (Cheutin et al., 2004; Keller et al., 2012; Rougemaille et al., 2012). Swi6 is thought to promote RNA degradation by escorting its associated RNAs to the RNA decay machinery (via TRAMP/exosome), thereby contributing to heterochromatic repression at the co- or post-transcriptional level (Keller et al., 2012; Motamedi et al., 2008). Interestingly, Swi6 cannot simultaneously bind RNA and H3K9me, leading to a highly dynamic localization of this HP1 protein to heterochromatin (Keller et al., 2012; Stunnenberg et al., 2015). Furthermore, Swi6 interacts through Ers1 with the RITS complex, RDRC and Dicer (Hayashi et al., 2012; Rougemaille et al., 2012), as well as with Epe1. Oligomerization of the Swi6, as well as the Chp2 chromoshadow domain and Tas3 in combination with the reader/writer ability of Clr4 is thought to mediate spreading of heterochromatin (Canzio et al., 2011; Sadaie et al., 2008; Zhang et al., 2008). Not only is RNAi important for CLRC recruitment, but also CLRC is important for RITS complex recruitment. Interaction of RITS to chromatin is lost upon mutation of Clr4 or the H3K9me binding chromodomain of Chp1 (Noma et al., 2004; Partridge et al., 2002). Furthermore, continuous amplification of siRNA is required for the recruitment of RITS to chromatin.

Amplification of siRNAs

A characteristic feature of small RNA-mediated nuclear gene silencing pathways is the continuous amplification of the small RNA pool. Many fungi (including *S. pombe*), plants, and nematodes rely on RdRPs for small RNA amplification (Dalmay et al., 2000; Henderson and Jacobsen, 2007; Motamedi et al., 2004; Sijen et al., 2001; Smardon et al., 2000; Volpe et al., 2002).

The *S. pombe* RdRP Rdp1 forms a complex together with the helicase Hrr1 and the putative poly(A) polymerase Cid12, termed RNA-dependent RNA polymerase complex (RDRC) (Motamedi et al., 2004). This complex is recruited to chromatin by the RITS complex through Stc1 and by Swi6 through Ers1 (Bayne et al., 2010; Hayashi et al., 2012; Motamedi et al., 2004; Rougemaille et al., 2012). RDRC uses the nascent transcript as a template to generate dsRNA. Interestingly, Rdp1 does not require a siRNA primer for *in vitro* RNA synthesis (Motamedi et al., 2004), suggesting that RITS acts by physical interaction as a "priming complex" and that the recruitment of the RDRC to a nascent transcript directs the specificity for RNA templates. Thus, siRNAs indirectly instruct dsRNA synthesis, which leads to an amplified RNAi response. The dsRNA is further processed into small RNAs by Dcr1, which is physically associated with RDRC (Colmenares et al., 2007). These siRNAs are assembled through the ARC complex into new RITS complexes, re-enforcing the positive feedback loop to H3K9 methylation.

Vertebrates and insects lack RdRP homologs (Zong et al., 2009). Instead, an RdRP-and Dicer-independent mechanism evolved in the metazoan germline to amplify the pool of small RNAs for silencing of transposons. For example, in the PIWI pathway small RNAs called piRNAs are amplified via the 'ping-pong' cycle mechanism (reviewed in Luteijn and Ketting, 2013).

3.2.2. The RNA-dependent DNA methylation pathway in *A. thaliana*

In plants, the major siRNA-mediated epigenetic pathway is RdDM, which has been most intensively studied in *A. thaliana* (Figure 7C) (reviewed in Law and Jacobsen, 2010; Matzke and Mosher, 2014; Wendte and Pikaard, 2017). This pathway was been shown to transcriptionally repress a subset of transposons and genes, mainly in euchromatic regions, and has been implicated in stress responses and pathogen defense, as well as in intercellular and interallelic communication (Matzke and Mosher, 2014). Similar to *S. pombe*, at the core of the RNA-directed pathway are siRNA-guided Argonaute complexes that bind to complementary nascent transcripts and recruit effectors that mediate chromatin modifications, siRNA amplification and silencing. In contrast to *S. pombe*, the RNA scaffold and the siRNA precursor originate from two different transcripts, synthesized by RNA Pol II-related RNA polymerases known as Pol IV and Pol V, which are both specialized for canonical RdDM (reviewed in Matzke and Mosher, 2014). Single-stranded RNA transcripts from Pol IV serve as template for the physically associated RNA-DEPENDENT RNA POLYMERASE 2 (RDR2) to synthesize dsRNAs (Haag et al., 2012; Singh et al., 2019), which are further processed by DICER-LIKE 3 (DCL3) into 24-nt siRNAs. In the cytoplasm, siRNAs are loaded onto AGO4, which is targeted back in the nucleus to complementary nascent transcripts of Pol V that serves as scaffold (Wierzbicki et al., 2008). AGO4 is furthermore recruited by the physical interaction with the AGO hook motifs of Pol V and of the putative transcription elongation factor KTF1 (Bies-Etheve et al., 2009; He et al., 2009). Binding leads to the recruitment of the *de novo* methyltransferase DRM2, additional DNA methyltransferases that methylate cytosines in several contexts (CG, CHG and CHH; H = A, C or T) and histone modification (reviewed in Wendte and Pikaard, 2017). H3K9me can act in a feedback loop with DNA methylation and thereby reinforce chromatin compaction and gene repression. Additionally, either modification can recruit the RdDM machinery, thereby further increasing chromatin compaction and gene repression in a positive feedback loop (Figure 7C).

3.2.3. Nuclear small RNA mediated gene silencing in *C. elegans*

In C. elegans, gene silencing can be triggered by several different classes of small RNAs generated through various biogenesis pathways (reviewed in Almeida et al., 2019; Luteijn and Ketting, 2013; Weiser and Kim, 2019). Importantly, primary small RNAs, like endo-siRNAs, piRNAs, and exo-siRNAs, can initiate the biogenesis of heritable secondary small RNAs, with a characteristic length of 22nt and a 5' guanine bias (22G RNAs) (Bagijn et al., 2012; Pak and Fire, 2007; Sijen et al., 2007). In contrast to yeast and plants, the secondary siRNAs in *C. elegans* are distinct from the primary small RNAs. 22G RNAs are bound by >12 of the 27 different worm-specific Argonaute proteins (WAGOs) (Weiser and Kim, 2019), which facilitate either post-transcriptional or transcriptional gene silencing (reviewed in Almeida et al., 2019).

For example, the germline-specific HRDE-1 (WAGO-9) binds together with HRDE-2 to 22G RNAs in the cytoplasm and upon translocation to the nucleus triggers transcriptional silencing of complementary target genes (Figure 7B) (Luteijn and Ketting, 2013; Spracklin et al., 2017). Furthermore, the WAGO protein NRDE-3 associates with endogenous, as well as exogenous small RNAs and also suppresses transcription (Guang et al., 2010; Guang et al., 2008). Analogous to fission yeast and plants, the Argonaute proteins NRDE-3 and HRDE-1 are thought to bind to RNA Pol II-transcribed nascent transcripts by base-pairing with their associated siRNA. Subsequently, factors of the nuclear RNAi pathway (Nuclear RNAi Defective NRDE-1/2&4) are recruited, leading to transcriptional silencing. On one hand, the NRDE pathway directs inhibition of RNA Pol II elongation (Guang et al., 2010). On the other hand, histone methyltransferases, such as MET-2, SET-25, and SET-32, are recruited, resulting in H3K9 methylation (Ashe et al., 2012; Buckley et al., 2012; Burkhart et al., 2011; Guang et al., 2008; Kalinava et al., 2017). Furthermore, the HP1-like proteins HPL-1 and HPL-2 were shown to play a role in silencing (Luteijn and Ketting, 2013). 22G RNAs are continuously amplified, which involves the RdRP activity of EGO-1 and RRF-1 and components of perinuclear foci (Bagijn et al., 2012; Phillips et al., 2012; Uebel et al., 2018).

Small RNA-mediated silencing responses can be inherited in the germline of C. elegans in the absence of triggering primary small RNAs. For example, 21U piRNAs can initiate a silencing response that can be independently maintained by a positive feedback loop through 22G RNAs (Ashe et al., 2012; Luteijn et al., 2012; Shirayama et al., 2012) (Figure 9). This phenomenon is consistent with the definition of "epigenetics" and has been dubbed "RNA-induced epigenetic silencing" (RNAe).

4. Mutations enabling RNAi-mediated facultative heterochromatin in *S. pombe*

In *S. pombe*, co-transcriptional silencing of the pericentromeric repeats is directed by complementary siRNAs. Whether siRNAs in *S. pombe* could also induce epigenetic gene silencing phenomena, as seen in *C. elegans,* has been unclear. Although expression of synthetic siRNAs was shown to promote H3K9 methylation *in trans* at a small number of loci, it is inefficient, locus dependent, and the silent state is highly unstable (Buhler et al., 2006; Iida et al., 2008; Sigova et al., 2004; Simmer et al., 2010). Therefore RNAi-mediated gene silencing of normally euchromatic loci was suggested to be under strict negative control. (Adapted from Duempelmann et al., 2020)

4.1. Transcription-associated factors counteract RNAe

Recent research has shown that synthetic siRNAs are able to initiate robust silencing responses in yeast strains with mutations in genes encoding transcription-associated factors. Those include subunits of the Paf1C, mRNA export factors Mlo3 and Dss1, transcription termination factors Ctf1 and Res2, and the acetyltransferase Mst2 (Duempelmann et al., 2019; Flury et al., 2017; Kowalik et al., 2015; Sadeghi et al., 2015; Verrier et al., 2015; Yu et al., 2018). Once initiated, silencing can be maintained across generations independently of the synthetic siRNA source in such mutants (Kowalik et al., 2015; Yu et al., 2018). Thus, in the presence of an "enabling" mutation, primary siRNAs can trigger an RNAe response in *S. pombe*. Secondary siRNA amplification is required for transgenerational inheritance (Duempelmann et al., 2019; Yu et al., 2018), as in *C. elegans*. (Adapted from Duempelmann et al., 2020)

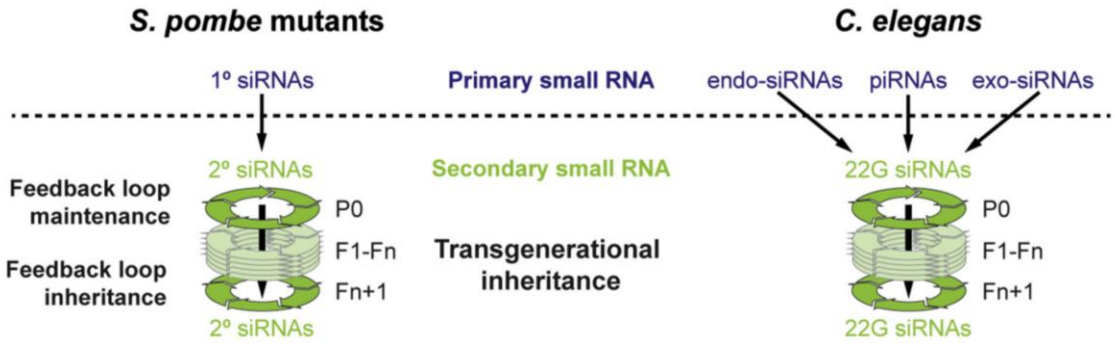

Figure 9. Primary siRNAs Initiate Silencing, Secondary siRNAs Maintain Silencing. *In S. pombe cells that harbor RNAi-enabling mutations, transcriptional gene silencing can be initiated by trans-acting primary (1°) siRNAs that derive from RNA hairpins [42] or centromeric heterochromatin [41]. Deposition of H3K9me3 leads to the production of secondary (2°) siRNAs, which re-enforce methylation of H3K9, creating a positive feedback loop sustained across generations independently of the triggering 1° siRNAs [41,43]. In C. elegans, 1° small RNAs, like endo-siRNAs, piRNAs, and exo-siRNAs, initiate the biogenesis of 2° 22G RNAs, which can be inherited over multiple generations. Figure re-used from Duempelmann et al., 2020 with permission.*

4.1.1. The Paf1 complex

During my PhD, I have induced RNAi-mediated silencing almost exclusively in the Paf1C mutant background. This evolutionary conserved complex functions as a regulator of RNA Pol II transcription and promotes specific transcription-coupled histone modifications. Paf1C participates in numerous cellular processes such as gene expression and silencing, DNA repair, cell cycle progression and prevention of disease states in higher eukaryotes (Tomson and Arndt, 2013). The Paf1C was initially discovered in *Saccharomyces cerevisiae* (*S. cerevisiae)* through its physical association with the C-terminal domain (CTD) of RNA Pol II subunit Rpb1 (Wade et al., 1996). In *S. cerevisiae* Paf1C comprises five subunits that stabilize each other in a complex: Paf1, Cdc73, Ctr9 (Tpr1 in *S. pombe*), Leo1 and Rtf1 (Prf1 in *S. pombe*) (Koch et al., 1999; Mbogning et al., 2013; Mueller and Jaehning, 2002; Squazzo et al., 2002; Wade et al., 1996). In fission yeast and multicellular organisms, Rtf1/Prf1 is less tightly associated with the other Paf1C subunits. The human Paf1C additionally contains Ski8, a subunit of the SKI complex, which together with the exosome mediates 3'-5' mRNA degradation (Tomson and Arndt, 2013; Zhu et al., 2005). All subunits are evolutionary conserved between *S. cerevisiae* and human with 19-22% overall amino acid identity (Tomson and Arndt, 2013). In yeast, deletions of individual Paf1C subunits result in various phenotypes indicative of defects in transcription elongation and chromatin, as well as sensitivity to cellular stress inducing compounds such as caffeine, cyclohexamide, rapamycin, hygromycin, and high temperature (Tomson and Arndt, 2013). Unlike for yeast (Mbogning et al., 2013; Shi et al., 1996), Paf1C is essential for the viability of multicellular organisms (Adelman et al., 2006; Kubota et al., 2014; Wang et al., 2008).

Paf1C localizes to active genes from the TSS to the poly(A) site (Adelman et al., 2006; Van Oss et al., 2017; Van Oss et al., 2016) through several interactions. The subunits Cdc73 and Rtf1 recruit the Paf1C to actively transcribed genes through binding of phosphorylated RNA Pol II CTD and Spt5-CTR repeat peptides. Additionally, Paf1C has been suggested to be recruited to transcribed genes by RNA binding of Leo1 (Dermody and Buratowski, 2010).

Multiple labs found that Paf1C affects and can facilitate RNA Pol II transcription elongation through multiple interactions (Kim et al., 2010; Tomson and Arndt, 2013). Paf1C interacts with the histone chaperone containing Spt16-Pob3/FACT (Facilitates Chromatin Transcription) complex and highly conserved transcription elongation factors including Spt4-Spt5/DSIF (DRB Sensitivity Inducing Factor) complex (Mueller and Jaehning, 2002; Adelman, 2006; Squazzo et al., 2002; Tomson, 2013). Furthermore, Paf1C and the elongation factor TFIIS cooperatively bind to RNA Pol II (Kim et al., 2010; Xu et al., 2017). FACT and TFIIS were both shown to promote transcription elongation (Formosa, 2012; Kim et al., 2010). Paf1C stimulates binding of each of those three complexes to RNA Pol II and is thereby suggested to play

a critical role in transcription elongation (Adelman et al., 2006; Chen et al., 2009; Kim et al., 2010; Tomson and Arndt, 2013).

Paf1C regulates transcription also by promoting specific histone modifications, which play an important role in transcription by altering chromatin accessibility and recruitment of chromatin remodelers and modifiers. The histone modification domain (HMD) of Rtf1 is necessary and sufficient for H2B monoubiquitylation (*S. cerevisiae* K123) *in vivo* by enhancing recruitment of the ubiquitin protein ligase Bre1 to chromatin (Tomson and Arndt, 2013). H2Bub in turn facilitates FACT function, transcription elongation and is essential for subsequent trimethylation of H3K4 and H3K79 by the methyltransferases Set1 and Dot1, respectively (Tomson and Arndt, 2013). Mutation of Paf1C leads to decreased promoter association of H3K4 trimethylation, as well as the co-transcriptionally deposited H3K36 trimethylation by Set2 histone methyltransferase (Chu et al., 2007). This might be partially due to the observed decrease of RNA Pol II CTD Serine 2 phosphorylation (Ser2P) levels in Paf1C mutant cells (Nordick et al., 2008).

Last but not least, Paf1C is also involved in transcription termination and processing. During transcription termination, 3'-end mRNA processing factors such as the Cleavage and Polyadenylation Factors (CPF) complex and the RNA processing complex (CF1A) are recruited. The subunits Cft1 (CPF) and Pcf11 (CF1A) were shown to directly associate with RNA Pol II CTD Ser2P. Furthermore, Cft1 associates with RNA Pol II CTD Ser5P in a Paf1C-dependent manner (Nordick et al., 2008). In mammals, mutation of Paf1C can additionally result in shortened poly(A) tails and change of the poly(A) site utilization. This might be caused by the CTD Ser2P levels, resulting in reduced recruitment of 3'-end processing factors (Nordick et al., 2008; Tomson and Arndt, 2013).

In summary, Paf1C is an important transcription-associated factor that promotes RNA Pol II elongation, histone modifications, and is involved in transcription termination and processing. Additionally, Paf1C counteracts RNAi-mediated silencing in *S. pombe* (Kowalik et al., 2015).

4.2. Models for RNAi-induced heterochromatin formation

The mechanisms by which the Paf1C and other transcription-associated factors counteract RNAe in *S. pombe* remain elusive. Two non-mutually exclusive models have been put forward (Figure 10).

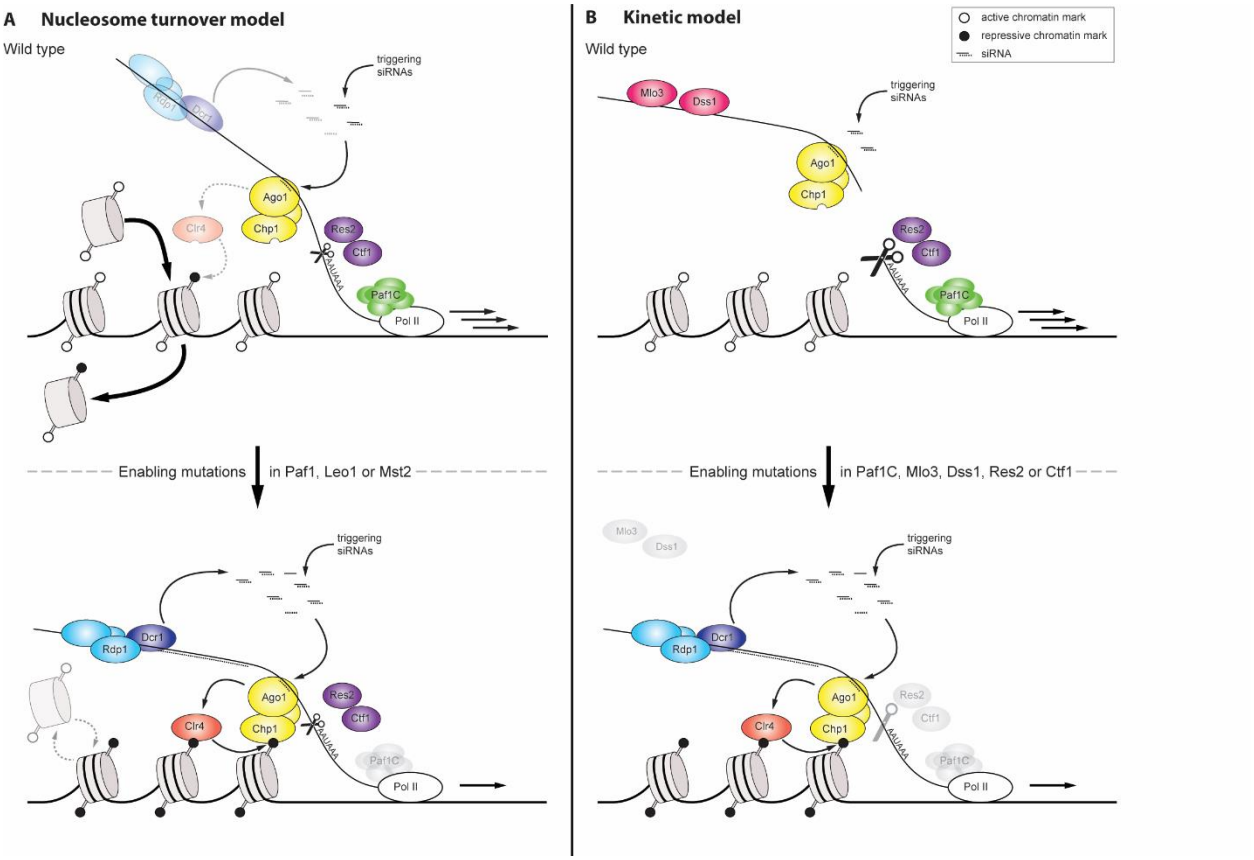

Figure 10. Enabling mutations in fission yeast and their potential modes of action. *(A) Nucleosome turnover model (model 1). Under wild type conditions (upper panel), triggering 1° siRNAs lead to the deposition of H3K9me2/3 marks at the complementary target locus. Because methylated nucleosomes are constantly exchanged, no stable heterochromatin can be established, weakening the feedback loop and preventing transcriptional gene silencing. Upon loss of the Paf1-Leo1 subcomplex (lower panel), nucleosome turnover rates are reduced and the persistence of methylated H3K9 promotes the RNAi feedback loop to form stable heterochromatin and reduce transcription at the target locus. (B) Kinetic model (model 2). Following transcription elongation, wild type cells rapidly terminate and release the siRNA target RNA from the site of transcription (upper panel). Kinetics of these processes are reduced when Paf1C, or termination and processing factors like Res2 and Ctf1, or RNA export factors such as Mlo3 and Dss1 are mutated. As a result, the nascent RNA transcript is maintained close to its site of transcription, allowing sufficient time for establishment of stable heterochromatin. Proteins with enabling mutations are depicted as transparent grey where their function is lost. Scissors depict the cleavage site for the transcript release. The polyadenylation signal is represented by the consensus motif AAUAAA. Figure re-used from Duempelmann et al., 2020 with permission.*

Model 1 suggests that reduced histone H3 exchange rates in *paf1*/*leo1* mutants (Sadeghi et al., 2015) may stabilize and thereby reduce dilution of K9 methylated H3 (Figure 10A). In line with this, the acetyltransferase Mst2 has also been proposed to promote histone turnover and *mst2* deletion drastically enhances the silencing initiation frequency in *paf1* mutants (Flury et al., 2017; Wang et al., 2015). Furthermore, reduced positioning of heterochromatin to the nuclear periphery has been suggested to elevate histone turnover and drastically reduce initiation and maintenance of ectopic heterochromatin (Holla et al., 2020). This model would predict that regions with low nucleosome turnover rates, such as lowly expressed genes, are more prone to RNAe, a hypothesis that remains to be tested.

Model 2 suggests that decelerated transcription kinetics or deferred release of the nascent transcript from chromatin allows sufficient time for RITS to recruit CLRC and methylate H3K9, enabling facultative heterochromatin formation (Figure 10B) (Kowalik et al., 2015). This model is supported by several observations: 1. Mutation of nascent transcript processing signals, which promote the release and export of the target RNA, enable siRNA-directed H3K9 methylation (Yu et al., 2014). 2. Deletion of certain transcription termination factors enables weak RNAi-mediated silencing (Kowalik et al., 2015). 3. siRNA-targeted introns close to the transcription start site have a lower silencing potential compared to distal introns (Shimada et al., 2016). 4. Forced release of the nascent transcript by ribozyme-mediated abolished initiation of silencing in Paf1C mutant cells (Kowalik et al., 2015). Model 2 would also explain why centromeric repeats are not under the control of Paf1C, as repeat transcripts do not contain strong cleavage and polyadenylation signals (Yu et al., 2014).

Inducing repression of protein-coding genes at the transcriptional level using siRNAs has been challenging in most organisms. This suggests that the mechanisms that antagonize silencing of euchromatic genes might be conserved. In accordance with this idea, Paf1C has recently been implicated in counteracting PIWI-dependent silencing in piRNA-targeted reporter assays in *D. melanogaster* (Clark et al., 2017). Furthermore, defects in RNA 3'-end processing complexes in *A. thaliana* have been shown to enhance the silencing phenotype (Herr et al., 2006), lending support for model 2. Thus, RNAe-related phenomena might be much more prevalent, but only revealed under specific conditions.

This chapter is adapted with permission from L. Duempelmann, M. Skribbe and M. Bühler; Small RNAs in the transgenerational inheritance of epigenetic information. Trends in Genetics (2020).

5. Propagation of small RNA-mediated silencing across generations

5.1. Introduction

Gene silencing can persist over multiple generations in the germline of C. elegans. Gene repression is typically maintained without the initial trigger for three to seven generations (Minkina and Hunter, 2018), and occasionally for tens of generations (Ashe et al., 2012; Luteijn et al., 2012; Shirayama et al., 2012; Vastenhouw et al., 2006). In contrast, silencing of somatically expressed genes mostly affects only the subsequent generation through non-epigenetic parental effects, with rare exceptions (Minkina and Hunter, 2017, 2018). Following the discovery of stably inherited silencing in the germline, forward genetic screens have identified various factors required for the propagation of the repressed state across generations.

5.2. Factors mediating RNAe

The nuclear Argonaute HRDE-1, which is dispensable for the initial silencing response, is essential for transgenerational inheritance (Ashe et al., 2012; Bagijn et al., 2012; Buckley et al., 2012; Luteijn et al., 2012; Shirayama et al., 2012), as are NRDE-1/-2/-4, RNA-dependent RNA polymerases (EGO-1, RRF-1) and the HP1 homolog HPL-2 (Minkina and Hunter, 2018; Rechavi and Lev, 2017). 22G RNAs are strictly required to propagate silencing across generations: RNAe responses cease if 22G RNAs are not continuously generated, which occurs in dedicated cellular compartments (Spracklin et al., 2017; Uebel et al., 2018; Wan et al., 2018; Weiser and Kim, 2019; Xu et al., 2018). There is evidence that 22G RNAs are paramutagenic: HRDE-1-22G-RNA complexes can be inherited and induce silencing of the homologous zygotic allele without transmission of the silenced locus and its chromatin marks (Sapetschnig et al., 2015). Further, the *in trans* silenced second allele remains silenced over tens of generations, even after the first allele is lost (Sapetschnig et al., 2015). Thus, it is tempting to speculate that RNAe in *C. elegans* could be propagated over multiple generations through transmissible HRDE-1-bound 22G RNAs. The role histone modifications play in propagation of a *C. elegans* RNAe response remains unclear. Although putative histone methyltransferases SET-25 and SET-32 are recruited to methylate H3K9, it is debated whether they are essential for the propagation of the silent state (Ashe et al., 2012; Kalinava et al., 2017; Minkina and Hunter, 2017; Spracklin et al., 2017; Woodhouse et al., 2018). Thus, more work is required to elucidate the crosstalk between RNA silencing and chromatin in worms.

5.3. Duration of RNAe

Although feedback loops could in principle lead to infinite silencing responses, the duration of epigenetically inherited silencing is typically restricted to a few generations in wild-type worms. Genetic screens designed to discover modifiers of RNAe (modified transgenerational epigenetic kinetics, MOTEK) revealed several factors that influence the duration of RNAe. Mutations in the gene heritable enhancer of RNAi (*heri-1*) gene prolong RNAe heritability by more than 20 generations (Perales et al., 2018). This nuclear, chromodomain-containing protein is expressed in the germline and its recruitment to an RNAi targeted gene unexpectedly depends on factors that drive co-transcriptional gene silencing, such as HRDE-1 and SET-32/HRDE-3. The authors hypothesize that HERI-1 restricts nuclear RNAi by allosteric inhibition and thereby limits RNAi-mediated inheritance. The duration of RNAe responses can also be modulated by shifting the balance between different small RNA pathways (Houri-Ze'evi et al., 2016). Many RNA silencing factors are shared between pathways, and defects in one pathway enhance parallel pathways as effector availability increases (Calo et al., 2017; Duchaine et al., 2006; Houri-Ze'evi et al., 2016; Lev et al., 2017). For example, a first RNAi response can be prolonged by a second RNAi response against an unrelated gene due to a shift from the endo- to the exo-siRNA pathway (Houri-Ze'evi et al., 2016). Upon mutation of met-2, small RNAs against repetitive elements decrease, potentiating the exo-siRNA pathway and leading to prolonged silencing response. Finally, endo-siRNAs against RNAi factor genes have been proposed to auto-inhibit RNAi and thereby also limit the duration of an RNAe response (Houri-Ze'evi et al., 2016).

5.4. The Role of H3K9me3 in *C. elegans* RNAe

In *C. elegans*, RNAe has generally been considered to correlate with enrichments of H3K9me3 at the target locus and to depend on the putative H3K9 methyltransferases set-25 and set-32 (Luteijn2012, Shirayama2012, Gu2012, Mao2015) (Ashe2012, Spracklin2017). However, recent reports challenged the requirement of H3K9me3 for silencing and RNAe in *C. elegans*. Histone methyltransferases were shown to be required for gene silencing of somatic, but not germline, genes (Minkina and Hunter, 2017). There may also be gene specific requirements, as, for example, repression of the oma-1 gene was reported to be inherited in the absence of H3K9me3 (Kalinava et al., 2017), and another study showed that initiation, but not maintenance, of gene silencing depends on H3K9me3 (Woodhouse et al., 2018).

5.5. RNAe in S. pombe

RNAe responses in *S. pombe* depend strictly on the continuous generation of secondary siRNAs, as in *C. elegans*. In contrast to *C. elegans*, however, amplification of siRNAs by the RNAi machinery and H3K9 methylation are mutually-dependent processes, and the tri-methylated state of H3K9 is necessary for transgenerational inheritance (see Results, Duempelmann et al., 2019). Thus, RNAe in fission yeast is not possible without the coupling of the RNAi pathway and H3K9 methylation (Yu et al., 2018). The mode of inheritance is more controversial and will be addressed in the DISCUSSION chapter 5.

6. Aim of this thesis

In fission yeast, RNAi-mediated silencing is under strict negative control and can only be induced in mutant backgrounds, such as mutations in genes encoding subunits of Paf1C. Once initiated in cells harboring such enabling mutations, silencing is stably maintained through mitotic divisions and can be inherited through meiosis (Kowalik et al., 2015). This finding raised the question whether also wild-type cells could maintain facultative heterochromatin. Because the silencing phenotype had not been observed when the enabling mutation was outcrossed (Kowalik et al., 2015; Bühler lab unpublished observations), it was assumed that there was no propagation of silent chromatin marks in wild type cells.

In my PhD project, I set out to address the following questions:

- Can exogenous signals enable RNAi-mediated silencing in wild-type cells, for example by modulation of Paf1C activity?
- Can *S. pombe* acquire resistance against a stressor through RNAi-mediated silencing?
- How does mutation of Paf1C lead to silencing?
- Does loss of a gene silencing phenotype always correlate with the erasure of all classical silencing marks?
- Can wild-type *S. pombe* maintain and inherit RNAi-mediated epimutations?

RESULTS

1. Inheritance of a Phenotypically Neutral Epimutation Evokes Gene Silencing in Later Generations

L. Duempelmann, F. Mohn, Y. Shimada, D. Oberti, A. Andriollo, S. Lochs and M. Bühler

The entire article can be found in the appendix section.

Highlighted in: M. Capella and S. Braun (2019). Neutral epigenetic inheritance: being prepared for future generations. Nat Struct Mol Biol. 26(6):391-392.

Summary

Small RNAs can trigger epigenetic gene silencing over many generations (Vastenhouw et al., 2006). In *S. pombe*, RNAi-mediated silencing of genes is under strong negative control and can only be initiated in the presence of an enabling mutation, such as in the Paf1C (Kowalik et al., 2015). We showed for the first time that in *S. pombe*, RNAe can be propagated for almost 20 generations in the Paf1C mutant background. Upon reversion of the enabling mutation, the silencing phenotype is lost, suggesting that the memory of a past silencing event also ceased. This raised the important question whether *S. pombe* cells can inherit epigenetic information in the absence of an enabling mutation at all. Unexpectedly, I discovered that wild-type cells, which could not inherit the silencing phenotype, can inherit a phenotypically neutral molecular mark, and reinstate silencing by repeated Paf1C impairment. I found that the previously repressed gene

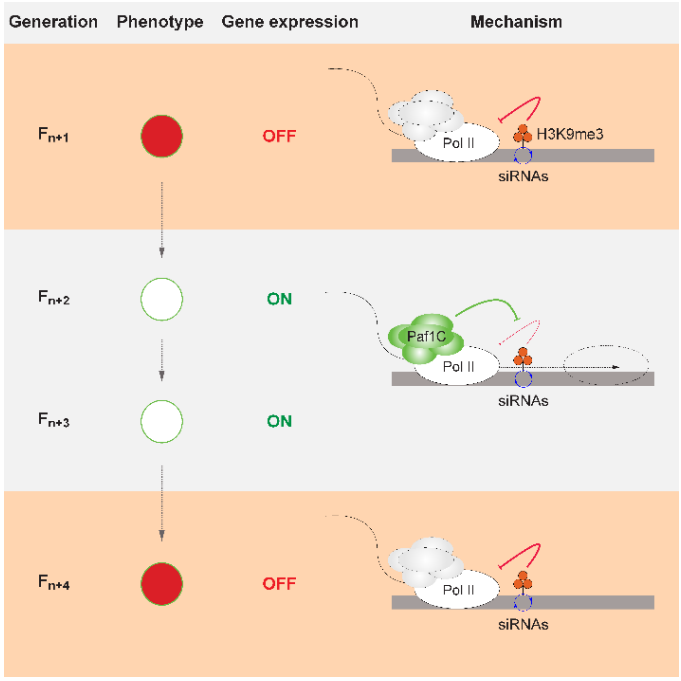

Figure 11. Schematic for inheritance of a phenotypic plastic epimutation. *In Paf1C mutants, H3K9me3 inhibits RNA Pol II transcription at ade6+, leading to a red silencing phenotype. In wild-type cells, ade6+ is transcribed normally, despite H3K9me3 enrichments (phenotypically neutral epimutation). Upon repeated Paf1C impairment, the silencing phenotype is reinstated. Thereby modulation of Paf1C can result in a phenotypic plastic epimutation. Figure re-used with permission from Duempelmann et al., 2019.*

was still H3K9 tri-methylated and produced siRNAs in phenotypically neutral cells, and therefore refer to this mark as “si3”. Both a functional RNAi pathway and H3K9me3 methylation are imperative for a stable propagation of the si3-mark, as is maximal binding activity of Clr4 to H3K9me3. My results show that H3K9me3 functions as epigenetic mark that must not necessarily be repressive *per se*, as has mostly been suggested in the past (Holoch and Moazed, 2015a). I propose a model in which Paf1C facilitates transcription elongation through H3K9me3 enriched genes, and I predict that modulation of Paf1C activity enables both acquisition and inheritance of phenotypically plastic epimutations.

My contributions

This paper comprises my main work and scientific findings of my PhD. Initially, members of the Bühler lab demonstrated that epigenetic silencing can be inherited over several generations in Paf1C mutant cells, but is lost in wild-type cells (see also Kowalik et al., 2015). In pursuit of exploring if *S. pombe* could also inherit epigenetic phenomena without an enabling mutation, I postulated that the silencing memory could potentially be uncoupled from the silencing phenotype. Indeed, I discovered that wild-type cells can inherit phenotypically neutral epimutations that can evoke gene silencing upon reintroducing an enabling mutation. I performed all experiments for the dissection of this peculiar ‘silencing memory’ and found that it consists and depends on H3K9me3 coupled to siRNAs. Furthermore, I performed parts of the computational analysis. The contributions of my dear colleagues to this project is given in the paper.

2. Bye1 UTR SNP segregates with the silencing phenotype

I showed that epigenetic silencing of *ade6+* could not be maintained in our wild-type background, despite high levels of H3K9me3 and siRNAs (Duempelmann et al., 2019). My results are inconsistent with a previous paper published by the Moazed lab, which reported inheritance of a strong silencing phenotype in wild-type cells across generations (Yu et al., 2018). Notably, they observed Mendelian inheritance of the silent state (Yu et al., 2018), which is rather uncommon for a purely epigenetic phenomena (see INTRODUCTION chapter 1.2.) (Horsthemke, 2018) and suggested to us that this phenomenon is likely linked to a genetic difference between the strains used in the two labs. The strains, in which silencing was initiated in the two studies, can be distinguished by few annotated genetic differences (Figure 12A, first two rows). We induced silencing of *trp1+::ade6+* by siRNAs from an RNA hairpin (*ade6-hp)* in a *paf1-Q264Stop* background (Duempelmann et al., 2019; Kowalik et al., 2015). In Yu et al. 2018, silencing of the endogenous *ade6+* was initiated by siRNAs from a centromeric *ade6+* copy (*cen::ade6*) in a *mlo3Δ* background (subsequently referred to as *mlo3Δ* Mlab strain) (Yu et al., 2018). Furthermore, they showed that silencing in a Buehler lab strain could only be stably propagated in the absence of an enabling mutation (*leo1Δ*) when initiated with *cen::ade6*, but not with a hairpin. Thus, they attributed the phenotypic discrepancy to the different siRNA source. However, in our lab changing the siRNA source to *cen::ade6,* as well as silencing the endogenous *ade6+* in the *paf1-Q264Stop* background did not result in inheritance of a silencing phenotype in wild-type cells (Figure 12A). Perplexingly, not even recreated *mlo3Δ cen::ade6* strains (n = 4) could induce silencing (referred to as *mlo3Δ* Blab strain), despite having the same annotated genetic features and being generated by crossing strains originating from the Moazed lab (Figure 12A). In comparison, the *mlo3Δ* Mlab strain had in our lab the same silencing initiation frequency (0.5 %) and showed Mendelian inheritance as reported (Yu et al., 2018), thus excluding environmental factors as cause of the observed phenotypic difference. The lack of silencing initiation in recreated *mlo3Δ cen::ade6* strains and observed Mendelian inheritance of silencing highly suggested a not annotated genetic difference.

To test this hypothesis, silenced colonies from the *mlo3Δ* Mlab strain were crossed out twice with an original wild-type strain (Figure 12B) and resulting silenced colonies were subjected to whole genome sequencing. Inheritance of the silencing phenotype correlated with a single nucleotide polymorphism (SNP) in the 3'-UTR of the gene *bye1* (Bypass of Ess1), a predicted negative regulator of RNA Pol II transcription elongation in *S. pombe* (Figure 12C) (Lock et al., 2018). Yukiko Shimada has previously found this identical SNP to correlate with a strong silencing phenotype (data not shown) (Kowalik et al., 2015). Therefore, we first asked whether the bye1 SNP, causing a three-fold increase of expression, would be

necessary for initiation of silencing. Reversion of this SNP to wild-type in the *mlo3Δ* Mlab strain obstructed silencing initiation in all transformants (n = 12) (Figure 12D), although directly after transformation, a very low silencing frequency was observed in three new strains, which was shortly after lost. This suggests that the *bye1* SNP is necessary for the initiation of silencing initiation in that background. Inexplicably, reintroduction of the *bye1+* 3'-UTR SNP into the *bye1Δ::ura4+ mlo3Δ* Mlab strain did not enable silencing initiation in tested transformants (n = 4, assessed colonies > 1000), implying very unstable silencing initiation in this genetic background that can be lost during manipulations such as transformations. Furthermore, the potential of silencing initiation could not be retained in descendants of *mlo3Δ* Mlab crossed with *mlo3Δ* Blab, even though all were *mlo3Δ cen::ade6* and 33% of the descendants carried the *bye1* SNP (Figure 12E). Therefore, the *bye1* SNP is sufficient in the *mlo3Δ cen::ade6* background for silencing initiation.

Next, I wondered if the *mlo3Δ* Mlab strain carried a pre-existing epigenetic mark that enables silencing initiation. Chronic heat stress causes Dicer to accumulate in the cytoplasm and heterochromatin to become unstable (Oberti et al., 2015; Woolcock et al., 2012). To find out if potential erasure of a pre-existing epigenetic mark would obviate silencing initiation, I exposed the *mlo3Δ* Mlab strain to chronic heat stress. Unexpectedly, antecedent heat shock did not inhibit, but increase silencing initiation of the *mlo3Δ* Mlab *bye1* SNP strain (Figure 12F) and enabled weak silencing of the *mlo3Δ* Blab *bye1* wild-type strain (faint pinkish colonies, not shown). This could result from erasure of epigenetic silencing of an enhancer of RNAi-mediated heterochromatin formation or by a compensatory mechanism, which enhances heterochromatin formation at high temperatures, and after return to standard temperature is propagated for some time.

In summary, I could not reproduce silencing initiation in newly created *cen::ade6 mlo3Δ::kan* strains, and the potential of silencing initiation could not be inherited from the *mlo3Δ* Mlab strain to *cen::ade6 mlo3Δ::kan* descendants with recombined backgrounds. Furthermore, a SNP in the bye1 3'-UTR correlated with the inheritance of *ade6+* silencing and might enhance silencing initiation under certain conditions, such as antecedent heat shock. However, the *bye1* SNP does not seem to be sufficient to disclose the fully penetrant silencing phenotype as described in Yu et al. 2018. Additional alleles that are different between the two strain backgrounds or additional unidentified factors might be required for the induction of silencing in *cen::ade6 mlo3Δ::kan* cells and Mendelian inheritance of silencing in wild-type yeast. Those results will be discussed in more detail in chapter 5 of the Discussion.

A

strain			silencing initiation	silencing maintenance*	source
enabling mutation	*ade6+* location	siRNA source			
mlo3Δ	*ade6+*	*cen::ade6+*	Yes	Yes	Moazed lab
paf1-Q264Stop	*trp1+::ade6+*	*ade6-hp*	Yes	No	Buehler lab
paf1-Q264Stop	*ade6+*	*ade6-hp*	Yes	No	Buehler lab
paf1-Q264Stop	*trp1+::ade6+*	*cen::ade6+*	Yes	No	Buehler lab
mlo3Δ	*ade6+*	*cen::ade6+*	No	n.d.	Buehler lab

B

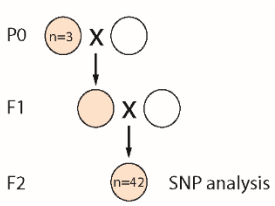

C

Chr	Start	Stop	Allele	Gene name	Consequence	IMPACT	%	Product description
III	1260881	1260882	A	SPCC645.13	3_prime_UTR_variant	MODIFIER	88.1	transcription elongation regulator, PHD finger Bye1 (predicted)
II	2908532	2908532	T	SPBP4H10.17c	5_prime_UTR_variant	MODIFIER	69	protein repair carboxyl methyl esterase (predicted)
III	1246664	1246664	T	rgf1	missense_variant	MODERATE	64.3	RhoGEF for Rho1, Rgf1
I	995016	995017	-	slp1	3_prime_UTR_variant	MODIFIER	54.8	substrate-specific mitotic metaphase/anaphase APC coactivator Slp1
II	2713912	2713912	T	pxl1	3_prime_UTR_variant	MODIFIER	54.8	paxillin-like protein Pxl1
II	662406	662407	-	SPBC947.06c	5_prime_UTR_variant	MODIFIER	52.4	spermidine family transmembrane transporter (predicted)
II	2689713	2689713	T	leu3	missense_variant	MODERATE	50	2-isopropylmalate synthase Leu3
I	4315335	4315335	A	pan1	missense_variant	MODERATE	42.9	actin cortical patch component, with EF hand and WH2 motif Panl (predicted)
II	154603	154603	C	mal1	missense_variant	MODERATE	42.9	maltase alpha-glucosidase Mal1
II	1104941	1104941	T	cyp3	5_prime_UTR_variant	MODIFIER	40.5	cyclophilin family peptidyl-prolyl cis-trans isomerase Cyp3
II	1104941	1104941	TTT	cyp3	5_prime_UTR_variant	MODIFIER	40.5	cyclophilin family peptidyl-prolyl cis-trans isomerase Cyp3
II	3984130	3984130	T	ste11	5_prime_UTR_variant	MODIFIER	40.5	transcription factor Ste11
II	962880	962880	G	ecl2	5_prime_UTR_variant	MODIFIER	40.5	extender of chronological lifespan protein Ecl2
III	253907	253907	T	SPCC794.16	frameshift_variant	HIGH	40.5	
I	3074001	3074001	T	otu1	missense_variant	MODERATE	35.7	ubiquitin-specific cysteine protease, OTU family, Otu1
I	4599222	4599222	A	tea5	missense_variant	MODERATE	35.7	pseudokinase Tea5
I	637916	637916	A	oct1	missense_variant	MODERATE	35.7	mitochondrial intermediate peptidase Oct1 (predicted)
I	3591910	3591910	T	SPAC17G6.03	5_prime_UTR_variant	MODIFIER	31	extracellular 5'-nucleotidase, human NT5E family (predicted)
II	1170025	1170025	T	SPBC409.17c	synonymous_variant	LOW	31	DUF1769 family protein
I	3342712	3342712	T	chc1	missense_variant	MODERATE	28.6	clathrin heavy chain Chc1 (predicted)
I	4822619	4822619	A	hus1	5_prime_UTR_variant	MODIFIER	26.2	checkpoint clamp complex protein Hus1
II	428123	428123	A	brc1	missense_variant	MODERATE	26.2	BRCT domain protein Brc1

D

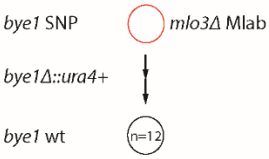

E

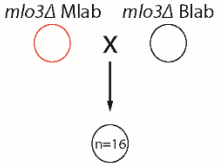

F

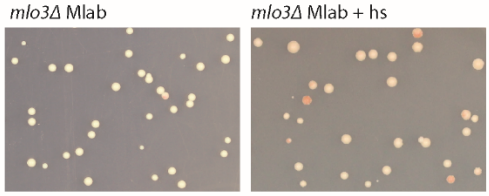

Figure 12. bye1 SNP highly correlates with inheritance of the ade6+ silencing phenotype. *(A) Table with observed silencing initiation and maintenance in wild type cells (*) is given for several different stains, created either in the Moazed or Buehler lab (source). 'Yes' signifies that at least one of >1000 colonies showed a silencing phenotype on YE plates, 'No' that all assessed colonies (>1000) were phenotypically white and 'n.d.' stands for not determined. Four strains of the genotype mlo3Δ::kan ade6+ cen::ade6 were independently created in the Buehler lab and none of the resulting colonies (n = 4079, 7840, 1970, 4310) displayed a silencing phenotype. (B) Crossing scheme to determine co-segregation of SNP with the ade6+ silencing phenotype. Silenced mlo3Δ Mlab colonies (red fill, n = 3) were twice outcrossed with an original wild-type strain (white circle). (C) Table with the frequency (%) of each detected SNPs (> 25%) in F2 colonies (mlo3+ cen+, n = 42), which could maintain the silencing phenotype during the outcrossing. The bye1 3'-UTR SNP highly correlated with the silencing phenotype (37/42 colonies). (D) Reversion of the bye1 SNP to bye1 wild-type (wt) in the mlo3Δ Mlab strain leads to loss of silencing initiation in all analyzed transformants (n = 12, for each >1000 plated colonies). Reversion of the SNP was achieved by replacing bye1+ 3'-UTR SNP with ura4+, followed by seamless reintegration of bye1+ 3'-UTR wt. (E) No descendants of mlo3Δ Mlab cells crossed with mlo3Δ Blab cells could induce silencing (white circle). At least 1000 colonies per descendant were assessed for the silencing phenotype. 33% of descendants (n =21) carried the bye1+ 3'-UTR SNP. (F) Images of mlo3Δ Mlab colonies and mlo3Δ Mlab colonies with a preceding three day heat shock at 37°C (hs). Both strains were grown on YE plates at 30°C.*

3. A fully automated deep learning pipeline for high-throughput colony segmentation and classification

Sarah H. Carl, Lea Duempelmann, Yukiko Shimada and Marc Bühler

The entire article can be found in the appendix section.

Summary

Adenine auxotrophy is commonly used by yeast researchers as a non-selective color readout for many different biological processes, such as recombination, chromosome loss and epigenetic gene regulation. For my main project alone (Duempelmann et al., 2019), we had to manually classify the phenotype of around 100'000 colonies, which was very time-consuming. Therefore, we developed a fully automated, high-throughput pipeline that can segment colonies and classify them as white or non-white. This pipeline consists of neural networks and has two steps. First, the segmentation task is performed with a U-net-like architecture, trained with full plate images and their corresponding Ilastik-generated masks, which contain positional information of the colonies. Second, classification is done with a Resnet-34 architecture, trained on individually cropped colony images. The pipeline predicts the number and phenotype of colonies from whole plate images with high validation accuracy (98.6%) and little deviation (0.26 - 5.1%) to previously manually classified colonies (Duempelmann et al., 2019). Furthermore, the pipeline increases reproducibility between different researchers and computer monitors and speeds up colony classification by 80-100x.

My contributions

Because I strongly felt that the time-consuming and tedious task of manually counting thousands of colonies could be optimized, I proposed to use neural networks to automate this process. I trained the program Ilastik for the prediction of colony positions within a plate image. Those predictions were used to train the U-net-like architecture for the segmentation of colonies. Furthermore, with combination of the Ilastik predictions and a Matlab script I generated hundreds of individually cropped colony images, which Yukiko Shimada classified. Based on those training datasets, our bioinformatician Sarah Carl successfully trained and tested the neural networks, wrote all scripts and compared automatic versus manual colony classification.

4. Review: Small RNAs in the transgenerational inheritance of epigenetic information

Lea Duempelmann*, Merle Skribbe* and Marc Bühler (*equal contribution)

The entire article can be found in the appendix section.

Summary

Small RNAs can induce chromatin changes that can persist over many generations in a truly epigenetic fashion through self-reinforcing feedback loops. In our review we focused on the nuclear small RNA-directed gene silencing pathways in *S. pombe*, *C. elegans* and *A. thaliana*. Amongst the substantial mechanistic differences, we particularly highlighted the general conserved key features. Those include nascent transcript binding of Argonaute by its associated siRNA and amplification of secondary siRNA through RNA-dependent RNA polymerases. In most organisms, induction of protein-coding gene repression with siRNAs has been challenging. In *S. pombe*, several transcription-associated factors were found to counteract RNAe. We discussed two non-mutually exclusive models on how mutation of such counteracting factors could enable RNAi-mediated ectopic heterochromatin formation. Once RNAi-mediated silencing has been initiated, it can occasionally be propagated over many generations. Various factors have been identified to be required for the inheritance of the repressed state, and few to counteract a potentially infinite silencing response. Transgenerational inheritance of RNAi-mediated silencing is mostly concurrent with H3K9me3 at the target locus. We also discussed the role of this histone mark in gene silencing and RNAe. Recent reports suggest that RNAe can also be triggered environmentally, with potential physiological roles in adaptation. We summaries those studies and propose a conceptual model for adaptation of populations with different strategies to a dynamic environment.

My contributions

This review was written in a very stimulating and gratifying teamwork together with Merle Skribbe and Marc Bühler. I wrote the last three chapters and Box, and made the final Figures in Illustrator.

DISCUSSION & OUTLOOK

Organisms constantly have to adapt to their changing environment and are often exposed to different sources of stress, sometimes over multiple generations. Therefore, inheritance of a beneficial epigenetic variation could potentially prepare progeny to cope with similar stressors, thereby possibly increasing their fitness. Especially small organisms with a short generation time could benefit from such adaptation. Nucleic acid induced RNAe can persist over tens of generations and there has been rapid progress in understanding the mechanisms for its propagation, mainly in *C. elegans*. Emerging evidence suggests that RNAe could not only be induced artificially, but also by environmental triggers. Whether this phenomenon is of any physiological relevance in heritable adaptation is controversial though.

For my PhD, I chose to study epigenetic phenomena in *S. pombe*, due to the extensively studied nuclear RNAi-silencing pathways. In this organism, RNAi-mediated induction of facultative heterochromatin is under strong negative control and can only be induced in the presence of an enabling mutation (Kowalik et al., 2015). Also, it was not known if RNAi-mediated epimutations could be maintained in wild-type yeast when I started my PhD. Therefore, my main achievement was to discover that RNAi-dependent H3K9me3 at an ectopic locus can be inherited in wild-type cells as phenotypically neutral epimutation. Upon modulation of the Paf1C, silencing can be reinstated. This phenomenon of phenotypic plastic epimutations could potentially have interesting implications in adaptation.

At the beginning of this discussion, I will introduce a conceptual framework for the adaptation to a dynamic environment and potential benefits of phenotypically neutral epimutations. Next, I will summarize reports that imply a potential physiological role of RNAe, found almost exclusively in *C. elegans*. Furthermore, I will discuss our efforts in finding compounds and conditions that would enable RNAi-mediated silencing and thereby phenotypic plastic epimutations in wild-type *S. pombe* cells. I will also deliberate on the phenotypic differences of the si3-mark in different backgrounds. Lastly, I will discuss the role of H3K9 tri-methylation in RNAe and show preliminary results on the potentially conserved role of Paf1C in transcription through H3K9me3.

1. Conceptual Framework of Adaptation to a Dynamic Environment

The fitness of a population in a dynamic environment strongly depends on the ability of individuals to adapt to the new condition as well as to remember, inherit, and forget such adaptation (Rechavi and Lev, 2017; van Boxtel et al., 2017). In this conceptual model, we compare the fitness of populations that adapt with different survival strategies: mutations, epimutations, or phenotypically plastic epimutations. For simplicity, we presume a dynamic environment consisting of two alternating states (Figure 13) where the transition between states creates a bottleneck. Consequently, individuals adapted to one state require mutations or epimutations to adapt to and propagate in the other state.

Individuals of a population can adapt by acquiring beneficial **mutations** (Figure 13A), leading to changes in protein function or gene expression (e.g. Calo et al., 2014). Such mutations mainly occur randomly and often affect only one gene directly. Exceptions might be operons or mutations in promoters/enhancers that drive expression of multiple genes. Adaptive mutations must originate in the germline to be inherited, and have full penetrance, once homozygous. Consequently, mutations beneficial in the red environment cannot be lost, and re-adaptation through another mutation is required should the environment change back to blue. However, the probability of a mutated gene regaining its original function/expression is low, leading to loss of the mal-adaptable population.

In contrast, **epimutations** (Figure 13B) tend to occur in hot spots, e.g. in stress-related or nutritional pathway genes, (Rechavi et al., 2014; Zheng et al., 2017), and can potentially silence several homologous genes simultaneously (Chang et al., 2019). As small RNAs from the soma can be amplified in the germline (Posner et al., 2019), and epimutations can be paramutagenic (Sapetschnig et al., 2015), they can increase the population fitness faster than a recessive mutation. Incomplete penetrance of a beneficial epimutation by stochastic loss of siRNAs (Houri-Ze'evi et al., 2016) can result in loss of adaptation in a given environment (red state), but can be beneficial if the previous blue state is re-established. Consequently, the population can quickly revive to full density. However, when the environment changes back to the red state, epimutations must initiate *de novo*, at the same low frequency as when the population first encountered this state.

This is different for populations that can maintain a small RNA-mediated memory of previously beneficial silencing events, without displaying the repressed state itself. This phenomenon, termed **phenotypically neutral epimutation** (Figure 13C), allows high-frequency re-establishment of the

epimutant phenotype in a pedigree founded by ancestors that have acquired the respective epimutation (Duempelmann et al., 2019). Consequently, individuals that adapt through epimutations and maintain the memory in a phenotypically neutral state, are predicted to have the greatest fitness advantages in a dynamic environment.

Thus, transient phenotypic plasticity through small RNA-mediated epigenetic mechanisms can provide the ideal strategy for adaptation over multiple generations in a dynamic environment, especially for organisms with short generation times. (Duempelmann et al., 2020).

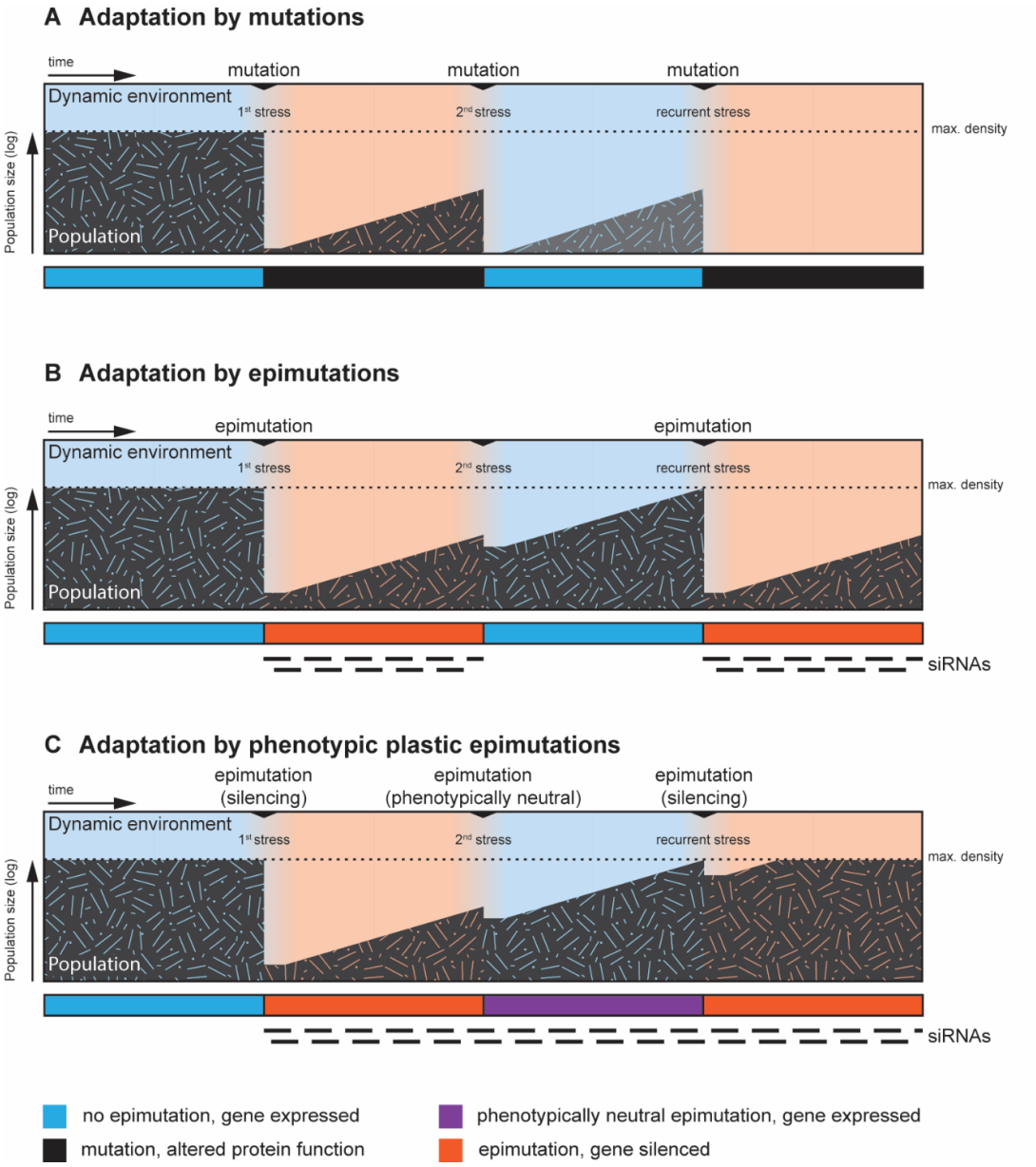

Figure 13. Population Adaptation Strategies to a Dynamic Two-State (Blue and Red) Environment. *(A) A well-adapted population (grey) is at its maximal density (dotted line) in a given niche until an environmental change (1st stress) creates a bottleneck. Only few individuals can adapt through mutations and repopulate the niche. After the environment changes back to the initial blue state, only individuals that acquire rare counteracting mutations survive, often leading to extinction of the population. (B) Individuals of a population in the red state can gain beneficial epimutations through siRNAs and repopulate the niche. When exposed again to the blue state, the epimutations can be quickly reversed and the population rapidly reaches maximal density. After recurrence of the red state, organisms establish de novo epimutations with the same low frequency as when they first encountered this state. (C) In contrast, organisms that can maintain the memory of a beneficial silencing event can quickly reestablish beneficial epimutations and grow to full density. Such memory can be maintained by phenotypically neutral epimutations, marked by the continuously high production of siRNAs without substantial reductions in the expression of a gene. Thus, a population that can adapt through phenotypically plastic epimutations is predicted to have a maximal fitness advantage in a dynamic environment. Figure re-used with permission from Duempelmann et al., 2020.*

This chapter is adapted with permission from L. Duempelmann, M. Skribbe and M. Bühler; Small RNAs in the transgenerational inheritance of epigenetic information. Trends in Genetics (2020).

2. Potential physiological role of RNAe

Insights into potential physiological roles of RNAe are only just emerging, even though substantial progress has been made in studying targeted RNAe responses triggered experimentally with nucleic acid (see INTRODUCTION chapter 5). Recent studies in *C. elegans* suggest that RNAe may facilitate sensing and reacting to a dynamic environment, potentially allowing adaptation to harsh conditions and transmitting the acquired epigenetic changes in gene expression to subsequent generations.

2.1. Starvation

Starvation was reported to induce expression of endogenous small RNAs that can potentially repress genes linked to nutrition. Because some small RNAs were still present in subsequent generations (F2/3) grown in nutritionally rich conditions, it is possible these animals might have inherited information on how to cope with starvation. Indeed, the F3 progeny of starved ancestors had a significantly increased life span and were more resistant to starvation (Rechavi et al., 2014). Inheritance of most starvation induced small RNAs depends on HRDE-1, suggesting that the memory of starvation is inherited through RNAi.
These worms also had an increased resistance to heat stress, suggesting that starvation might lead to epigenetic inheritance of general stress resistance (Jobson et al., 2015). However, the mechanism of cross-stress resistance and the functional relationship between the inherited small RNAs and lifespan requires further study (Jobson et al., 2015; Rechavi et al., 2014).

2.2. Heat stress

Temperature has been shown to change the abundance of small RNA populations, resulting in gene expression changes that lasted for several generations, independent of the temperature that triggered the change (Klosin et al., 2017; Ni et al., 2016; Schott et al., 2014). Heat stress in *hrde-1* mutant animals resulted in the up-regulation of a large number of genes (>280). In wild-type worms these genes are H3K9 methylated and produce abundant HRDE-1-associated siRNAs, suggesting that RNAe can also act to dampen heat-induced transcriptional gene activation (Ni et al., 2016).

2.3. Learned behavior

Recently, small RNAs have even been implicated in the heritability of learned behavior in *C. elegans* (Moore et al., 2019; Posner et al., 2019) (Figure 14). In its natural habitat, *C. elegans* is surrounded by nutritious, but also pathogenic food sources, which can drastically reduce its life span. Worms learn within hours to avoid virulent bacteria. Descendants (F4) inheriting the avoidance behavior escape faster from the same pathogen and thereby have significantly increased lifespan and an adaptive survival advantage. This heritable behavior was found to depend on the expression change of the neuronal expressed, HRDE-1-targeted gene *daf-7*. It also required nuclear RNAi factors (*mut-7*, *rrf-1*, *set-25* and *hpl-2*), as well as the germline expressed PRG-1 (Moore et al., 2019). Another study found RNAe induced by neuronal endo-siRNAs to be important for chemotaxis (Posner et al., 2019). Those findings suggest that learned behavior is inherited by RNAe, and that RNAe is involved in adaptive responses in nematodes.

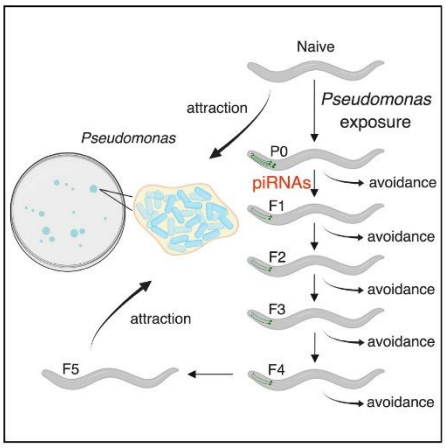

Figure 14. Inheritance of avoidance behavior in C. elegans. *Worms can learn to avoid pathogenic food sources and inherit such behavior over four generations, thereby increasing the fitness of offspring.*

R. S. Moore, R. Kaletsky, C. T. Murphy, Piwi/PRG-1 Argonaute and TGF-b Mediate Transgenerational Learned Pathogenic Avoidance, Cell 177, 1827–1841, © (2019), with permission from Elsevier

Interestingly, avoidance training of pathogenic Pseudomonas also causes worms to avoid non-pathogenic Pseudomonas, which could otherwise serve as adequate nutrition. The authors therefore speculate that forgetting the learned avoidance behavior after a few generations might be beneficial for worms, since this puts the non-pathogenic Pseudomonas back on their menu, thereby increasing the food sources. Transgenerational epigenetic inheritance of specific pathogen avoidance can therefore provide an ideal survival strategy for short-lived organisms and their progeny in a dynamic environment (Moore et al., 2019). However, while epigenetic variation can respond to the environment, it is far from clear whether this has any real-world impact on adaptive fitness. (Adapted from Duempelmann et al., 2020)

2.4. RNAi-mediated drug resistance

In contrast to *C. elegans*, evidence for RNAe-related phenomena in other animals is scarce and we thus should be cautious about inferring RNAe is a widely conserved phenomenon. Even if not widely conserved, current literature suggests that a thorough understanding of RNAe may be of significant biomedical relevance. *Mucor circinelloides* is one of the major agents of mucormycosis, a deadly fungal infection. Mucor can acquire resistance against antifungal agents either through mutation, or by small RNA-mediated epigenetic silencing of the gene, called epimutations, that encodes the respective drug target (Figure 13, Calo et al., 2014; Chang et al., 2019). Upon several passages of growth in drug-free medium, previously drug-resistant epimutants lose their endogenous small RNAs, restore target gene mRNA levels, and revert to being drug-sensitive, similar to the parental wild-type. It remains to be tested whether drug resistance is stable through meiosis. The acquisition rate of small RNA-induced epimutations in wild-type Mucor (20-30%) can be enhanced to 80-100% by impairing the other RNAi-related pathways of Mucor (Calo et al., 2017; Calo et al., 2014), reminiscent of enhanced RNAi in *C. elegans* (Houri-Ze'evi et al., 2016; Lev et al., 2017). Virulent isolates of Mucor from human and other mammals have an enhanced ability to develop drug resistance through epimutations (76-96%) (Calo et al., 2017). It seems worth exploring if the resistance of those Mucor isolates is higher because of acquired genetic mutations in its other RNAi-related pathways or by RNAe-enabling mutations such as those described in *S. pombe*.

In *S. pombe*, the mechanism that evolved to maintain heterochromatin at the centromeres differs from other eukaryotes with a similar centromere architecture. This raises the intriguing idea, that RNAi-mediated silencing might also serve additional purposes, such as in adaptation. That *S. pombe* can gain drug resistance through epimutations, as shown for Mucor, has so far only been reported once (Torres-Garcia et al., 2019) and whether the underlying mechanism is RNAi-mediated remains to be elucidated. It is of great interest to find out if *S. pombe* can adapt to stressors by its well-studied RNAi pathway. As a first step, we tried to discover compounds and conditions that would enable RNAi-mediated silencing of strains that already express a synthetic source of siRNAs against a euchromatic locus, which will be discussed in the next chapter.

3. Can certain conditions stimulate wild-type *S. pombe* for RNAi-mediated silencing?

As described above, recent studies suggest that RNAe can be induced by environmental triggers in *C. elegans*, potentially preparing progeny to cope with similar conditions. Furthermore, the fungus *Mucor* can acquire drug resistance through RNAi-dependent epimutations. In *S. pombe*, RNAi-mediated silencing is under strict negative control and could only be induced stably and heritably after mutation of counteracting factors (Kowalik et al., 2015; Yu et al., 2018). Such mutations can have a detrimental effect on viability (Duempelmann et al., 2019; Kowalik et al., 2015). We speculated that the standard lab conditions did not provide the adequate environment, but different stress conditions or compounds might enable RNAi-mediated silencing, potentially resulting in beneficial epimutations that increase survival under stress.

In Paf1C mutants, sporadic siRNA peaks occur at several loci (Duempelmann et al., 2019). My dear colleague Daniele Oberti observed a siRNA peak over *sty1+* in a *paf1-Q264Stop* colony (Duempelmann et al., 2019). Sty1 is part of the MAPK pathway, involved in multiple stress responses such as heavy metal toxicity, osmotic stress, nutrient limitation, oxidative stress and high temperature. Mutation of *sty1+* results in, amongst others, Cobalt Chloride ($CoCl_2$)-resistance (Ryuko et al., 2012). We were curious to find out if *S. pombe* could establish $CoCl_2$-resistance through RNAi-mediated silencing without enabling mutations. Daniele and I exposed an *ade6-hp* expressing strain to $CoCl_2$ (5-7mM) and isolated 49 $CoCl_2$-resistant colonies that simultaneously also silenced *ade6+* (Figure 15A). In half of the analyzed colonies (5/10), the $CoCl_2$ resistance depends on *ago1+*, *dcr1+* and *clr4+*, and showed phenotypic plasticity (Figure 15B and 15C). Unfortunately, each isolated strain had on average 35 SNPs, making it impossible to assert a purely RNAi-dependent nature of $CoCl_2$-resistance without enabling mutations.

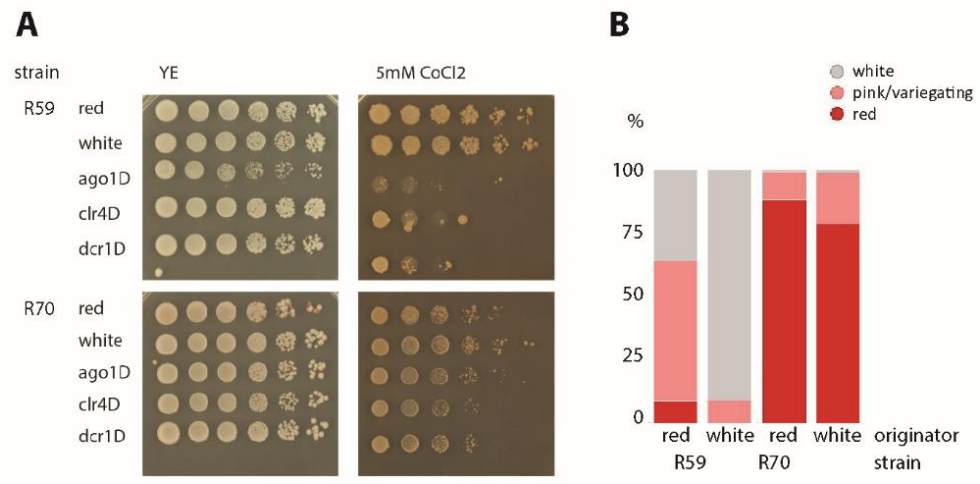

Figure 15. RNAi-mediated CoCl2 resistance. *(**A**) CoCl2 resistance depends in 5 of 10 strains on the RNAi (ago1+, dcr1+) and H3K9me (clr4+), as visible in the spotting assay for strain R59, but not for R70. (**B**) ade6+ silencing only of RNAi-mediated CoCl2 resistant colonies is phenotypic plastic.*

The fungus Mucor can gain resistance to the antifungal agent 5-fluoroorotic acid (5-FOA) by RNAi-mediated epimutations and downregulation of two enzymes in the uracil biosynthetic pathway (Chang et al., 2019). The homologous *S. pombe* proteins Ura4 and Ura5 also convert 5-FOA, which is structurally similar to a Uracil precursor, into a toxic compound (Bach, 1987; Boeke et al., 1987; Mudge et al., 2012). Under exposure to 5-FOA, cells can only grow upon mutation or silencing of *ura4+* or *ura5+* (Mudge et al., 2012). We found that a strain, producing siRNAs from a hairpin against *ura4+*, can form 5-FOA resistant colonies, however closer analysis of 30 colonies revealed that resistance was not RNAi-mediated (not shown). We hypothesized that additional natural compounds, which are encountered by yeast in its natural habitat, might be necessary to enable RNAi-mediated silencing. In collaboration with Novartis, we exposed an *ura4*-siRNA producing strain to 15'000 natural compounds and assessed growth under 5-FOA exposure (Figure 16). Additionally, in order to increase drug sensitivity, we deleted in the screening cell line a transcription factor for drug efflux pumps (Prt1) and an ABC transporter (Brf1) (Kawashima et al., 2012). Of the 323 hits, 73 responded in an *ago1+* and dose-dependent growth. However, this dose-dependent growth could not be consistently reproduced. Furthermore, exposure of *ade6*-siRNA producing cells to the 73 hit compounds did not induce silencing of *ade6+*. In conclusion, so far I have not found natural compounds that stimulated *S. pombe* to silence a target gene, even in the presence of artificially provided siRNAs.

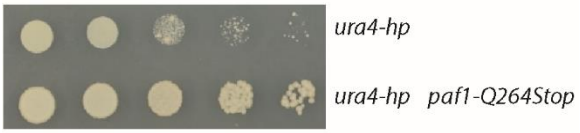

Figure 16. Screening window for the natural compound screen. *Silencing assay performed with the screening cell line (trp1+::ura4+ ura4-hp) and as control for maximal expected growth the screening cell line with paf1-Q264Stop.*

This might have several technical reasons. We might have not tested the optimal enabling concentration (Torres-Garcia et al., 2019). Another reasons could be that the subset of 15'000 compounds did not include the 'right' ones, despite covering a large range of chemical structures, or that the media and temperature might have not been adequate.

Conceptually, yeast would mainly benefit from epimutations to overcome temporal stress. Yet, frequent occurrence of sporadic epimutations could be detrimental, especially when essential genes would be targeted. Therefore, a natural compound that does not impose stress on yeast but constantly enables sporadic RNAi-mediated silencing would be disadvantageous, especially when yeast often encounters such a compound in its natural habitat. Therefore, such an adverse mechanism would be under strong negative selection. Instead, it would be much more beneficial if a stress condition itself or a *S. pombe* produced metabolite as response to stress could activate a pathway that enables RNAi-mediated silencing. To test additional stressors, I exposed a strain producing siRNAs against *ade6+* to different pHs, grew them at 16°C and under oxygen-poor conditions, and exposed this traditional brewing strain to different concentrations of EtOH. None of those conditions led to silencing of *ade6+*.

In a recent preprint, *S. pombe* was found to gain caffeine resistance through two different mechanisms, both without permanently changing the genome (Torres-Garcia et al., 2019). First, and similar to Mucor (Calo et al., 2014), genes were silenced through H3K9me-dependent epimutations, conferring caffeine resistance. Those ectopic heterochromatin domains are only detectable after caffeine treatment and concur with small RNA generation. The most frequently occurring domain was previously described as a heterochromatic 'island' (Zofall et al., 2012) and forms dynamically in response to different caffeine concentrations. Second, mini duplication and concomitant upregulation of a gene enhanced caffeine resistance, and could maintain it upon loss of heterochromatin. Interestingly, caffeine-resistant isolates also show cross-resistance to a fungicide. It will be challenging, but relevant to identify if more plant and human pathogenic fungi also gain anti-fungal resistance through epimutations, and if such resistant strains could alternatively be treated by blocking epimutation pathways (Torres-Garcia et al., 2019). Furthermore, it will be a very exciting task to find out if the caffeine induced epimutations (Torres-

Garcia et al., 2019) depend on RNAi. I observed a silencing phenotype in about half of the colonies from cells expressing an *ade6-hp* on caffeine plates (1, 5 and 10 mM) (Figure 17). It remains to be determined if facultative heterochromatin was successfully established and if this phenotype is RNAi-dependent. If so, caffeine would be such an external stimulus, which is what we were seeking in the Novartis natural compound screen.

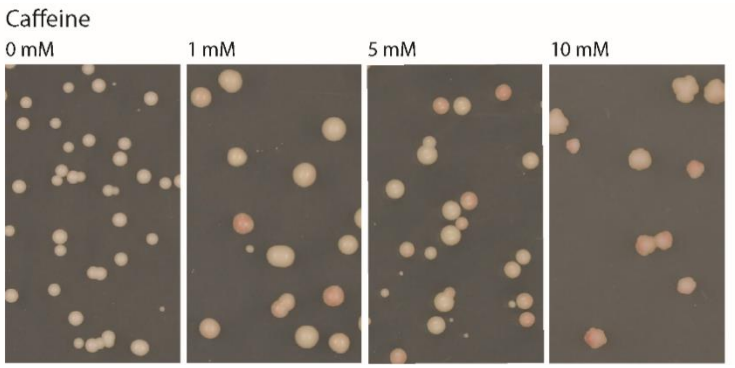

Figure 17. Caffeine induces an ade6+ silencing phenotype. *An ade6-hp expressing strain frequently forms pink/red colonies at different caffeine concentrations (1, 5, 10 mM) but not on control YE plates.*

If caffeine could indeed enable RNAi-mediated silencing, it would be of immense interest to discover by which mechanism, for example by activation of a general stress pathway that could also be stimulated by other stress conditions or stress-imposing compounds. It also remains to be determined if caffeine resistance is heritable over multiple generations, such as RNAe. We discovered phenotypic plastic epimutations upon genetic modulation of the Paf1C (Duempelmann et al., 2020). Based on that finding, I would predict that modulation through a compound of Paf1C activity or another repressor of RNAi-mediated silencing would enables both acquisition and inheritance of phenotypically plastic epimutations. It remains to be tested if such phenomena can be evoked by addition and removal of caffeine.

4. Induction and duration of RNAi-mediated silencing

Despite the adaptive advantages RNAe of endogenous genes could potentially yield, its directed induction by dsRNA has been inherently difficult. In *C. elegans*, heritable silencing was successfully established in only 13 of 171 targeted endogenous genes, and in *S. pombe* a sensitized background is required for induction of RNAe (Kowalik et al., 2015; Vastenhouw et al., 2006). However, a low induction frequency of silencing can be beneficial for an organism to prevent detrimental silencing of essential genes. Mechanisms evolved that counteract silencing of euchromatic regions (Flury et al., 2017; Houri-Ze'evi et al., 2016; Kowalik et al., 2015; Pisacane and Halic, 2017; Spracklin et al., 2017). Spontaneous silencing under stress or in a sensitized background often happens in hot spots, suggesting that different gene properties facilitate silencing. Those were suggested to include anti-sense transcription, convergent gene expression, specific expression ranges and homologies to frequently silenced loci or pseudogenes. Such a facilitated silencing of e.g. genes in stress or nutrition pathways might have evolved to enable a faster response to frequently encountered stress (Leung et al., 2016; Rechavi et al., 2014; Zheng et al., 2017). Several sporadic siRNA peaks, often in hotspots, also appear in *S. pombe* Paf1C mutants. So far, we could not determine any common features which would facilitate ectopic heterochromatin formation at these loci. Thus, it will be an important future task to identify more hot spots of silencing, perhaps in enhanced RNAi-backgrounds, and thereby uncover currently unidentified features of loci that can be heritably silenced.

Once established, silencing can be inherited for multiple generations by feedback loops that continuously amplify small RNAs and could in principle lead to an infinite silencing response. However, inheritance of adaptation to stress is only beneficial, as long as the progeny is still exposed to the same stress. The duration of epigenetic inherited silencing is typically lost after few generations. Recently, new mechanisms were discovered that modify and limit the duration of RNAe (Houri-Ze'evi et al., 2016; Spracklin et al., 2017). Also, RNAe is typically inherited with less than 100% penetrance (Duempelmann et al., 2019; Moore et al., 2019; Vastenhouw et al., 2006). Thus, upon cessation of the stress, organisms have the ability to forget the adaptation (Moore et al., 2019). Alternatively, cells could also inherit phenotypically neutral epimutations with a very high penetrance, but only induce silencing under certain stress conditions (Duempelmann et al., 2019). It will be an exciting task to find stress conditions or compounds that enable *S. pombe* to initiate and transiently induce such silencing.

5. Phenotypic differences between si3-marked 'wild type' yeast

My experiments revealed that wild type descendants from epigenetically silenced *paf1-Q264Stop* parents lose the silencing phenotype, despite high levels of siRNAs and H3K9me3 (si3-mark) at the *ade6+* gene (Duempelmann et al., 2019). Silencing can be reinstated in later generations if Paf1C is impaired. Hence, the silencing phenotype strictly depends on the enabling *paf1-Q264Stop* mutation (Duempelmann et al., 2019; Kowalik et al., 2015). In contrast, Yu et al. reported stable inheritance of silencing, in the absence of the original siRNA source and enabling mutation (Yu et al., 2018). This heritability was found to depend on concurrent spreading of secondary siRNAs and H3K9me to neighboring areas of the target gene. Multigenerational inheritance is propagated by a positive-feedback loop coupling siRNA generation and H3K9 methylation, as in our study (Duempelmann et al., 2019; Yu et al., 2018). Furthermore, they reported a predominant *in cis* inheritance of silencing, different to the typically non-Mendelian inheritance of epigenetic phenomena and to our observations in Paf1C mutants (Duempelmann et al., 2019; Yu et al., 2018) (see INTRODUCTION chapter 1.3).

The difference in heritability of silencing in wild type cells was previously explained to result from the source of triggering siRNA (Yu et al., 2018). When silencing was induced in *leo1Δ* cells with a hairpin, no spreading of secondary small RNAs was observed (Yu et al., 2018) (Figure 17A). In contrast, when *cen::ade6* was used as silencing trigger, spreading extended to *ade6+* neighboring genes (Yu et al., 2018) (Figure 17A and 18C). Yu et al. speculated that only such an extensive heterochromatic domain could be inherited in wild-type cells, concurrent with the silencing phenotype. This explanation is unlikely to be the cause, since we observed equal spreading of facultative heterochromatin initiated with an *ade6-hp* in the *paf1-Q264Stop* background (Figure 17B). Additionally, spreading extended upstream of the *trp1* locus in some cases, whereas equal ratio of siRNAs and H3K9me3 chromatin immunoprecipitation sequencing (ChIP-seq) read counts covered the mutated endogenous and the functional trp1+::a*de6+* copies. Furthermore, silencing induced with *cen::ade6* in the *paf1-Q264Stop* background could not be phenotypically inherited to wild-type cells in our lab (Figure 17A).

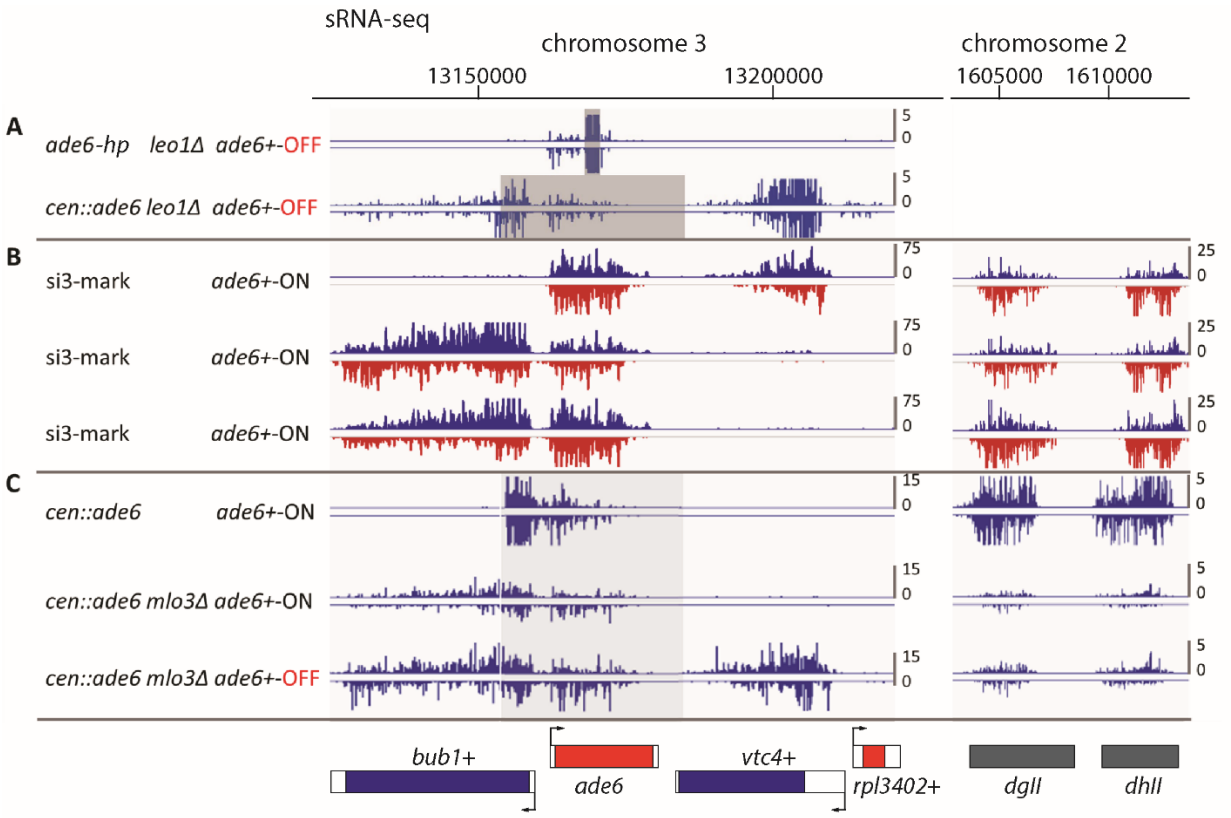

Figure 17. Spreading of small RNAs is independent of the silencing trigger. *(A) Secondary small RNA spreading in leo1Δ is limited when induced with ade6+ hairpin (HP) in comparison to extensive spreading in cen::ade6 cells (Yu et al., 2018). (B) Wild-type cells with the si3-mark show extensive small RNA spreading at neighboring genes of ade6+ (Buehler lab). (C) Secondary small RNAs are generated in cen::ade6 strains only in the presence of an enabling mutation, such as mlo3Δ, and also spread to neighboring genes (Yu et al., 2018).*

Inheritance of the silencing phenotype in wild-type cells (Yu et al., 2018) correlated with several SNPs (Figure 12). The top hit was a SNP in the UTR of *bye1+*, a predicted negative transcriptional regulator, leading to a threefold upregulation of expression. Reversion of the SNP to wild-type obscures silencing initiation of the *mlo3Δ* Mlab strain (Figure 12).

S. pombe Bye1 is a nuclear protein (Matsuyama et al., 2006), and is annotated with a PHD zinc-finger (Plant HomeoDomain), a central TFIIS (Transcription elongation factor S-II) and SPOC (Spen Paralogue and Orthologue C-terminal) domain (Howe et al., 2020; UniProt, 2019). To my knowledge, there are no reports on *bye1+* in *S. pombe*, other than in listings of whole genome and -omics data without follow-up (e.g. Kettenbach et al., 2015; Roguev et al., 2008).

In *S. cerevisiae*, BYE1 was originally discovered as negative elongation factor of RNA Pol II transcription (Wu et al., 2003; Wu et al., 2000). BYE1 binds to the beginning of active genes through high affinity to H3K4me3, typically enriched at promoters, and to early RNA Pol II elongation complexes with its TFIIS domain (Kinkelin et al., 2013). Consistent with its role as a negative transcriptional regulator, deletion of *bye1+* leads to a global increase of RNA Pol II density throughout gene bodies, as well as decreased RNA Pol II density near the promoter (Harlen and Churchman, 2017). Unlike the transcription elongation factor TFIIS, BYE1 does not alter the confirmation or *in vitro* functions of RNA Pol II (Kinkelin et al., 2013). Since BYE1 and TFIIS bind to the same domain of RNA Pol II, elevated expression of BYE1 might outcompete and sterically inhibit binding of TFIIS, thereby reducing RNA Pol II transcription and additionally sequester RNA Pol II at H3K4 methylated promoter regions. Furthermore, Paf1C binding to RNA Pol II is stimulated by the elongation factor TFIIS, but unlikely to be stimulated by BYE1 (Kim et al., 2010; Xu et al., 2017). Thus, elevated expression of the negative transcription regulator Bye1, resulting from the UTR SNP, could enable RNAi-mediated silencing of actively transcribed genes. To test this, *bye1+* could be overexpressed in cells that produce siRNAs against *ade6+*. RNAi-dependent facultative heterochromatin formation at the *ade6+* locus and downregulation of *ade6+* mRNA would reveal that elevated levels of Bye1 is sufficient to enable RNAi-mediated silencing of transcribed genes. If this is not the case, Bye1 could still play a role in maintenance, rather than initiation of silencing. Therefore, I would suggest to cross epigenetically silenced Paf1C mutant cells to cells that contain *Pnmt1::bye1+* and are otherwise wild-type (analogous to Figure 2A in Duempelmann et al., 2019). Thiamine represses the *nmt1* promoter activity and thereby *bye1+* expression. After plating the cross on low adenine PMG plates with different concentrations of thiamine, the phenotype of si3-marked *Pnmt1::bye1+ paf1+* cells can be assessed. Silencing of si3-marked cells only at low thiamine concentrations would imply that high expression of Bye1 can maintain RNAi-mediated silencing in the absence of an enabling mutation or additional siRNA source against the target gene. Interestingly, the *bye1+* 3'-UTR SNP is only 60 kb upstream of *ade6+*, potentially explaining the Mendelian *in cis* inheritance. It is surprising that a RNA Pol II binding protein and potential modulator of transcription received so little attention in the past. Independent of the results from the suggested experiments, Bye1 seems to be an interesting candidate to follow up on to improve our understanding of gene expression regulation in *S. pombe*.

The PHD domains of the BYE1 homologs in *Drosophila* (PPS) and human (DIDO) bind H3K4me3 in a pH dependent manner, potentially providing a mechanism for environmental regulation (Tencer et al., 2017). This behavior is lost in *S. cerevisiae* (Tencer et al., 2017) and exposure of an *ade6-hp* expressing *S. pombe* strain to different pHs did not lead to silencing initiation (see DISCUSSION chapter 3). The conservation

from human to yeast is low (8% pairwise AA identity) and the critical residue becoming positively charged upon pH change is not conserved (PPS H919, Tencer et al., 2017). Therefore, it is unlikely that a change in pH would increase *S. pombe* Bye1 PHD binding affinity to H3K4me3 in the same manner as other organisms and enable RNAi-mediated silencing in an environment dependent fashion. However, Bye1 was a hit in several phospho screens. It is completely unknown how phosphorylation of Bye1 is mediated and regulated, and it is also unknown if and how phosphorylation impacts Bye1's function as transcription regulator. It will be a very interesting future task to discover the functions of Bye1 in transcription and determine modes of regulation of this protein.

Even though silencing initiation is lost in the *mlo3Δ* Mlab strain upon reversion of the SNP to wild-type 3'-UTR, *bye1+* SNP is not sufficient to enable silencing initiation of *cen::ade6 mlo3Δ::kan ade6+* cells with other backgrounds (Figure 12). Therefore, either a combination of multiple SNPs (Roguev et al., 2008), or additional unidentified factors are required for silencing initiation in *cen::ade6 mlo3Δ* cells, and potentially also for the Mendelian inheritance in *cen+ mlo3+* cells. The different silencing phenotype of the strains that both contain high levels of H3K9me3 and siRNAs (Duempelmann et al., 2019; Yu et al., 2018) might provide a great opportunity to study such additional factors.

6. The role of H3K9me3 in RNAe

In S*. pombe*, H3K9me is indespensible for RNAe and strictly required for a targeted amplification of siRNAs (Kowalik et al., 2015; Yu et al., 2018). Until recently, small RNA-directed H3K9me3 deposition had always been associated with persistent gene silencing (Holoch and Moazed, 2015a; Rechavi and Lev, 2017). Whether mechanisms exist that allow transgenerational inheritance of H3K9me3 without the associated repressed state, as a form of "silencing memory", was unknown. I showed that H3K9me3 functions as a stable epigenetic mark, but is not repressive *per se*, and can retain information of a previous gene-silencing event. Upon deposition of H3K9me3, the silencing phenotype is dependent on the modulation of Paf1C function (Duempelmann et al., 2019).

The Paf1C is thought to regulate RNA Pol II transcription and facilitates elongation through several interactions (see INTRODUCTION chapter 4.1.1). Paf1C physically and genetically interacts with the transcription elongation factors Spt4-Spt5/DSIF and Spt16-Pob3/FACT (Squazzo et al., 2002; Van Oss et al., 2017). Furthermore, Paf1C binds RNA Pol II cooperatively with the elongation factor TFIIS, globally facilitating transcription (Kim et al., 2010; Xu et al., 2017). During my PhD, I most commonly initiated silencing in a Paf1C mutant (*paf1-Q264Stop*) that truncates Paf1 by more than half (Kowalik et al., 2015). This could reduce or inhibit Paf1C stability and/or its interactions with the transcription elongation factors, leading to frequent stalling of RNA Pol II during transcription of H3K9 methylated genes. In wild-type cells, those factors could facilitate RNA Pol II transcription through si3-marked genes, observable as phenotypically neutral epimutation. An immunoprecipitation coupled to mass spectrometry (IP–MS) might give insights into the specific loss of interactions of Paf1-Q264Stop in comparison to Paf1 and could serve as starting point for further dissection of how a functional Paf1C facilitates transcription through H3K9me3 marked regions. This observation gives rise to the idea that H3K9me3 is only repressive under specific conditions in fission yeast.

Consistent with such a model, the peculiar transcription factor Moonshiner enables transcription within the heterochromatic, H3K9me3-enriched piRNA clusters in *Drosophila* (Andersen et al., 2017). Furthermore, transposons can become expressed upon changes in chromatin accessibility, without a reduction in H3K9me3 enrichment (Iwasaki et al., 2016). For some fly genes H3K9 methylation is even a pre-requisite for efficient expression (Schultz, 1936; Yasuhara and Wakimoto, 2006). Transcription of

H3K9 methylated protein-coding genes has also been observed in mammalian cells. The KRAB zinc finger protein ZNF274 was shown to mediate H3K9me3 deposition on the expressed and highly homologous zinc finger genes, supposedly to counteract homologous recombination (Frietze et al., 2010; Vakoc et al., 2005; Vogel et al., 2006). It is not known if Paf1C also facilitates transcription of H3K9me3 methylated regions in mammals, as we observed in yeast (Duempelmann et al., 2019).

7. Is the role of Paf1C in transcription through H3K9me3 marked loci conserved?

We found Paf1C to promote RNA Pol II transcription through an H3K9me3 marked locus in yeast. In the absence of functional Paf1C, RNA Pol II accumulates at the 5' gene end and co-transcriptional H3K36me3 levels are reduced, probably due to frequent stalling of RNA Pol II (Duempelmann et al., 2019). Akin, Paf1C was recently shown to mediate transcription of toxic disease-associated repeat expansions in *Drosophila*. Those GC-rich repeats likely reduce RNA Pol II transcription by forming secondary structures, and they are only transcribed efficiently in the presence of a functional Paf1C (Goodman et al., 2019). It is unknown whether or not the function of Paf1C in promoting RNA Pol II transcription through hard to transcribe regions is conserved in mammals.

Anelya Rankova, a former PhD student in our lab, had performed an RNA-seq time course experiment in which she conditionally knocked out (cKO) the Paf1C subunit *Leo1* in mouse embryonic stem cells (Figure 18A). I analyzed her data and found that differentially expressed genes that overlapped with an H3K9me3 peak had on average an increased expression 8 days after *Leo1* cKO in comparison to not H3K9me3 enriched genes (Figure 18B). This is consistent with the hypothesis that Paf1C is required for transcription of H3K9me3 marked genes. However, the enrichment level of H3K9me3 anti-correlated with increase of expression (not shown). During the time course, the RNA level of the differentially expressed, H3K9me3 enriched genes increases in half of the genes, whereas the other genes showed decreased expression (Figure 18C). The difference of expression between those two groups cannot be explained by the position of H3K9me3 peak overlap (Figure 18C, side annotation). Furthermore, neither peak strength (qvalue) nor location within and in proximity of each gene correlated with the expression change at any measured time point. We hypothesized that H3K27me3, another common repressive mark in mammals, but absent in *S. pombe*, might correlate with gene expression changes. This seemed not to be the case. Conditional deletion of the *Paf1*, *Ctr9*, or *Ski8* genes in mESCs also did not result in reduced RNA expression of genes with enriched levels of H3K9me3.

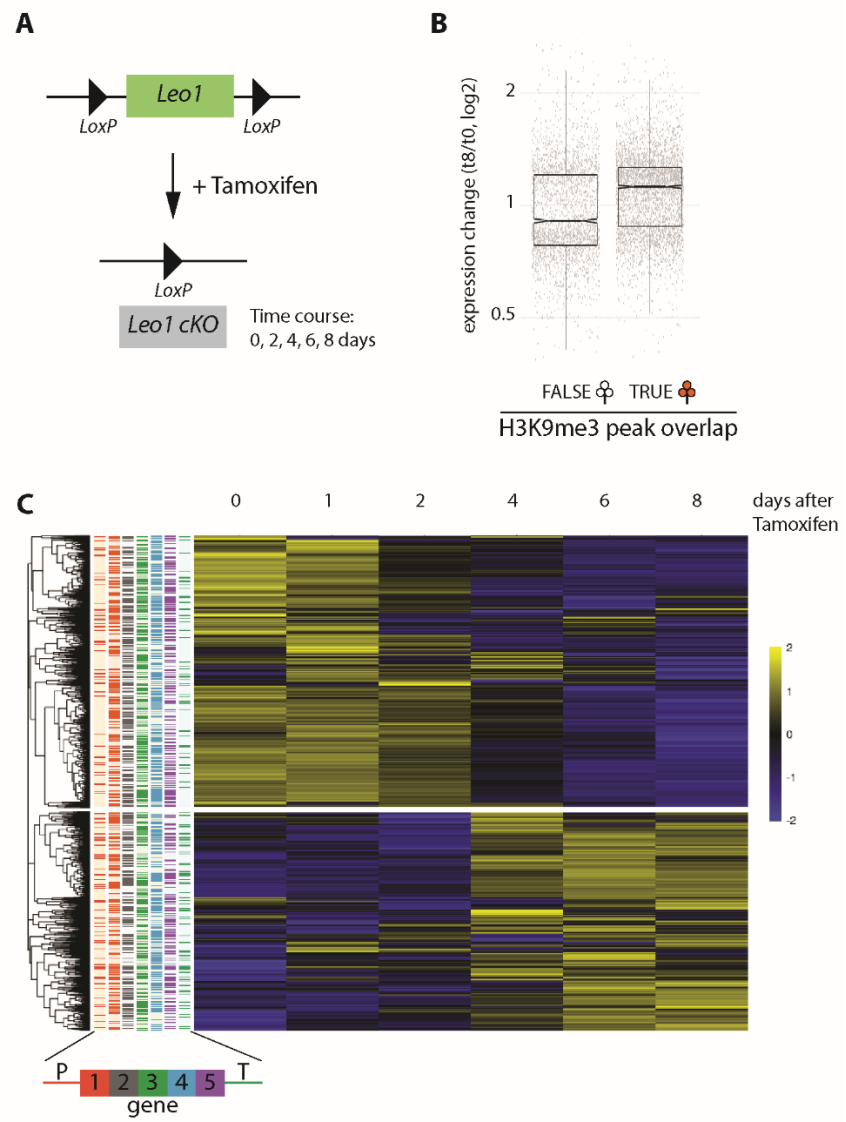

Figure 18. Conditional knockout of Leo1 in mouse ESCs leads to many expression changes. *(A) Leo1 is flanked by LoxP sites, that upon addition of tamoxifen recombine, leading to a conditional Leo1 knockout (Leo1 cKO). (B) Box plot of expression change between day 8 and day 0 after tamoxifen treatment. The genes are divided according to their overlap with an H3K9me3 peak. (C) Heatmap of all differentially expressed genes that overlap with an H3K9me3 peak. The side annotation marks the position of overlap with each gene. Therefore, each gene was divided into 5 equal parts (1-5). P stands for promoter (2000 base pairs upstream of the transcription start site) and T for terminator (2000 base pairs downstream of the transcription stop site).*

Based on this preliminary analysis, I suggest to repeat such experiments with more replicates, H3K9me3 ChIP-seq at each time point and native elongating transcript-Sequencing (NET-Seq) instead of RNA-seq for a more direct readout of transcription. This I expect to reveal whether the function of Paf1C in facilitating transcription through H3K9me3 enriched loci is conserved in mammalian cells.

ACKNOWLEDGEMENTS

First and foremost, I would like to express my gratitude to my PhD advisor Marc Bühler for giving me the opportunity to do my PhD in his lab, his great scientific guidance and that I could work on so many exciting projects over the years. Thanks a lot for regularly discussing my progress during group meetings, for providing valuable feedback and at the same time giving me the freedom to also pursue own ideas. I am very grateful that I could seek support when needed and Marc always made time to talk, his shared enthusiasm for science and input throughout my PhD. I also very much appreciate Marc always being so incredibly fast with corrections, giving helpful advice on manuscripts and for proofreading my thesis. A huge thanks also to Daniele Oberti, who gave me such a wonderful start into my PhD, for sharing his passion for science, love for *S. pombe* and getting me started in the lab. Without all the inspiring discussions and shared curiosity with Marc and Daniele, the projects I finally pursued might have never started. Also a huge thanks to Xian for the interesting and inspiring science lunch discussions that motivated me throughout my PhD and his universal advice. A big thanks also to Vincent Colot and Helge Grosshans for investing their time to being on my PhD thesis committee, and for their valuable advice and input during our meetings. Thanks also to Antoine Peters for chairing my PhD defense.

I could have never worked so efficiently on the projects without Yukiko's and Motty's great organization of the lab and databases, and advice from Yukiko on yeast experiments. Without their valuable support, my PhD would have taken at least twice as long;) どうもありがとうございました!! A big thanks also to Sarah Carl for successfully establishing the classification pipeline, which gave me terrible headaches for more than a year, and for saving the Blab yeasties and researchers around the globe many hours of colony counting. It was wonderful working together! As I joined the Blab, I was a complete novice to shell scripting and R. Throughout my PhD I learned a lot from Fabio, Michi and Alex and am very grateful for their advice, support and efficient solutions, which saved me from spending a lot of time on Stack Overflow. Furthermore, I never expected that writing a review could be so much fun and want to give a huge thanks to Merle for all the fun discussions about (obscure) papers from tomato to sparrow, and also on projects, random ideas and art pieces :) A big thanks also to Aude for having been a great student and supporting me during the end phase of my main project. And a big thanks the terrific mentorship of Woltjen-sensei, having saved me a lot of experimental time. Furthermore, I am grateful to my Novartis collaborators for sharing compounds and giving me advice on screen performance and analysis, and to Katrin Volkmann also for advice and analysis of the screening data. A huge thanks also to all the Buehler lab members who made working in the lab fun and were always willing to help and share. Furthermore, all my projects wouldn't have been possible without the support of the great FMI facilities.

My deepest gratitude to Kieran, my family and friends for their endless love, support and fun times.

REFERENCES

Adelman, K., Wei, W., Ardehali, M.B., Werner, J., Zhu, B., Reinberg, D., and Lis, J.T. (2006). Drosophila Paf1 modulates chromatin structure at actively transcribed genes. Mol Cell Biol *26*, 250-260.
Andersen, P.R., Tirian, L., Vunjak, M., and Brennecke, J. (2017). A heterochromatin-dependent transcription machinery drives piRNA expression. Nature *549*, 54-59.
Arteaga-Vazquez, M.A., and Chandler, V.L. (2010). Paramutation in maize: RNA mediated trans-generational gene silencing. Curr Opin Genet Dev *20*, 156-163.
Ashe, A., Sapetschnig, A., Weick, E.M., Mitchell, J., Bagijn, M.P., Cording, A.C., Doebley, A.L., Goldstein, L.D., Lehrbach, N.J., Le Pen, J*., et al.* (2012). PiRNAs can trigger a multigenerational epigenetic memory in the germline of C. elegans. Cell *150*, 88-99.
Bach, M.L. (1987). Cloning and Expression of the Omp Decarboxylase Gene Ura4 from Schizosaccharomyces-Pombe. Curr Genet *12*, 527-534.
Bagijn, M.P., Goldstein, L.D., Sapetschnig, A., Weick, E.M., Bouasker, S., Lehrbach, N.J., Simard, M.J., and Miska, E.A. (2012). Function, targets, and evolution of Caenorhabditis elegans piRNAs. Science *337*, 574-578.
Bannister, A.J., Zegerman, P., Partridge, J.F., Miska, E.A., Thomas, J.O., Allshire, R.C., and Kouzarides, T. (2001). Selective recognition of methylated lysine 9 on histone H3 by the HP1 chromo domain. Nature *410*, 120-124.
Bayne, E.H., White, S.A., Kagansky, A., Bijos, D.A., Sanchez-Pulido, L., Hoe, K.-L., Kim, D.-U., Park, H.-O., Ponting, C.P., Rappsilber, J*., et al.* (2010). Stc1: A Critical Link between RNAi and Chromatin Modification Required for Heterochromatin Integrity. Cell *140*, 666-677.
Bernstein, E., Caudy, A.A., Hammond, S.M., and Hannon, G.J. (2001). Role for a bidentate ribonuclease in the initiation step of RNA interference. Nature *409*, 363-366.
Bertozzi, T.M., and Ferguson-Smith, A.C. (2020). Metastable epialleles and their contribution to epigenetic inheritance in mammals. Semin Cell Dev Biol *97*, 93-105.
Bies-Etheve, N., Pontier, D., Lahmy, S., Picart, C., Vega, D., Cooke, R., and Lagrange, T. (2009). RNA-directed DNA methylation requires an AGO4-interacting member of the SPT5 elongation factor family. EMBO Rep *10*, 649-654.
Boeke, J.D., Trueheart, J., Natsoulis, G., and Fink, G.R. (1987). 5-Fluoroorotic Acid as a Selective Agent in Yeast Molecular-Genetics. Method Enzymol *154*, 164-175.
Buchwalter, A., Kaneshiro, J.M., and Hetzer, M.W. (2019). Coaching from the sidelines: the nuclear periphery in genome regulation. Nat Rev Genet *20*, 39-50.
Buckley, B.A., Burkhart, K.B., Gu, S.G., Spracklin, G., Kershner, A., Fritz, H., Kimble, J., Fire, A., and Kennedy, S. (2012). A nuclear Argonaute promotes multigenerational epigenetic inheritance and germline immortality. Nature *489*, 447-451.
Buehler, M., Haas, W., Gygi, S.P., and Moazed, D. (2007). RNAi-dependent and -independent RNA turnover mechanisms contribute to heterochromatic gene silencing. Cell *129*, 707-721.
Buhler, M., and Gasser, S.M. (2009). Silent chromatin at the middle and ends: lessons from yeasts. EMBO J *28*, 2149-2161.
Buhler, M., Spies, N., Bartel, D.P., and Moazed, D. (2008). TRAMP-mediated RNA surveillance prevents spurious entry of RNAs into the Schizosaccharomyces pombe siRNA pathway. Nat Struct Mol Biol *15*, 1015-1023.
Buhler, M., Verdel, A., and Moazed, D. (2006). Tethering RITS to a nascent transcript initiates RNAi- and heterochromatin-dependent gene silencing. Cell *125*, 873-886.
Buker, S.M., Iida, T., Buhler, M., Villen, J., Gygi, S.P., Nakayama, J., and Moazed, D. (2007). Two different Argonaute complexes are required for siRNA generation and heterochromatin assembly in fission yeast. Nat Struct Mol Biol *14*, 200-207.

Burkhart, K.B., Guang, S., Buckley, B.A., Wong, L., Bochner, A.F., and Kennedy, S. (2011). A Pre-mRNA-Associating Factor Links Endogenous siRNAs to Chromatin Regulation. Plos Genetics *7*.
Calo, S., Nicolas, F.E., Lee, S.C., Vila, A., Cervantes, M., Torres-Martinez, S., Ruiz-Vazquez, R.M., Cardenas, M.E., and Heitman, J. (2017). A non-canonical RNA degradation pathway suppresses RNAi-dependent epimutations in the human fungal pathogen Mucor circinelloides. PLoS Genet *13*, e1006686.
Calo, S., Shertz-Wall, C., Lee, S.C., Bastidas, R.J., Nicolas, F.E., Granek, J.A., Mieczkowski, P., Torres-Martinez, S., Ruiz-Vazquez, R.M., Cardenas, M.E*., et al.* (2014). Antifungal drug resistance evoked via RNAi-dependent epimutations. Nature *513*, 555-558.
Cam, H.P., Sugiyama, T., Chen, E.S., Chen, X., FitzGerald, P.C., and Grewal, S.I. (2005). Comprehensive analysis of heterochromatin- and RNAi-mediated epigenetic control of the fission yeast genome. Nat Genet *37*, 809-819.
Canzio, D., Chang, E.Y., Shankar, S., Kuchenbecker, K.M., Simon, M.D., Madhani, H.D., Narlikar, G.J., and Al-Sady, B. (2011). Chromodomain-mediated oligomerization of HP1 suggests a nucleosome-bridging mechanism for heterochromatin assembly. Mol Cell *41*, 67-81.
Capella, M., and Braun, S. (2019). Neutral epigenetic inheritance: being prepared for future generations. Nat Struct Mol Biol *26*, 391-392.
Chandler, V.L. (2007). Paramutation: from maize to mice. Cell *128*, 641-645.
Chandler, V.L. (2010). Paramutation's properties and puzzles. Science *330*, 628-629.
Chang, Z., Billmyre, R.B., Lee, S.C., and Heitman, J. (2019). Broad antifungal resistance mediated by RNAi-dependent epimutation in the basal human fungal pathogen Mucor circinelloides. PLoS Genet *15*, e1007957.
Chen, Y., Yamaguchi, Y., Tsugeno, Y., Yamamoto, J., Yamada, T., Nakamura, M., Hisatake, K., and Handa, H. (2009). DSIF, the Paf1 complex, and Tat-SF1 have nonredundant, cooperative roles in RNA polymerase II elongation. Genes & Development *23*, 2765-2777.
Cheutin, T., Gorski, S.A., May, K.M., Singh, P.B., and Misteli, T. (2004). In vivo dynamics of Swi6 in yeast: evidence for a stochastic model of heterochromatin. Mol Cell Biol *24*, 3157-3167.
Chow, J.C., Ciaudo, C., Fazzari, M.J., Mise, N., Servant, N., Glass, J.L., Attreed, M., Avner, P., Wutz, A., Barillot, E*., et al.* (2010). LINE-1 activity in facultative heterochromatin formation during X chromosome inactivation. Cell *141*, 956-969.
Chu, Y., Simic, R., Warner, M.H., Arndt, K.M., and Prelich, G. (2007). Regulation of histone modification and cryptic transcription by the Bur1 and Paf1 complexes. Embo Journal *26*, 4646-4656.
Clark, J.P., Rahman, R., Yang, N., Yang, L.H., and Lau, N.C. (2017). Drosophila PAF1 Modulates PIWI/piRNA Silencing Capacity. Curr Biol *27*, 2718-2726 e2714.
Coe, E.H. (1959). A regular and continuing conversion-type phenomenon at the B locus in maize. Proc Natl Acad Sci U S A *45:828-832*.
Colmenares, S.U., Buker, S.M., Buhler, M., Dlakic, M., and Moazed, D. (2007). Coupling of double-stranded RNA synthesis and siRNA generation in fission yeast RNAi. Mol Cell *27*, 449-461.
Colome-Tatche, M., Cortijo, S., Wardenaar, R., Morgado, L., Lahouze, B., Sarazin, A., Etcheverry, M., Martin, A., Feng, S., Duvernois-Berthet, E*., et al.* (2012). Features of the Arabidopsis recombination landscape resulting from the combined loss of sequence variation and DNA methylation. Proc Natl Acad Sci U S A *109*, 16240-16245.
Cortijo, S., Wardenaar, R., Colome-Tatche, M., Gilly, A., Etcheverry, M., Labadie, K., Caillieux, E., Hospital, F., Aury, J.M., Wincker, P*., et al.* (2014). Mapping the epigenetic basis of complex traits. Science *343*, 1145-1148.
Croce, C.M., and Calin, G.A. (2005). miRNAs, cancer, and stem cell division. Cell *122*, 6-7.
Cropley, J.E., Suter, C.M., Beckman, K.B., and Martin, D.I. (2006). Germ-line epigenetic modification of the murine A vy allele by nutritional supplementation. Proc Natl Acad Sci U S A *103*, 17308-17312.
Dahm, R. (2005). Friedrich Miescher and the discovery of DNA. Dev Biol *278*, 274-288.

Dalmay, T., Hamilton, A., Rudd, S., Angell, S., and Baulcombe, D.C. (2000). An RNA-Dependent RNA polymerase gene in Arabidopsis is required for posttranscriptional gene silencing mediated by a transgene but not by a virus. Cell *101*, 543-553.
Daxinger, L., and Whitelaw, E. (2012). Understanding transgenerational epigenetic inheritance via the gametes in mammals. Nat Rev Genet *13*, 153-162.
Debeauchamp, J.L., Moses, A., Noffsinger, V.J., Ulrich, D.L., Job, G., Kosinski, A.M., and Partridge, J.F. (2008). Chp1-Tas3 interaction is required to recruit RITS to fission yeast centromeres and for maintenance of centromeric heterochromatin. Mol Cell Biol *28*, 2154-2166.
Dermody, J.L., and Buratowski, S. (2010). Leo1 subunit of the yeast paf1 complex binds RNA and contributes to complex recruitment. J Biol Chem *285*, 33671-33679.
Duchaine, T.F., Wohlschlegel, J.A., Kennedy, S., Bei, Y., Conte, D., Jr., Pang, K., Brownell, D.R., Harding, S., Mitani, S., Ruvkun, G.*, et al.* (2006). Functional proteomics reveals the biochemical niche of C. elegans DCR-1 in multiple small-RNA-mediated pathways. Cell *124*, 343-354.
Duempelmann, L., Mohn, F., Shimada, Y., Oberti, D., Andriollo, A., Lochs, S., and Buhler, M. (2019). Inheritance of a Phenotypically Neutral Epimutation Evokes Gene Silencing in Later Generations. Mol Cell.
Duempelmann, L., Skribbe, M., and Buhler, M. (2020). Small RNAs in the Transgenerational Inheritance of Epigenetic Information. Trends Genet.
Duhl, D.M., Vrieling, H., Miller, K.A., Wolff, G.L., and Barsh, G.S. (1994). Neomorphic agouti mutations in obese yellow mice. Nat Genet *8*, 59-65.
Festenstein, R., Pagakis, S.N., Hiragami, K., Lyon, D., Verreault, A., Sekkali, B., and Kioussis, D. (2003). Modulation of heterochromatin protein 1 dynamics in primary Mammalian cells. Science *299*, 719-721.
Fire, A., Xu, S., Montgomery, M.K., Kostas, S.A., Driver, S.E., and Mello, C.C. (1998). Potent and specific genetic interference by double-stranded RNA in Caenorhabditis elegans. Nature *391*, 806-811.
Flury, V., Georgescu, P.R., Iesmantavicius, V., Shimada, Y., Kuzdere, T., Braun, S., and Buhler, M. (2017). The Histone Acetyltransferase Mst2 Protects Active Chromatin from Epigenetic Silencing by Acetylating the Ubiquitin Ligase Brl1. Mol Cell *67*, 294-307 e299.
Formosa, T. (2012). The role of FACT in making and breaking nucleosomes. Biochimica Et Biophysica Acta-Gene Regulatory Mechanisms *1819*, 247-255.
Frietze, S., O'Geen, H., Blahnik, K.R., Jin, V.X., and Farnham, P.J. (2010). ZNF274 recruits the histone methyltransferase SETDB1 to the 3' ends of ZNF genes. PLoS One *5*, e15082.
Goodman, L.D., Prudencio, M., Kramer, N.J., Martinez-Ramirez, L.F., Srinivasan, A.R., Lan, M., Parisi, M.J., Zhu, Y., Chew, J., Cook, C.N.*, et al.* (2019). Toxic expanded GGGGCC repeat transcription is mediated by the PAF1 complex in C9orf72-associated FTD. Nat Neurosci *22*, 863-874.
Greer, E.L., and Shi, Y. (2012). Histone methylation: a dynamic mark in health, disease and inheritance. Nat Rev Genet *13*, 343-357.
Grewal, S.I., and Jia, S. (2007). Heterochromatin revisited. Nat Rev Genet *8*, 35-46.
Grewal, S.I., and Moazed, D. (2003). Heterochromatin and epigenetic control of gene expression. Science *301*, 798-802.
Grewal, S.I.S., and Klar, A.J.S. (1997). A Recombinationally Repressed Region Between mat2 and mat3 Loci Shares Homology to Centromeric Repeats and Regulates Directionality of Mating-Type Switching in Fission Yeast. Genetics *146*, 1221.
Guang, S., Bochner, A.F., Burkhart, K.B., Burton, N., Pavelec, D.M., and Kennedy, S. (2010). Small regulatory RNAs inhibit RNA polymerase II during the elongation phase of transcription. Nature *465*, 1097-1101.
Guang, S., Bochner, A.F., Pavelec, D.M., Burkhart, K.B., Harding, S., Lachowiec, J., and Kennedy, S. (2008). An Argonaute transports siRNAs from the cytoplasm to the nucleus. Science *321*, 537-541.

Haag, J.R., Ream, T.S., Marasco, M., Nicora, C.D., Norbeck, A.D., Pasa-Tolic, L., and Pikaard, C.S. (2012). In Vitro Transcription Activities of Pol IV, Pol V, and RDR2 Reveal Coupling of Pol IV and RDR2 for dsRNA Synthesis in Plant RNA Silencing. Molecular Cell *48*, 811-818.
Halfmann, R., and Lindquist, S. (2010). Epigenetics in the extreme: prions and the inheritance of environmentally acquired traits. Science *330*, 629-632.
Halic, M., and Moazed, D. (2010). Dicer-independent primal RNAs trigger RNAi and heterochromatin formation. Cell *140*, 504-516.
Hall, I.M., Shankaranarayana, G.D., Noma, K., Ayoub, N., Cohen, A., and Grewal, S.I. (2002). Establishment and maintenance of a heterochromatin domain. Science *297*, 2232-2237.
Hamilton, A.J., and Baulcombe, D.C. (1999). A species of small antisense RNA in posttranscriptional gene silencing in plants. Science *286*, 950-952.
Hammond, S.M., Bernstein, E., Beach, D., and Hannon, G.J. (2000). An RNA-directed nuclease mediates post-transcriptional gene silencing in Drosophila cells. Nature *404*, 293-296.
Harlen, K.M., and Churchman, L.S. (2017). Subgenic Pol II interactomes identify region-specific transcription elongation regulators. Mol Syst Biol *13*, 900.
Hayashi, A., Ishida, M., Kawaguchi, R., Urano, T., Murakami, Y., and Nakayama, J.-i. (2012). Heterochromatin protein 1 homologue Swi6 acts in concert with Ers1 to regulate RNAi-directed heterochromatin assembly. Proceedings of the National Academy of Sciences of the United States of America *109*, 6159-6164.
He, X.J., Hsu, Y.F., Zhu, S., Wierzbicki, A.T., Pontes, O., Pikaard, C.S., Liu, H.L., Wang, C.S., Jin, H., and Zhu, J.K. (2009). An effector of RNA-directed DNA methylation in arabidopsis is an ARGONAUTE 4- and RNA-binding protein. Cell *137*, 498-508.
Heard, E., and Martienssen, R.A. (2014). Transgenerational epigenetic inheritance: myths and mechanisms. Cell *157*, 95-109.
Henderson, I.R., and Jacobsen, S.E. (2007). Epigenetic inheritance in plants. Nature *447*, 418-424.
Henry, D. (2006). Aristotle on the Mechanism of Inheritance. Journal of the History of Biology *39*, 425-455.
Herr, A.J., Molnar, A., Jones, A., and Baulcombe, D.C. (2006). Defective RNA processing enhances RNA silencing and influences flowering of Arabidopsis. Proc Natl Acad Sci U S A *103*, 14994-15001.
Holla, S., Dhakshnamoorthy, J., Folco, H.D., Balachandran, V., Xiao, H., Sun, L.L., Wheeler, D., Zofall, M., and Grewal, S.I.S. (2020). Positioning Heterochromatin at the Nuclear Periphery Suppresses Histone Turnover to Promote Epigenetic Inheritance. Cell *180*, 150-164 e115.
Holoch, D., and Moazed, D. (2015a). RNA-mediated epigenetic regulation of gene expression. Nat Rev Genet *16*, 71-84.
Holoch, D., and Moazed, D. (2015b). Small-RNA loading licenses Argonaute for assembly into a transcriptional silencing complex. Nat Struct Mol Biol *22*, 328-335.
Horsthemke, B. (2018). A critical view on transgenerational epigenetic inheritance in humans. Nat Commun *9*, 2973.
Houri-Ze'evi, L., Korem, Y., Sheftel, H., Faigenbloom, L., Toker, I.A., Dagan, Y., Awad, L., Degani, L., Alon, U., and Rechavi, O. (2016). A Tunable Mechanism Determines the Duration of the Transgenerational Small RNA Inheritance in C. elegans. Cell *165*, 88-99.
Howe, K.L., Contreras-Moreira, B., De Silva, N., Maslen, G., Akanni, W., Allen, J., Alvarez-Jarreta, J., Barba, M., Bolser, D.M., Cambell, L*., et al.* (2020). Ensembl Genomes 2020-enabling non-vertebrate genomic research. Nucleic Acids Res *48*, D689-D695.
Iglesias, N., Currie, M.A., Jih, G., Paulo, J.A., Siuti, N., Kalocsay, M., Gygi, S.P., and Moazed, D. (2018). Automethylation-induced conformational switch in Clr4 (Suv39h) maintains epigenetic stability. Nature *560*, 504-508.

Iida, T., Nakayama, J., and Moazed, D. (2008). siRNA-mediated heterochromatin establishment requires HP1 and is associated with antisense transcription. Mol Cell *31*, 178-189.
Irvine, D.V., Zaratiegui, M., Tolia, N.H., Goto, D.B., Chitwood, D.H., Vaughn, M.W., Joshua-Tor, L., and Martienssen, R.A. (2006). Argonaute slicing is required for heterochromatic silencing and spreading. Science *313*, 1134-1137.
Iwasaki, Y.W., Murano, K., Ishizu, H., Shibuya, A., Iyoda, Y., Siomi, M.C., Siomi, H., and Saito, K. (2016). Piwi Modulates Chromatin Accessibility by Regulating Multiple Factors Including Histone H1 to Repress Transposons. Mol Cell *63*, 408-419.
Jansen, A., and Verstrepen, K.J. (2011). Nucleosome positioning in Saccharomyces cerevisiae. Microbiol Mol Biol Rev *75*, 301-320.
Jia, S., Noma, K., and Grewal, S.I. (2004). RNAi-independent heterochromatin nucleation by the stress-activated ATF/CREB family proteins. Science *304*, 1971-1976.
Jih, G., Iglesias, N., Currie, M.A., Bhanu, N.V., Paulo, J.A., Gygi, S.P., Garcia, B.A., and Moazed, D. (2017). Unique roles for histone H3K9me states in RNAi and heritable silencing of transcription. Nature *547*, 463-467.
Job, G., Brugger, C., Xu, T., Lowe, B.R., Pfister, Y., Qu, C.X., Shanker, S., Sanz, J.I.B., Partridge, J.F., and Schalch, T. (2016). SHREC Silences Heterochromatin via Distinct Remodeling and Deacetylation Modules. Molecular Cell *62*, 207-221.
Jobson, M.A., Jordan, J.M., Sandrof, M.A., Hibshman, J.D., Lennox, A.L., and Baugh, L.R. (2015). Transgenerational Effects of Early Life Starvation on Growth, Reproduction, and Stress Resistance in Caenorhabditis elegans. Genetics *201*, 201-+.
Johannes, F., Porcher, E., Teixeira, F.K., Saliba-Colombani, V., Simon, M., Agier, N., Bulski, A., Albuisson, J., Heredia, F., Audigier, P*., et al.* (2009). Assessing the Impact of Transgenerational Epigenetic Variation on Complex Traits. PLOS Genetics *5*, e1000530.
Kalinava, N., Ni, J.Z., Peterman, K., Chen, E., and Gu, S.G. (2017). Decoupling the downstream effects of germline nuclear RNAi reveals that H3K9me3 is dispensable for heritable RNAi and the maintenance of endogenous siRNA-mediated transcriptional silencing in Caenorhabditis elegans. Epigenetics Chromatin *10*, 6.
Kanoh, J., Sadaie, M., Urano, T., and Ishikawa, F. (2005). Telomere binding protein Taz1 establishes Swi6 heterochromatin independently of RNAi at telomeres. Curr Biol *15*, 1808-1819.
Kawashima, S.A., Takemoto, A., Nurse, P., and Kapoor, T.M. (2012). Analyzing fission yeast multidrug resistance mechanisms to develop a genetically tractable model system for chemical biology. Chem Biol *19*, 893-901.
Kazachenka, A., Bertozzi, T.M., Sjoberg-Herrera, M.K., Walker, N., Gardner, J., Gunning, R., Pahita, E., Adams, S., Adams, D., and Ferguson-Smith, A.C. (2018). Identification, Characterization, and Heritability of Murine Metastable Epialleles: Implications for Non-genetic Inheritance. Cell *175*, 1259-1271.e1213.
Keller, C., Adaixo, R., Stunnenberg, R., Woolcock, K.J., Hiller, S., and Buhler, M. (2012). HP1(Swi6) mediates the recognition and destruction of heterochromatic RNA transcripts. Mol Cell *47*, 215-227.
Kim, H.S., Choi, E.S., Shin, J.A., Jang, Y.K., and Park, S.D. (2004). Regulation of Swi6/HP1-dependent heterochromatin assembly by cooperation of components of the mitogen-activated protein kinase pathway and a histone deacetylase Clr6. J Biol Chem *279*, 42850-42859.
Kim, J., Guermah, M., and Roeder, R.G. (2010). The Human PAF1 Complex Acts in Chromatin Transcription Elongation Both Independently and Cooperatively with SII/TFIIS. Cell *140*, 491-503.
Kinkelin, K., Wozniak, G.G., Rothbart, S.B., Lidschreiber, M., Strahl, B.D., and Cramer, P. (2013). Structures of RNA polymerase II complexes with Bye1, a chromatin-binding PHF3/DIDO homologue. Proc Natl Acad Sci U S A *110*, 15277-15282.
Klosin, A., Casas, E., Hidalgo-Carcedo, C., Vavouri, T., and Lehner, B. (2017). Transgenerational transmission of environmental information in C. elegans. Science *356*, 320-323.

Koch, C., Wollmann, P., Dahl, M., and Lottspeich, F. (1999). A role for Ctr9p and Paf1p in the regulation G(1) cyclin expression in yeast. Nucleic Acids Research *27*, 2126-2134.
Kooke, R., Johannes, F., Wardenaar, R., Becker, F., Etcheverry, M., Colot, V., Vreugdenhil, D., and Keurentjes, J.J. (2015). Epigenetic basis of morphological variation and phenotypic plasticity in Arabidopsis thaliana. Plant Cell *27*, 337-348.
Kornberg, R.D., and Thomas, J.O. (1974). Chromatin structure; oligomers of the histones. Science *184*, 865-868.
Kowalik, K.M., Shimada, Y., Flury, V., Stadler, M.B., Batki, J., and Buhler, M. (2015). The Paf1 complex represses small-RNA-mediated epigenetic gene silencing. Nature *520*, 248-252.
Kubota, Y., Tsuyama, K., Takabayashi, Y., Haruta, N., Maruyama, R., Iida, N., and Sugimoto, A. (2014). The PAF1 complex is involved in embryonic epidermal morphogenesis in Caenorhabditis elegans. Dev Biol *391*, 43-53.
Law, J.A., and Jacobsen, S.E. (2010). Establishing, maintaining and modifying DNA methylation patterns in plants and animals. Nat Rev Genet *11*, 204-220.
Leung, C., Breton, S., and Angers, B. (2016). Facing environmental predictability with different sources of epigenetic variation. Ecology and evolution *6*, 5234-5245.
Lev, I., Seroussi, U., Gingold, H., Bril, R., Anava, S., and Rechavi, O. (2017). MET-2-Dependent H3K9 Methylation Suppresses Transgenerational Small RNA Inheritance. Curr Biol *27*, 1138-1147.
Li, H., Motamedi, M.R., Yip, C.K., Wang, Z., Walz, T., Patel, D.J., and Moazed, D. (2009). An alpha motif at Tas3 C terminus mediates RITS cis spreading and promotes heterochromatic gene silencing. Mol Cell *34*, 155-167.
Liegard, B., Baillet, V., Etcheverry, M., Joseph, E., Lariagon, C., Lemoine, J., Evrard, A., Colot, V., Gravot, A., Manzanares-Dauleux, M.J.*, et al.* (2019). Quantitative resistance to clubroot infection mediated by transgenerational epigenetic variation in Arabidopsis. New Phytol *222*, 468-479.
Liu, J., Carmell, M.A., Rivas, F.V., Marsden, C.G., Thomson, J.M., Song, J.J., Hammond, S.M., Joshua-Tor, L., and Hannon, G.J. (2004). Argonaute2 is the catalytic engine of mammalian RNAi. Science *305*, 1437-1441.
Liu, Y., and Chen, Q. (2018). 150 years of Darwin's theory of intercellular flow of hereditary information. Nature Reviews Molecular Cell Biology *19*, 749-750.
Lock, A., Rutherford, K., Harris, M.A., and Wood, V. (2018). PomBase: The Scientific Resource for Fission Yeast. Methods Mol Biol *1757*, 49-68.
Luger, K., Rechsteiner, T.J., Flaus, A.J., Waye, M.M., and Richmond, T.J. (1997). Characterization of nucleosome core particles containing histone proteins made in bacteria. J Mol Biol *272*, 301-311.
Luteijn, M.J., and Ketting, R.F. (2013). PIWI-interacting RNAs: From generation to transgenerational epigenetics. Nature Reviews Genetics *14*, 523-534.
Luteijn, M.J., van Bergeijk, P., Kaaij, L.J., Almeida, M.V., Roovers, E.F., Berezikov, E., and Ketting, R.F. (2012). Extremely stable Piwi-induced gene silencing in Caenorhabditis elegans. EMBO J *31*, 3422-3430.
Marasovic, M., Zocco, M., and Halic, M. (2013). Argonaute and Triman generate dicer-independent priRNAs and mature siRNAs to initiate heterochromatin formation. Mol Cell *52*, 173-183.
Martienssen, R., and Moazed, D. (2015). RNAi and heterochromatin assembly. Cold Spring Harb Perspect Biol *7*, a019323.
Matsuyama, A., Arai, R., Yashiroda, Y., Shirai, A., Kamata, A., Sekido, S., Kobayashi, Y., Hashimoto, A., Hamamoto, M., Hiraoka, Y.*, et al.* (2006). ORFeome cloning and global analysis of protein localization in the fission yeast Schizosaccharomyces pombe. Nat Biotechnol *24*, 841-847.
Matzke, M.A., and Mosher, R.A. (2014). RNA-directed DNA methylation: an epigenetic pathway of increasing complexity. Nature Reviews Genetics *15*, 394-408.

Mbogning, J., Nagy, S., Page, V., Schwer, B., Shuman, S., Fisher, R.P., and Tanny, J.C. (2013). The PAF Complex and Prf1/Rtf1 Delineate Distinct Cdk9-Dependent Pathways Regulating Transcription Elongation in Fission Yeast. Plos Genetics *9*.
Mette, M.F., van der Winden, J., Matzke, M.A., and Matzke, A.J.M. (1999). Production of aberrant promoter transcripts contributes to methylation and silencing of unlinked homologous promoters in trans. Embo Journal *18*, 241-248.
Minkina, O., and Hunter, C.P. (2017). Stable Heritable Germline Silencing Directs Somatic Silencing at an Endogenous Locus. Mol Cell *65*, 659-670 e655.
Minkina, O., and Hunter, C.P. (2018). Intergenerational Transmission of Gene Regulatory Information in Caenorhabditis elegans. Trends Genet *34*, 54-64.
Moore, R.S., Kaletsky, R., and Murphy, C.T. (2019). Piwi/PRG-1 Argonaute and TGF-beta Mediate Transgenerational Learned Pathogenic Avoidance. Cell *177*, 1827-1841 e1812.
Morgan, H.D., Sutherland, H.G., Martin, D.I., and Whitelaw, E. (1999). Epigenetic inheritance at the agouti locus in the mouse. Nat Genet *23*, 314-318.
Motamedi, M.R., Hong, E.J., Li, X., Gerber, S., Denison, C., Gygi, S., and Moazed, D. (2008). HP1 proteins form distinct complexes and mediate heterochromatic gene silencing by nonoverlapping mechanisms. Mol Cell *32*, 778-790.
Motamedi, M.R., Verdel, A., Colmenares, S.U., Gerber, S.A., Gygi, S.P., and Moazed, D. (2004). Two RNAi complexes, RITS and RDRC, physically interact and localize to noncoding centromeric RNAs. Cell *119*, 789-802.
Mudge, D.K., Hoffman, C.A., Lubinski, T.J., and Hoffman, C.S. (2012). Use of a ura5(+)-lys7(+) cassette to construct unmarked gene knock-ins in Schizosaccharomyces pombe. Curr Genet *58*, 59-64.
Mueller, C.L., and Jaehning, J.A. (2002). Ctr9, Rtf1, and Leo1 are components of the Paf1/RNA polymerase II complex. Molecular and Cellular Biology *22*, 1971-1980.
Nakayam, J., Rice, J.C., Strahl, B.D., Allis, C.D., and Grewal, S.I.S. (2001). Role of histone H3 lysine 9 methylation in epigenetic control of heterochromatin assembly. Science *292*, 110-113.
Nakayama, J., Rice, J.C., Strahl, B.D., Allis, C.D., and Grewal, S.I. (2001). Role of histone H3 lysine 9 methylation in epigenetic control of heterochromatin assembly. Science *292*, 110-113.
Napoli, C., Lemieux, C., and Jorgensen, R. (1990). Introduction of a Chimeric Chalcone Synthase Gene into Petunia Results in Reversible Co-Suppression of Homologous Genes in trans. Plant Cell *2*, 279-289.
Ni, J.Z., Kalinava, N., Chen, E., Huang, A., Trinh, T., and Gu, S.G. (2016). A transgenerational role of the germline nuclear RNAi pathway in repressing heat stress-induced transcriptional activation in C-elegans. Epigenetics & Chromatin *9*.
Nicoglou, A., and Wolfe, C.T. (2018). Introduction: sketches of a conceptual history of epigenesis. Hist Philos Life Sci *40*, 64.
Noble, D. (2015). Conrad Waddington and the origin of epigenetics. J Exp Biol *218*, 816-818.
Noma, K., Sugiyama, T., Cam, H., Verdel, A., Zofall, M., Jia, S., Moazed, D., and Grewal, S.I. (2004). RITS acts in cis to promote RNA interference-mediated transcriptional and post-transcriptional silencing. Nat Genet *36*, 1174-1180.
Nordick, K., Hoffman, M.G., Betz, J.L., and Jaehning, J.A. (2008). Direct interactions between the Paf1 complex and a cleavage and polyadenylation factor are revealed by dissociation of Paf1 from RNA polymerase II. Eukaryotic Cell *7*, 1158-1167.
Oberti, D., Biasini, A., Kirschmann, M.A., Genoud, C., Stunnenberg, R., Shimada, Y., and Buhler, M. (2015). Dicer and Hsp104 function in a negative feedback loop to confer robustness to environmental stress. Cell Rep *10*, 47-61.
Olins, A.L., and Olins, D.E. (1974). Spheroid chromatin units (v bodies). Science *183*, 330-332.

Painter, R.C., Osmond, C., Gluckman, P., Hanson, M., Phillips, D.I., and Roseboom, T.J. (2008). Transgenerational effects of prenatal exposure to the Dutch famine on neonatal adiposity and health in later life. BJOG *115*, 1243-1249.
Pak, J., and Fire, A. (2007). Distinct populations of primary and secondary effectors during RNAi in C-elegans. Science *315*, 241-244.
Partridge, J.F., Scott, K.S.C., Bannister, A.J., Kouzarides, T., and Allshire, R.C. (2002). cis-Acting DNA from Fission Yeast Centromeres Mediates Histone H3 Methylation and Recruitment of Silencing Factors and Cohesin to an Ectopic Site. Current Biology *12*, 1652-1660.
Penny, D. (2015). Epigenetics, Darwin, and Lamarck. Genome biology and evolution *7*, 1758-1760.
Perales, R., Pagano, D., Wan, G., Fields, B.D., Saltzman, A.L., and Kennedy, S.G. (2018). Transgenerational Epigenetic Inheritance Is Negatively Regulated by the HERI-1 Chromodomain Protein. Genetics *210*, 1287-1299.
Phillips, C.M., Montgomery, T.A., Breen, P.C., and Ruvkun, G. (2012). MUT-16 promotes formation of perinuclear mutator foci required for RNA silencing in the C. elegans germline. Genes Dev *26*, 1433-1444.
Pisacane, P., and Halic, M. (2017). Tailing and degradation of Argonaute-bound small RNAs protect the genome from uncontrolled RNAi. Nat Commun *8*, 15332.
Posner, R., Toker, I.A., Antonova, O., Star, E., Anava, S., Azmon, E., Hendricks, M., Bracha, S., Gingold, H., and Rechavi, O. (2019). Neuronal Small RNAs Control Behavior Transgenerationally. Cell *177*, 1814-1826 e1815.
Ptashne, M. (2007). On the use of the word 'epigenetic'. Curr Biol *17*, R233-236.
Ptashne, M. (2013). Epigenetics: core misconcept. Proc Natl Acad Sci U S A *110*, 7101-7103.
Rakyan, V.K., Chong, S., Champ, M.E., Cuthbert, P.C., Morgan, H.D., Luu, K.V., and Whitelaw, E. (2003). Transgenerational inheritance of epigenetic states at the murine Axin(Fu) allele occurs after maternal and paternal transmission. Proc Natl Acad Sci U S A *100*, 2538-2543.
Rechavi, O., Houri-Ze'evi, L., Anava, S., Goh, W.S.S., Kerk, S.Y., Hannon, G.J., and Hobert, O. (2014). Starvation-induced transgenerational inheritance of small RNAs in C. elegans. Cell *158*, 277-287.
Rechavi, O., and Lev, I. (2017). Principles of Transgenerational Small RNA Inheritance in Caenorhabditis elegans. Current Biology *27*, R720-R730.
Roguev, A., Bandyopadhyay, S., Zofall, M., Zhang, K., Fischer, T., Collins, S.R., Qu, H., Shales, M., Park, H.O., Hayles, J.*, et al.* (2008). Conservation and rewiring of functional modules revealed by an epistasis map in fission yeast. Science *322*, 405-410.
Rougemaille, M., Braun, S., Coyle, S., Dumesic, P.A., Garcia, J.F., Isaac, R.S., Libri, D., Narlikar, G.J., and Madhani, H.D. (2012). Ers1 links HP1 to RNAi. Proceedings of the National Academy of Sciences of the United States of America *109*, 11258-11263.
Ryuko, S., Ma, Y., Ma, N., Sakaue, M., and Kuno, T. (2012). Genome-wide screen reveals novel mechanisms for regulating cobalt uptake and detoxification in fission yeast. Mol Genet Genomics *287*, 651-662.
Sadaie, M., Iida, T., Urano, T., and Nakayama, J. (2004). A chromodomain protein, Chp1, is required for the establishment of heterochromatin in fission yeast. EMBO J *23*, 3825-3835.
Sadaie, M., Kawaguchi, R., Ohtani, Y., Arisaka, F., Tanaka, K., Shirahige, K., and Nakayama, J. (2008). Balance between distinct HP1 family proteins controls heterochromatin assembly in fission yeast. Mol Cell Biol *28*, 6973-6988.
Sadeghi, L., Prasad, P., Ekwall, K., Cohen, A., and Svensson, J.P. (2015). The Paf1 complex factors Leo1 and Paf1 promote local histone turnover to modulate chromatin states in fission yeast. EMBO Reports *16*, 1673-1687.
Sapetschnig, A., Sarkies, P., Lehrbach, N.J., and Miska, E.A. (2015). Tertiary siRNAs Mediate Paramutation in C. elegans. Plos Genetics *11*.

Schalch, T., Job, G., Noffsinger, V.J., Shanker, S., Kuscu, C., Joshua-Tor, L., and Partridge, J.F. (2009). High-affinity binding of Chp1 chromodomain to K9 methylated histone H3 is required to establish centromeric heterochromatin. Mol Cell *34*, 36-46.
Schott, D., Yanai, I., and Hunter, C.P. (2014). Natural RNA interference directs a heritable response to the environment. Scientific Reports *4*.
Schultz, J. (1936). Variegation in Drosophila and the Inert Chromosome Regions. Proc Natl Acad Sci U S A *22*, 27-33.
Shi, X., Finkelstein, A., Wolf, A.J., Wade, P.A., Burton, Z.F., and Jaehning, J.A. (1996). Paf1p, an RNA polymerase II-associated factor in Saccharomyces cerevisiae, may have both positive and negative roles in transcription. Molecular and Cellular Biology *16*, 669-676.
Shimada, Y., Mohn, F., and Buhler, M. (2016). The RNA-induced transcriptional silencing complex targets chromatin exclusively via interacting with nascent transcripts. Genes Dev *30*, 2571-2580.
Shirayama, M., Seth, M., Lee, H.-C., Gu, W., Ishidate, T., Conte, D., Jr., and Mello, C.C. (2012). piRNAs Initiate an Epigenetic Memory of Nonself RNA in the C. elegans Germline. Cell *150*, 65-77.
Shogren-Knaak, M., Ishii, H., Sun, J.M., Pazin, M.J., Davie, J.R., and Peterson, C.L. (2006). Histone H4-K16 acetylation controls chromatin structure and protein interactions. Science *311*, 844-847.
Sigova, A., Rhind, N., and Zamore, P.D. (2004). A single Argonaute protein mediates both transcriptional and posttranscriptional silencing in Schizosaccharomyces pombe. Genes Dev *18*, 2359-2367.
Sijen, T., Fleenor, J., Simmer, F., Thijssen, K.L., Parrish, S., Timmons, L., Plasterk, R.H.A., and Fire, A. (2001). On the role of RNA amplification in dsRNA-triggered gene silencing. Cell *107*, 465-476.
Sijen, T., Steiner, F.A., Thijssen, K.L., and Plasterk, R.H.A. (2007). Secondary siRNAs result from unprimed RNA synthesis and form a distinct class. Science *315*, 244-247.
Simmer, F., Buscaino, A., Kos-Braun, I.C., Kagansky, A., Boukaba, A., Urano, T., Kerr, A.R., and Allshire, R.C. (2010). Hairpin RNA induces secondary small interfering RNA synthesis and silencing in trans in fission yeast. EMBO Rep *11*, 112-118.
Singh, J., Mishra, V., Wang, F., Huang, H.Y., and Pikaard, C.S. (2019). Reaction Mechanisms of Pol IV, RDR2, and DCL3 Drive RNA Channeling in the siRNA-Directed DNA Methylation Pathway. Mol Cell *75*, 576-589 e575.
Smardon, A., Spoerke, J.M., Stacey, S.C., Klein, M.E., Mackin, N., and Maine, E.M. (2000). EGO-1 is related to RNA-directed RNA polymerase and functions in germ-line development and RNA interference in C-elegans. Current Biology *10*, 169-178.
Song, J.J., Smith, S.K., Hannon, G.J., and Joshua-Tor, L. (2004). Crystal structure of argonaute and its implications for RISC slicer activity. Science *305*, 1434-1437.
Spracklin, G., Fields, B., Wan, G., Becker, D., Wallig, A., Shukla, A., and Kennedy, S. (2017). The RNAi Inheritance Machinery of Caenorhabditis elegans. Genetics *206*, 1403-1416.
Squazzo, S.L., Costa, P.J., Lindstrom, D.L., Kumer, K.E., Simic, R., Jennings, J.L., Link, A.J., Arndt, K.M., and Hartzog, G.A. (2002). The Paf1 complex physically and functionally associates with transcription elongation factors in vivo. Embo Journal *21*, 1764-1774.
Steiner, N.C., Hahnenberger, K.M., and Clarke, L. (1993). Centromeres of the fission yeast Schizosaccharomyces pombe are highly variable genetic loci. Mol Cell Biol *13*, 4578-4587.
Strahl, B.D., and Allis, C.D. (2000). The language of covalent histone modifications. Nature *403*, 41-45.
Stunnenberg, R., Kulasegaran-Shylini, R., Keller, C., Kirschmann, M.A., Gelman, L., and Buhler, M. (2015). H3K9 methylation extends across natural boundaries of heterochromatin in the absence of an HP1 protein. EMBO J *34*, 2789-2803.
Sugiyama, T., Cam, H.P., Sugiyama, R., Noma, K., Zofall, M., Kobayashi, R., and Grewal, S.I. (2007). SHREC, an effector complex for heterochromatic transcriptional silencing. Cell *128*, 491-504.

Tencer, A.H., Gatchalian, J., Klein, B.J., Khan, A., Zhang, Y., Strahl, B.D., van Wely, K.H.M., and Kutateladze, T.G. (2017). A Unique pH-Dependent Recognition of Methylated Histone H3K4 by PPS and DIDO. Structure *25*, 1530-1539 e1533.
Thon, G., and Verhein-Hansen, J. (2000). Four chromo-domain proteins of Schizosaccharomyces pombe differentially repress transcription at various chromosomal locations. Genetics *155*, 551-568.
Tomson, B.N., and Arndt, K.M. (2013). The many roles of the conserved eukaryotic Paf1 complex in regulating transcription, histone modifications, and disease states. Biochim Biophys Acta *1829*, 116-126.
Torres-Garcia, S., Audergon, P.N.C.B., Shukla, M., White, S.A., Pidoux, A.L., and Allshire, R.C. (2019).
Towbin, B.D., Gonzalez-Sandoval, A., and Gasser, S.M. (2013). Mechanisms of heterochromatin subnuclear localization. Trends Biochem Sci *38*, 356-363.
Trojer, P., and Reinberg, D. (2007). Facultative heterochromatin: is there a distinctive molecular signature? Mol Cell *28*, 1-13.
Uebel, C.J., Anderson, D.C., Mandarino, L.M., Manage, K.I., Aynaszyan, S., and Phillips, C.M. (2018). Distinct regions of the intrinsically disordered protein MUT-16 mediate assembly of a small RNA amplification complex and promote phase separation of Mutator foci. PLoS Genet *14*, e1007542.
UniProt, C. (2019). UniProt: a worldwide hub of protein knowledge. Nucleic Acids Res *47*, D506-D515.
Vaiserman, A.M., Koliada, A.K., and Jirtle, R.L. (2017). Non-genomic transmission of longevity between generations: potential mechanisms and evidence across species. Epigenetics Chromatin *10*, 38.
Vakoc, C.R., Mandat, S.A., Olenchock, B.A., and Blobel, G.A. (2005). Histone H3 lysine 9 methylation and HP1gamma are associated with transcription elongation through mammalian chromatin. Mol Cell *19*, 381-391.
van Boxtel, C., van Heerden, J.H., Nordholt, N., Schmidt, P., and Bruggeman, F.J. (2017). Taking chances and making mistakes: non-genetic phenotypic heterogeneity and its consequences for surviving in dynamic environments. J R Soc Interface *14*.
Van Oss, S.B., Cucinotta, C.E., and Arndt, K.M. (2017). Emerging Insights into the Roles of the Paf1 Complex in Gene Regulation. Trends Biochem Sci *42*, 788-798.
Van Oss, S.B., Shirra, M.K., Bataille, A.R., Wier, A.D., Yen, K., Vinayachandran, V., Byeon, I.L., Cucinotta, C.E., Heroux, A., Jeon, J.*, et al.* (2016). The Histone Modification Domain of Paf1 Complex Subunit Rtf1 Directly Stimulates H2B Ubiquitylation through an Interaction with Rad6. Mol Cell *64*, 815-825.
Van Speybroeck, L. (2002). From epigenesis to epigenetics: the case of C. H. Waddington. Ann N Y Acad Sci *981*, 61-81.
van Steensel, B., and Belmont, A.S. (2017). Lamina-Associated Domains: Links with Chromosome Architecture, Heterochromatin, and Gene Repression. Cell *169*, 780-791.
Vasicek, T.J., Zeng, L., Guan, X.J., Zhang, T., Costantini, F., and Tilghman, S.M. (1997). Two dominant mutations in the mouse fused gene are the result of transposon insertions. Genetics *147*, 777-786.
Vasil, I.K. (2008). A history of plant biotechnology: from the Cell Theory of Schleiden and Schwann to biotech crops. Plant Cell Rep *27*, 1423-1440.
Vastenhouw, N.L., Brunschwig, K., Okihara, K.L., Mueller, F., Tijsterman, M., and Plasterk, R.H.A. (2006). Long-term gene silencing by RNAi. Nature *442*, 882-882.
Vaughn, M.W., Tanurdzic, M., Lippman, Z., Jiang, H., Carrasquillo, R., Rabinowicz, P.D., Dedhia, N., McCombie, W.R., Agier, N., Bulski, A.*, et al.* (2007). Epigenetic natural variation in Arabidopsis thaliana. PLoS Biol *5*, e174.
Verdel, A., Jia, S., Gerber, S., Sugiyama, T., Gygi, S., Grewal, S.I., and Moazed, D. (2004). RNAi-mediated targeting of heterochromatin by the RITS complex. Science *303*, 672-676.
Verdel, A., and Moazed, D. (2005). RNAi-directed assembly of heterochromatin in fission yeast. FEBS Lett *579*, 5872-5878.
Verrier, L., Taglini, F., Barrales, R.R., Webb, S., Urano, T., Braun, S., and Bayne, E.H. (2015). Global regulation of heterochromatin spreading by Leo1. Open Biology *5*, 150045.

Vogel, M.J., Guelen, L., de Wit, E., Peric-Hupkes, D., Loden, M., Talhout, W., Feenstra, M., Abbas, B., Classen, A.K., and van Steensel, B. (2006). Human heterochromatin proteins form large domains containing KRAB-ZNF genes. Genome Res *16*, 1493-1504.
Volpe, T.A., Kidner, C., Hall, I.M., Teng, G., Grewal, S.I., and Martienssen, R.A. (2002). Regulation of heterochromatic silencing and histone H3 lysine-9 methylation by RNAi. Science *297*, 1833-1837.
Waddington, C.H. (2012). The epigenotype. 1942. Int J Epidemiol *41*, 10-13.
Wade, P.A., Werel, W., Fentzke, R.C., Thompson, N.E., Leykam, J.F., Burgess, R.R., Jaehning, J.A., and Burton, Z.F. (1996). A novel collection of accessory factors associated with yeast RNA polymerase II. Protein Expression and Purification *8*, 85-90.
Wan, G., Fields, B.D., Spracklin, G., Shukla, A., Phillips, C.M., and Kennedy, S. (2018). Spatiotemporal regulation of liquid-like condensates in epigenetic inheritance. Nature *557*, 679-683.
Wang, J., Reddy, B.D., and Jia, S. (2015). Rapid epigenetic adaptation to uncontrolled heterochromatin spreading. Elife *4*.
Wang, P., Bowl, M.R., Bender, S., Peng, J., Farber, L., Chen, J., Ali, A., Zhang, Z., Alberts, A.S., Thakker, R.V.*, et al.* (2008). Parafibromin, a component of the human PAF complex, regulates growth factors and is required for embryonic development and survival in adult mice. Molecular and Cellular Biology *28*, 2930-2940.
Wassenegger, M., Heimes, S., Riedel, L., and Sanger, H.L. (1994). RNA-directed de novo methylation of genomic sequences in plants. Cell *76*, 567-576.
Waterland, R.A., and Jirtle, R.L. (2003). Transposable elements: targets for early nutritional effects on epigenetic gene regulation. Mol Cell Biol *23*, 5293-5300.
Weiser, N.E., and Kim, J.K. (2019). Multigenerational Regulation of the Caenorhabditis elegans Chromatin Landscape by Germline Small RNAs. Annu Rev Genet.
Wendte, J.M., and Pikaard, C.S. (2017). The RNAs of RNA-directed DNA methylation. Biochim Biophys Acta Gene Regul Mech *1860*, 140-148.
Wierzbicki, A.T., Haag, J.R., and Pikaard, C.S. (2008). Noncoding Transcription by RNA Polymerase Pol IVb/Pol V Mediates Transcriptional Silencing of Overlapping and Adjacent Genes. Cell *135*, 635-648.
Wilhelm, B.T., Marguerat, S., Watt, S., Schubert, F., Wood, V., Goodhead, I., Penkett, C.J., Rogers, J., and Bahler, J. (2008). Dynamic repertoire of a eukaryotic transcriptome surveyed at single-nucleotide resolution. Nature *453*, 1239-1243.
Woodhouse, R.M., Buchmann, G., Hoe, M., Harney, D.J., Low, J.K.K., Larance, M., Boag, P.R., and Ashe, A. (2018). Chromatin Modifiers SET-25 and SET-32 Are Required for Establishment but Not Long-Term Maintenance of Transgenerational Epigenetic Inheritance. Cell Rep *25*, 2259-2272 e2255.
Woolcock, K.J., Stunnenberg, R., Gaidatzis, D., Hotz, H.R., Emmerth, S., Barraud, P., and Buhler, M. (2012). RNAi keeps Atf1-bound stress response genes in check at nuclear pores. Genes Dev *26*, 683-692.
Wu, X., Rossettini, A., and Hanes, S.D. (2003). The ESS1 prolyl isomerase and its suppressor BYE1 interact with RNA pol II to inhibit transcription elongation in Saccharomyces cerevisiae. Genetics *165*, 1687-1702.
Wu, X., Wilcox, C.B., Devasahayam, G., Hackett, R.L., Arevalo-Rodriguez, M., Cardenas, M.E., Heitman, J., and Hanes, S.D. (2000). The Ess1 prolyl isomerase is linked to chromatin remodeling complexes and the general transcription machinery. EMBO J *19*, 3727-3738.
Xu, F., Feng, X., Chen, X., Weng, C., Yan, Q., Xu, T., Hong, M., and Guang, S. (2018). A Cytoplasmic Argonaute Protein Promotes the Inheritance of RNAi. Cell Rep *23*, 2482-2494.
Xu, Y., Bernecky, C., Lee, C.-T., Maier, K.C., Schwalb, B., Tegunov, D., Plitzko, J.M., Urlaub, H., and Cramer, P. (2017). Architecture of the RNA polymerase II-Paf1C-TFIIS transcription elongation complex. Nature Communications *8*, 15741.
Yasuhara, J.C., and Wakimoto, B.T. (2006). Oxymoron no more: the expanding world of heterochromatic genes. Trends Genet *22*, 330-338.

Yu, R., Jih, G., Iglesias, N., and Moazed, D. (2014). Determinants of heterochromatic siRNA biogenesis and function. Mol Cell *53*, 262-276.
Yu, R., Wang, X., and Moazed, D. (2018). Epigenetic inheritance mediated by coupling of RNAi and histone H3K9 methylation. Nature *558*, 615-619.
Zhang, K., Mosch, K., Fischle, W., and Grewal, S.I. (2008). Roles of the Clr4 methyltransferase complex in nucleation, spreading and maintenance of heterochromatin. Nat Struct Mol Biol *15*, 381-388.
Zhang, Y.Y., Fischer, M., Colot, V., and Bossdorf, O. (2013). Epigenetic variation creates potential for evolution of plant phenotypic plasticity. New Phytol *197*, 314-322.
Zhao, J., Sun, B.K., Erwin, J.A., Song, J.J., and Lee, J.T. (2008). Polycomb proteins targeted by a short repeat RNA to the mouse X chromosome. Science *322*, 750-756.
Zhao, Y., and Garcia, B.A. (2015). Comprehensive Catalog of Currently Documented Histone Modifications. Cold Spring Harb Perspect Biol *7*, a025064.
Zheng, X., Chen, L., Xia, H., Wei, H., Lou, Q., Li, M., Li, T., and Luo, L. (2017). Transgenerational epimutations induced by multi-generation drought imposition mediate rice plant's adaptation to drought condition. Sci Rep *7*, 39843.
Zhu, B., Mandal, S.S., Main, A.D., Zheng, Y., Erdjument-Bromage, H., Batra, S.K., Tempst, P., and Reinberg, D. (2005). The human PAF complex coordinates transcription with events downstream of RNA synthesis. Genes & Development *19*, 1668-1673.
Zofall, M., Yamanaka, S., Reyes-Turcu, F.E., Zhang, K., Rubin, C., and Grewal, S.I. (2012). RNA elimination machinery targeting meiotic mRNAs promotes facultative heterochromatin formation. Science *335*, 96-100.
Zong, J., Yao, X., Yin, J., Zhang, D., and Ma, H. (2009). Evolution of the RNA-dependent RNA polymerase (RdRP) genes: duplications and possible losses before and after the divergence of major eukaryotic groups. Gene *447*, 29-39.

APPENDIX

Inheritance of a Phenotypically Neutral Epimutation Evokes Gene Silencing in Later Generations

Lea Duempelmann, Fabio Mohn, Yukiko Shimada, Daniele Oberti, Aude Andriollo, Silke Lochs and Marc Bühler

A fully automated deep learning pipeline for high-throughput colony segmentation and classification

Sarah H. Carl, Lea Duempelmann, Yukiko Shimada and Marc Bühler

Review: Small RNAs in the transgenerational inheritance of epigenetic information

Lea Duempelmann*, Merle Skribbe* and Marc Bühler (*equal contribution)

Curriculum vitae

Article

Molecular Cell

Inheritance of a Phenotypically Neutral Epimutation Evokes Gene Silencing in Later Generations

Graphical Abstract

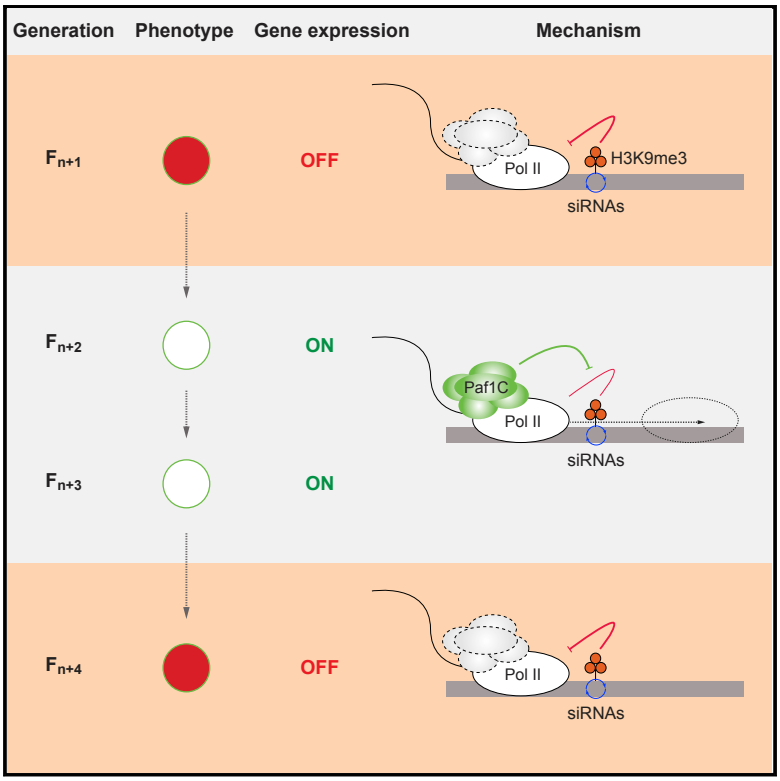

Highlights

- *S. pombe* remembers and reinstates silencing that occurred in a previous generation
- Paf1 modulation enables acquisition of a new trait that is plastic and inheritable
- H3K9me3 functions as an epigenetic mark that is not repressive per se
- Paf1C facilitates transcription elongation through H3K9-methylated nucleosomes

Authors

Lea Duempelmann, Fabio Mohn, Yukiko Shimada, Daniele Oberti, Aude Andriollo, Silke Lochs, Marc Bühler

Correspondence

marc.buehler@fmi.ch

In Brief

Duempelmann et al. describe an H3K9me3 and siRNA-dependent epimutation, which is installed during gene silencing and inherited across generations, even upon reactivation of the silenced gene. Yet silencing is reinstated in later generations if Paf1C is impaired, revealing H3K9me3 as a stable epigenetic mark that is not repressive per se.

Duempelmann et al., 2019, Molecular Cell *74*, 534–541
May 2, 2019
https://doi.org/10.1016/j.molcel.2019.02.009

CellPress

CellPress

Molecular Cell
Article

Inheritance of a Phenotypically Neutral Epimutation Evokes Gene Silencing in Later Generations

Lea Duempelmann,[1,2] Fabio Mohn,[1] Yukiko Shimada,[1] Daniele Oberti,[1] Aude Andriollo,[1] Silke Lochs,[3] and Marc Bühler[1,2,4,*]

[1]Friedrich Miescher Institute for Biomedical Research, Maulbeerstrasse 66, 4058 Basel, Switzerland
[2]University of Basel, Petersplatz 10, 4003 Basel, Switzerland
[3]Oncode Institute, Hubrecht Institute-KNAW and University Medical Centre Utrecht, Uppsalalaan 8, 3584 Utrecht, the Netherlands
[4]Lead Contact
*Correspondence: marc.buehler@fmi.ch
https://doi.org/10.1016/j.molcel.2019.02.009

SUMMARY

Small RNAs trigger the formation of epialleles that are silenced across generations. Consequently, RNA-directed epimutagenesis is associated with persistent gene repression. Here, we demonstrate that small interfering RNA-induced epimutations in fission yeast are still inherited even when the silenced gene is reactivated, and descendants can reinstate the silencing phenotype that only occurred in their ancestors. This process is mediated by the deposition of a phenotypically neutral molecular mark composed of tri-methylated histone H3 lysine 9 (H3K9me3). Its stable propagation is coupled to RNAi and requires maximal binding affinity of the Clr4/Suvar39 chromodomain to H3K9me3. In wild-type cells, this mark has no visible impact on transcription but causes gene silencing if RNA polymerase-associated factor 1 complex (Paf1C) activity is impaired. In sum, our results reveal a distinct form of epigenetic memory in which cells acquire heritable, transcriptionally active epialleles that confer gene silencing upon modulation of Paf1C.

INTRODUCTION

Phenotypic effects caused by epimutations rather than changes in DNA sequence have been described in various organisms. Epimutations are potentially adaptive if inherited across generations and might even respond to environmental challenges. Yet experimental evidence is scarce (Heard and Martienssen, 2014). Prominent examples of heritable phenotypic changes caused by epimutations are paramutation in plants and RNA-induced epigenetic silencing (RNAe) in nematodes, in which small RNAs trigger the formation of epialleles that are stably silenced across generations (Ashe et al., 2012; Chandler, 2007; Erhard and Hollick, 2011; Grentzinger et al., 2012; Luteijn et al., 2012; Shirayama et al., 2012). A similar phenomenon has recently been described in the fission yeast *Schizosaccharomyces pombe* (Yu et al., 2018), demonstrating that long-lasting gene silencing responses mediated by small RNAs are widespread. Consequently, RNA-directed epimutagenesis is associated with persistent gene repression.

Whereas it is now well established that RNA-induced repression of genes is heritable across generations, it has remained unknown whether mechanisms exist that robustly convey transgenerational memory of a silencing "experience," without establishing a permanently repressed state. Here, we report the discovery of such a phenomenon in *S. pombe*: we show that RNAe, triggered by transient expression of hairpin-derived small interfering RNAs (siRNAs) coupled with mutation of the polymerase-associated factor 1 (Paf1), is stably propagated for at least 18 generations. Upon reintroduction of Paf1, the silent state is lost but resumes if Paf1 is again impaired in later generations, even in the absence of the original siRNA trigger. This process is mediated by the deposition of a phenotypically neutral molecular mark composed of tri-methylated histone H3 lysine 9 (H3K9me3), and its stable propagation is coupled to RNAi. Our results reveal that H3K9me3 functions as an epigenetic mark that is not repressive per se and imply that Paf1C's function in promoting transcription elongation is particularly important within difficult-to-transcribe chromatin.

RESULTS

A Point Mutation in Paf1 Enables Multi-generational Inheritance of Gene Silencing

In *S. pombe*, ectopic expression of primary siRNAs mediates *de novo* silencing of euchromatic genes through the formation of heterochromatin. These silent epialleles are only established upon the concurrent mutation of factors that negatively regulate this process (Flury et al., 2017; Kowalik et al., 2015; Yu et al., 2018), including mutations in subunits of the Paf1C, such as a nonsense mutation in the *paf1*$^+$ gene (*paf1-Q264Stop*). We used this system to study mechanisms of epigenetic inheritance by expressing an RNA hairpin (*ade6-hp*) from a euchromatic locus (Figures S1A and S1B), which leads to the generation of primary siRNAs that induce strong heterochromatin-mediated silencing of *ade6*$^+$ expression in *paf1-Q264Stop* cells (Kowalik

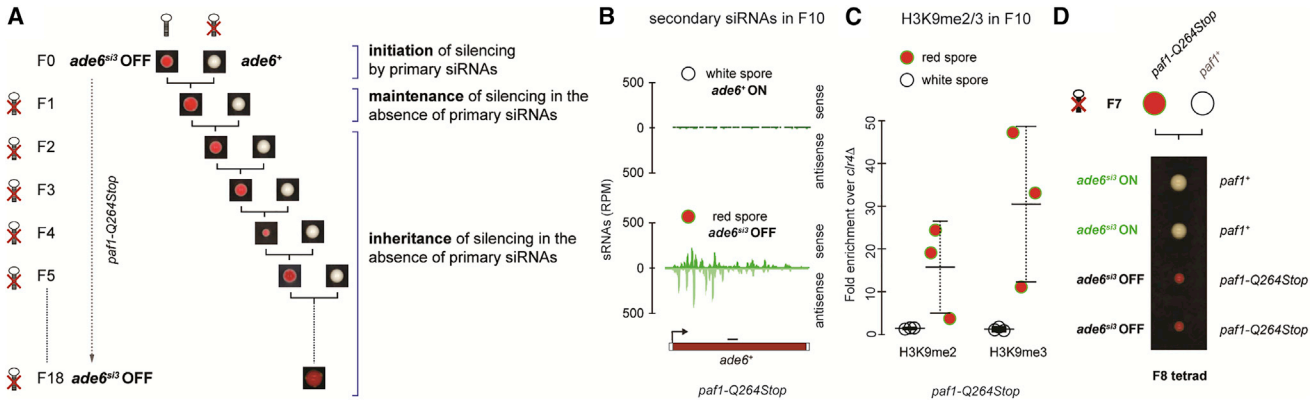

Figure 1. Transgenerational Inheritance of siRNA-Directed Gene Silencing

(A) Silencing of the *ade6*$^+$ gene was initiated in *trans* by a primary siRNA-producing *ade6*-hairpin (denoted by the symbol) in *paf1-Q264Stop* cells (F0). F0 cells with a silent epiallele (*ade6*$^+$ OFF, red phenotype) were then crossed with *paf1-Q264Stop* cells lacking the *ade6*-hairpin (*ade6*$^+$, white phenotype), followed by spore dissection on YE plates. Colonies forming from F1 spores that inherited the *ade6*$^+$ OFF allele (red), but not the *ade6*-hairpin, were selected and again crossed with naive *paf1-Q264Stop ade6*$^+$ cells (white). This was repeated until generation 18 (F18; see also Figure S1C).

(B) Small RNA (sRNA) sequencing performed with red (*ade6*$^+$ OFF) or white (*ade6*$^+$ ON) colonies from F10 spores. Read counts were normalized to library size. Black line denotes the part of *ade6*$^+$ that is complementary to the primary siRNA-producing *ade6*-hairpin. One representative of many sequenced spores is shown.

(C) Chromatin immunoprecipitation (ChIP)-qPCR measuring H3K9me2 and H3K9me3 enrichments at *ade6*$^+$ ON and *ade6*$^+$ OFF epialleles, normalized to *adh1*$^+$ and relative to a *clr4Δ* background control. n = 3 independent white or red colonies formed from F10 spores. Center values denote the mean; error bars denote SD.

(D) Tetrad dissection of F7 *paf1-Q264Stop ade6*$^+$ OFF (red) cells crossed with naive *paf1*$^+$ cells. F8 *paf1*$^+$ spores never grew as red colonies (see also Figure S1E).

et al., 2015). Because silencing of *ade6*$^+$ causes a phenotypic switch from white to red cells when grown on limiting adenine plates, *ade6*$^+$ ON (white) and *ade6*$^+$ OFF (red) epialleles can be visually distinguished. The red phenotype of cells bearing an *ade6*$^+$ OFF epiallele is stably propagated to the next generation in the same *paf1-Q264Stop* background, even in the absence of the primary siRNAs that induced the silent state, demonstrating epigenetic inheritance (Kowalik et al., 2015).

Using this approach, we have previously demonstrated that siRNA-mediated repression of *ade6*$^+$ in the absence of Paf1C is mitotically stable and mediated by heterochromatic histone H3 lysine 9 (H3K9) modifications and secondary *ade6*$^+$ siRNA production at the target locus (Kowalik et al., 2015). To test whether the repressed state of *ade6*$^+$ is also stably maintained over multiple generations in the absence of the primary siRNA trigger, we repeatedly crossed red *paf1-Q264Stop ade6*$^+$ OFF cells with white *paf1-Q264Stop ade6*$^+$ ON cells (Figure 1A) and analyzed the degree of inheritance by tetrad dissection (Figures S1C and S1D). In total, we examined three independent pedigrees for 5 generations (F5), of which one we continued until F18. Spores of the 18th generation still formed red colonies (Figures 1A and S1C), indicating that the repressed phenotype is stably inherited. Segregation of the red phenotype was non-Mendelian (Figure S1C), excluding DNA sequence changes as the underlying cause for the observed heritability. Occasionally, we observed the red phenotype in more than 2 spores of a tetrad (Figure S1C), indicating that the *ade6*$^+$ OFF allele can be paramutagenic (Chandler, 2010). Similar to RNAe in *Caenorhabditis elegans* (Luteijn and Ketting, 2013), we observed secondary *ade6*$^+$ siRNAs in *paf1-Q264Stop ade6*$^+$ OFF cells, but not in *paf1-Q264Stop ade6*$^+$ ON cells derived from F10 spores (Figure 1B). These siRNAs spread up and downstream of the region initially targeted by the hairpin (Figure 1B). They also correlated well with enrichment of the heterochromatic histone modifications H3K9me2 and H3K9me3 (Figure 1C), which are associated with gene silencing (Jih et al., 2017). Consistent with a recent study (Yu et al., 2018), inheritance of the red silencing phenotype remained strictly dependent on the *paf1-Q264Stop* mutation, as all spores that inherited the *paf1*$^+$ allele formed white colonies (Figures 1D and S1E). Thus, if primary siRNAs are transiently expressed from a euchromatic locus, acquisition and epigenetic inheritance of the *ade6*$^+$ OFF silencing phenotype (red colonies) is only possible if Paf1C activity is impaired.

H3K9me3 and Secondary siRNAs Are Inherited with No Apparent Silencing Phenotype in Wild-Type Cells

H3K9 methylation is a well-established "repressive" histone modification. Hence, we concluded that the loss of the RNAe phenotype in all *paf1*$^+$ progeny from heterozygous *paf1-Q264Stop* × *paf1*$^+$ crosses must result from a failure to maintain methylated H3K9 in wild-type cells. However, we discovered that H3K9me2 and H3K9me3 marks were not erased from the reactivated *ade6*$^+$ epiallele (Figures 2A–C). Furthermore, the secondary *ade6*$^+$ siRNAs were also still produced in the *paf1*$^+$ cells (Figures 2D, 2E, and S2). This demonstrates that H3K9 methylation marks and secondary siRNAs are stably propagated to the next generation, despite no apparent silencing phenotype. Therefore, we hypothesized that H3K9 methylation functions as a phenotypically neutral epimutation, conferring a cellular memory of the ancestral *ade6*$^+$-silencing phenotype that might be reinstated by repeated Paf1C impairment. To test this, we

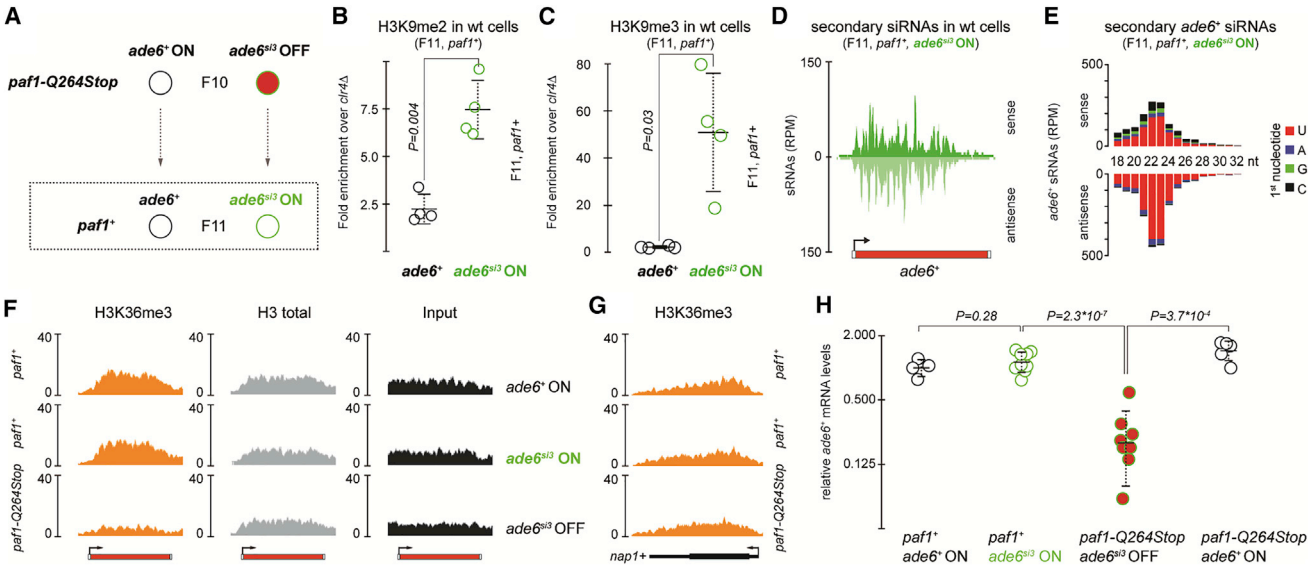

Figure 2. H3K9 Methyl Marks Remain, even when the Silenced *ade6*$^{+}$ Gene Is Reactivated

(A) Schematic illustrating that the *ade6*^{si3} OFF epiallele from a red *paf1-Q264Stop* parent retains a molecular mark (*ade6*^{si3}) in *paf1*$^{+}$ daughter cells (indicated by green color), although the silent state was lost (*ade6*^{si3} ON). If the silent state had already been lost in the *paf1-Q264Stop* parental generation (*ade6*$^{+}$ ON), no mark was inherited to the next generation (*ade6*$^{+}$).

(B and C) ChIP-qPCR measuring H3K9me2 (B) and H3K9me3 (C) enrichments at *ade6*$^{+}$ genes in marked and non-marked wild-type cells, which show no silencing phenotype. Values are normalized to *adh1*$^{+}$ and relative to a *clr4Δ* background control. n = 4 independent colonies growing from unrelated F11 *paf1*$^{+}$ spores. Center values denote the mean, error bars denote SD, and p values were calculated with a two-tailed Student's t test.

(D) sRNA sequencing performed with wild-type cells carrying the *ade6*^{si3} ON epiallele. Same cells as used in (B) and (C) are shown. See Figure S2 for all 4 biological replicates.

(E) Length distribution and 5′ U bias of small RNAs shown in (D), which are characteristic of siRNAs. Read counts in (D) and (E) were normalized to library size.

(F and G) University of California Santa Cruz (UCSC) genome browser shots of *ade6*$^{+}$ (F) and an unrelated euchromatic gene *nap1*$^{+}$(G). ChIP sequencing (ChIP-seq) profiles for H3K36me3, total H3, and input for wild-type (with and without marked *ade6*$^{+}$) and *paf1-Q264Stop* (with marked *ade6*$^{+}$) cells are normalized to library size. All 3 biological replicates are shown in Figures S3E and 5.

(H) qRT-PCR measurement of *ade6*$^{+}$ mRNA levels in wild-type and *paf1-Q264Stop* cells, with and without the molecular mark. mRNA levels were normalized to *act1*+ and shown relative to *paf1*$^{+}$ *ade6*$^{+}$ ON. n = 4–9 biological replicates (individual data points). Center values denote the mean, error bars denote SD, and p values were calculated using two-tailed Student's t tests.

(A–H) F10 *paf1-Q264Stop ade6*^{imp} OFF cells were the same as shown in Figure 1.

crossed the *paf1*$^{+}$ cells that had lost the silencing phenotype with *paf1-Q264Stop* cells and monitored gene silencing in the next generation (Figure S3A). Indeed, in almost half of the crosses, *ade6*$^{+}$ silencing was re-established in *paf1-Q264Stop* cells, which was again stably maintained through mitosis (Figures S3B–S3D). Silencing occurred at the level of transcription, as H3K36me3 levels were strongly reduced on the *ade6*$^{+}$ gene (Figures 2F and S3E). The *paf1-Q264Stop* allele did not affect transcription of other genes, and we only observed repression of *ade6*$^{+}$ in *paf1-Q264Stop* cells if the ancestral strain had been exposed to *ade6*$^{+}$ siRNAs (Figures 2G, 2H, and 5). These results demonstrate that RNAe installs a molecular mark—involving H3K9 methylation and secondary siRNA production—that is also compatible with active transcription. Because this mark resists erasure upon reactivation of the silent allele, it confers a cellular memory of gene silencing that had occurred in past generations. We hereafter refer to the marked *ade6*$^{+}$ epiallele as *ade6*^{si3}.

We assessed the mitotic stability of *ade6*^{si3} in Paf1C wild-type cells by exponentially growing *paf1*$^{+}$ *ade6*^{si3} ON cells in liquid culture and crossing a sample every 3 days (30–40 mitotic divisions) with *paf1-Q264Stop* cells (Figure 3A). This revealed recurrence of the silent state in *paf1-Q264Stop* progeny even after 17 days of exponential growth (~180 mitotic divisions) of the *paf1*$^{+}$ *ade6*^{si3} ON parental cells, although this gradually declined with the number of cell divisions (Figure 3B). We next evaluated transgenerational inheritance of *ade6*^{si3} in the *paf1*$^{+}$ background. We found that *paf1*$^{+}$ grandparents were able to pass on the *ade6*^{si3} ON allele to a *paf1*$^{+}$ parent, and silencing could still be re-established in their *paf1-Q264Stop* progeny (Figures 3C and 3D). Thus, the marked *ade6*^{si3} epiallele is stably maintained during both mitosis and meiosis.

In summary, impaired Paf1C activity enables primary siRNAs to install a molecular mark on the homologous protein-coding gene, which results in a strong silencing phenotype that is inherited over many generations. Upon reactivation of Paf1C, the silencing phenotype is lost, but the phenotypically neutral mark (secondary siRNA production and H3K9 methylation; si3) is still inherited by subsequent generations, even in the absence of the primary siRNAs that triggered marking in the ancestral strain. If Paf1C is again compromised, silencing is re-established and extremely stably maintained.

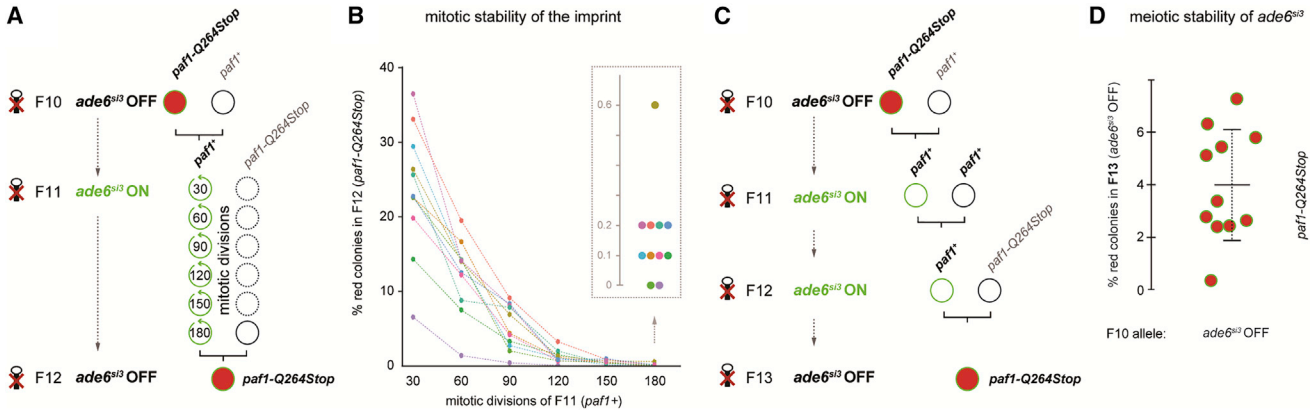

Figure 3. The *ade6^{si3}* Epiallele Is Stable across Generations in Wild-Type Cells

(A) Crossing scheme for testing the mitotic stability of the marked *ade6^{si3}* epiallele. F11 *paf1^{+} ade6^{si3}* ON colonies were grown in liquid culture and crossed to *paf1-Q264Stop ade6^{+}* cells every 30–40 mitotic divisions. Restoration of silencing phenotype in F12 *paf1-Q264Stop* was assessed by random spore analysis.

(B) Analysis of silencing restoration as depicted in (A), which was performed eleven times. At least 1,000 F12 colonies (spores) per cross were inspected for the silencing phenotype.

(C) Crossing scheme for testing the meiotic stability of the marked *ade6^{si3}* epiallele. Colonies grown from F11 *paf1^{+} ade6^{si3}* ON spores (A) were crossed to wild-type cells and subsequently to *paf1-Q264Stop ade6^{+}* cells.

(D) Restoration of the silencing phenotype in F13 *paf1-Q264Stop* cells was assessed by random spore analysis. At least 1,000 colonies grown from those spores per cross were inspected for the silencing phenotype. n = 11 different crosses. Centre values denote the mean; error bars denote SD.

(A–D) F10 *paf1-Q264Stop ade6^{imp}* OFF cells were the same as shown in Figure 1.

Epigenetic Memory of an Ancestral Gene-Silencing Episode Is Mediated by Coupling of Secondary siRNA Amplification and H3K9 Tri-methylation

Coupling of RNAi and histone H3K9 methylation is important to maintain the silent state of an RNAe response triggered by centromeric siRNAs (Yu et al., 2018). To investigate whether such coupling also mediates transgenerational inheritance of the marked *ade6^{si3}* epiallele, we crossed *paf1-Q264Stop ade6^{si3}* OFF cells with *paf1^{+}* cells lacking key RNAi factors (Ago1, Dcr1, or Rdp1) or the H3K9 methyltransferase Clr4 (Figure 4A). These were then crossed with *paf1-Q264Stop* cells expressing Clr4, Ago1, Dcr1, and Rdp1 to see whether the marked *ade6^{si3}* epiallele had been inherited and the silencing state could be re-established. However, in the next-generation *paf1-Q264Stop* cells, *ade6^{+}* could no longer be silenced (Figure 4B). Furthermore, secondary *ade6^{+}* siRNA production ceased in these mutants (Figures 4C, 4D, and S4). *ade6^{+}* siRNAs were also absent in the parental *paf1^{+} clr4Δ* cells (Figures 4C and S4B), and H3K9me3 and H3K9me2 were abolished in the parental *paf1^{+}* RNAi mutants (Figures 4E and 4F). This demonstrates coupling of siRNA production and histone H3K9 methylation in *paf1^{+}* cells for the transgenerational inheritance of the marked allele. To further dissect the requirement of specific H3K9 methylation states for stable marking, we employed a Clr4 mutant (Clr4-F449Y) that is deficient in catalyzing specifically H3K9me3 (Jih et al., 2017). We observed that *ade6^{+}* siRNA production was abolished in Clr4-F449Y-expressing cells (Figures 4C and S4B) and that the silencing phenotype was not re-established in the next generation (Figure 4B). In contrast, H3K9me2 was only lost in *clr4-F449Y* cells at the marked locus, but not at centromeric repeats (Figures 4F and 4H; Jih et al., 2017), where siRNA production was maintained (Figures 4D and S4C). Therefore, we conclude that epigenetic inheritance of the *ade6^{si3}* allele is mediated by coupling of secondary siRNA amplification and H3K9 tri-methylation. H3K9me2 catalysis alone (i.e., in the presence of Clr4-F449Y) is not sufficient to maintain the mark (Figures 4B, 4C, and 4F).

Inheritance of the Phenotypically Neutral Epimutation Depends on Maximal Binding Affinity of the Clr4/Suvar39 Chromodomain to H3K9me3

We next investigated how H3K9 tri-methylation maintains inheritance of the *ade6^{si3}* epiallele. Methylation of H3K9 creates a binding site for chromodomain-containing proteins. The chromodomains of Chp1 and Clr4, both essential factors for RNAi-directed heterochromatin silencing, bind H3K9me3 more tightly than H3K9me2, and the chromodomain of Chp1 has the highest binding affinity for H3K9me (Schalch et al., 2009). Chp1 forms the RNA-induced transcriptional silencing complex (RITS) together with Ago1 and Tas3 (Verdel et al., 2004). Such high-affinity binding between Chp1 and H3K9me3 is critical for *de novo* formation of heterochromatin at centromeric repeats, but it is not required for the maintenance of heterochromatin once it is established (Schalch et al., 2009). In agreement with these observations, we observed that *ade6^{si3}* was maintained in cells expressing a mutant of Chp1, Chp1-F61A (Figure 4A and 4I). This mutant binds H3K9me3 with lower affinity, which is similar to the affinity of wild-type Chp1 binding to H3K9me2 (Schalch et al., 2009). Thus, high-affinity binding of the RITS complex to H3K9me3 is not a prerequisite for inheritance of the *ade6^{si3}* epiallele (Figures 4A and 4I). However, in cells expressing Chp1-V24R, which cannot bind methylated H3K9 at all, the mark was lost (Figure 4I). To test whether the requirement of H3K9me3 for stable marking is also linked to Clr4, we reduced the high H3K9me3 binding affinity of the Clr4 chromodomain to the lower affinity for H3K9me2

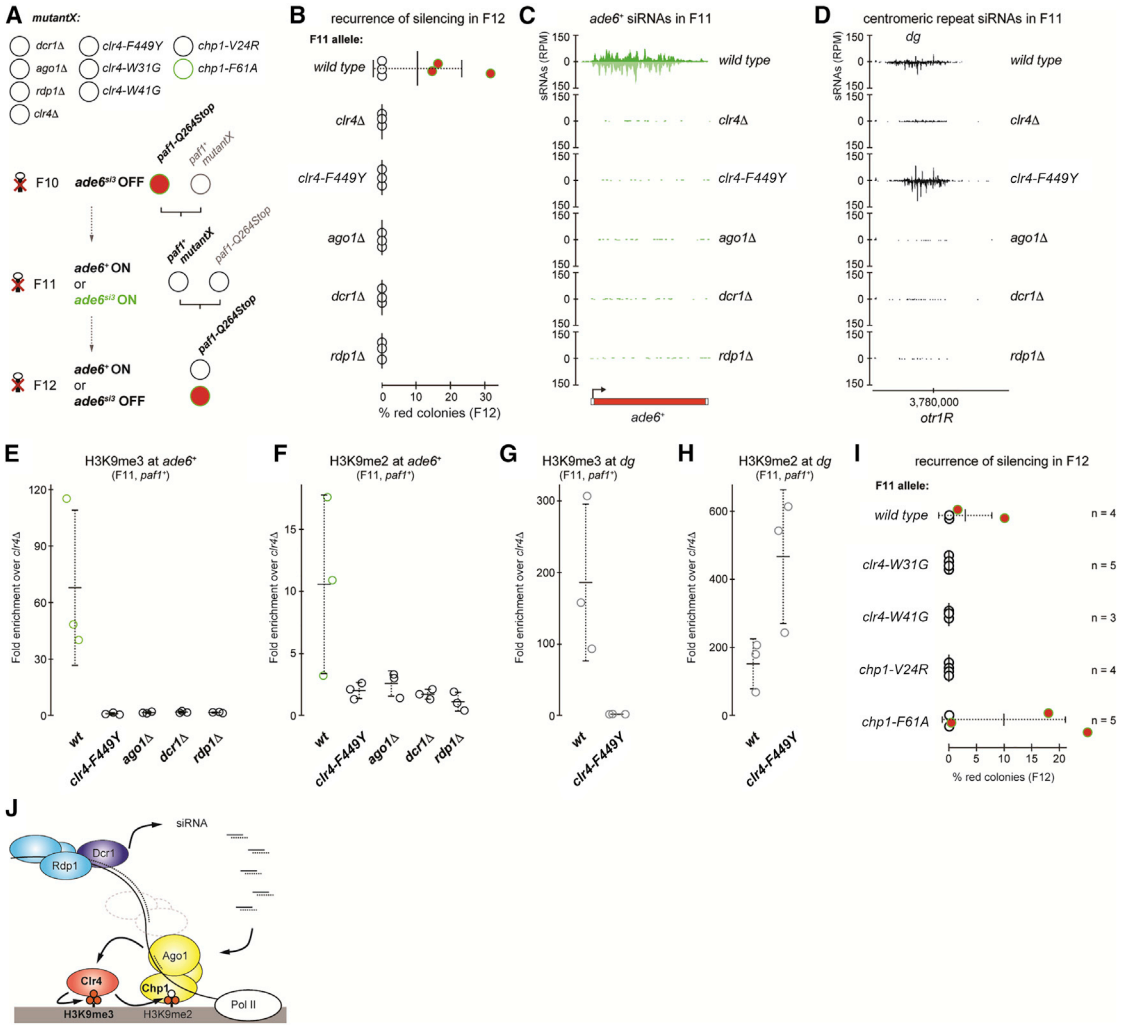

Figure 4. H3K9me3 and siRNAs Preserve the *ade6*^{si3} Epiallele in *paf1*$^{+}$ Cells without Affecting Transcription

(A) Crossing scheme for testing the requirement of H3K9me3 and RNAi for the heritability of the molecular mark (B–H) or for testing heritability of the mark if the affinity of Chp1 or Clr4 for H3K9me3 is reduced (Chp1-F61A and Clr4-W31G) or abolished (Chp1-V24R and Clr4-W41G) in otherwise wild-type cells (I).

(B) Restoration of the silencing phenotype in F12 *paf1-Q264Stop* cells (otherwise wild-type), assessed by random spore analysis. If the F11 *paf1*$^{+}$ parent was mutant for any of the factors depicted (*mutantX*), silencing was never re-established. Number of colonies grown from F12 spores that were inspected for the silencing phenotype is as follows: 442, 1,161, and 1,167 (*wild-type, ade6*^{si3}); 4,892, 5,070, and 4,982 (*wild-type, ade6*$^{+}$); 2,549, 1,586, and 1,906 (*clr4Δ*); 2,743, 651, and 631 (*clr4-F449Y*); 1,368, 2,019, and 2,219 (*ago1Δ*); 1,980, 1,444, and 1,447 (*dcr1Δ*); and 2,063, 1,775, and 1,918 (*rdp1Δ*). Center values denote the mean; error bars denote SD.

(C and D) sRNA sequencing was performed with F11 wild-type *ade6*^{si3} and *paf1*$^{+}$ *mutantX* cells. Enrichments are shown at *ade6*$^{+}$ (C) and *dg* (D). Counts were normalized to library size. All biological triplicates of *wild-type ade6*^{si3} and *mutantX* are shown in Figure S4.

(E–H) ChIP-qPCR measuring H3K9me2 and H3K9me3 enrichments at *ade6*$^{+}$ genes (E and F) and the centromeric *dg* repeat (G and H), normalized to *adh1*$^{+}$ and relative to a *clr4Δ* background control in F11 wild-type *ade6*^{si3} and *paf1*$^{+}$ *mutantX* cells that produced F12 spores analyzed in (B). Center values denote the mean; error bars denote SD.

(B–H) n ≥ 3 different crosses (pedigrees) for each genetic background.

(I) Restoration of the silencing phenotype in F12, in which Chp1 and Clr4 had again normal affinities for H3K9me3, was assessed by random spore analysis (see A for crossing scheme). Number of F12 *paf1-Q264Stop* colonies (otherwise wild-type) that were inspected for the silencing phenotype is as follows: 1,113, 1,049, 1,372, and 1,294 (*wild-type*); 2,308, 1,113, 2,200, 1,077, and 1,317 (*clr4-W31G*); 1,615, 708, and 2,155 (*clr4-W41G*); 1,196, 1,249, 1,035, and 1,292 (*chp1-V24R*); and 2,146, 1,012, 1,014, 1,015, and 652 (*chp1-F61A*). Center values denote the mean; error bars denote SD; n, number of crosses (pedigrees) for each genetic background.

(J) Model depicting positive feedback loops that preserve the marked epiallele. Clr4 recognizes H3K9me3 and catalyzes H3K9 methylation on newly deposited histones. H3K9me2 is sufficient to stabilize RITS binding to chromatin. RITS together with H3K9me3 retain Clr4 activity at the marked locus. Amplification of secondary siRNAs further stabilizes RITS association with the marked locus, promoting recruitment of Clr4 activity.

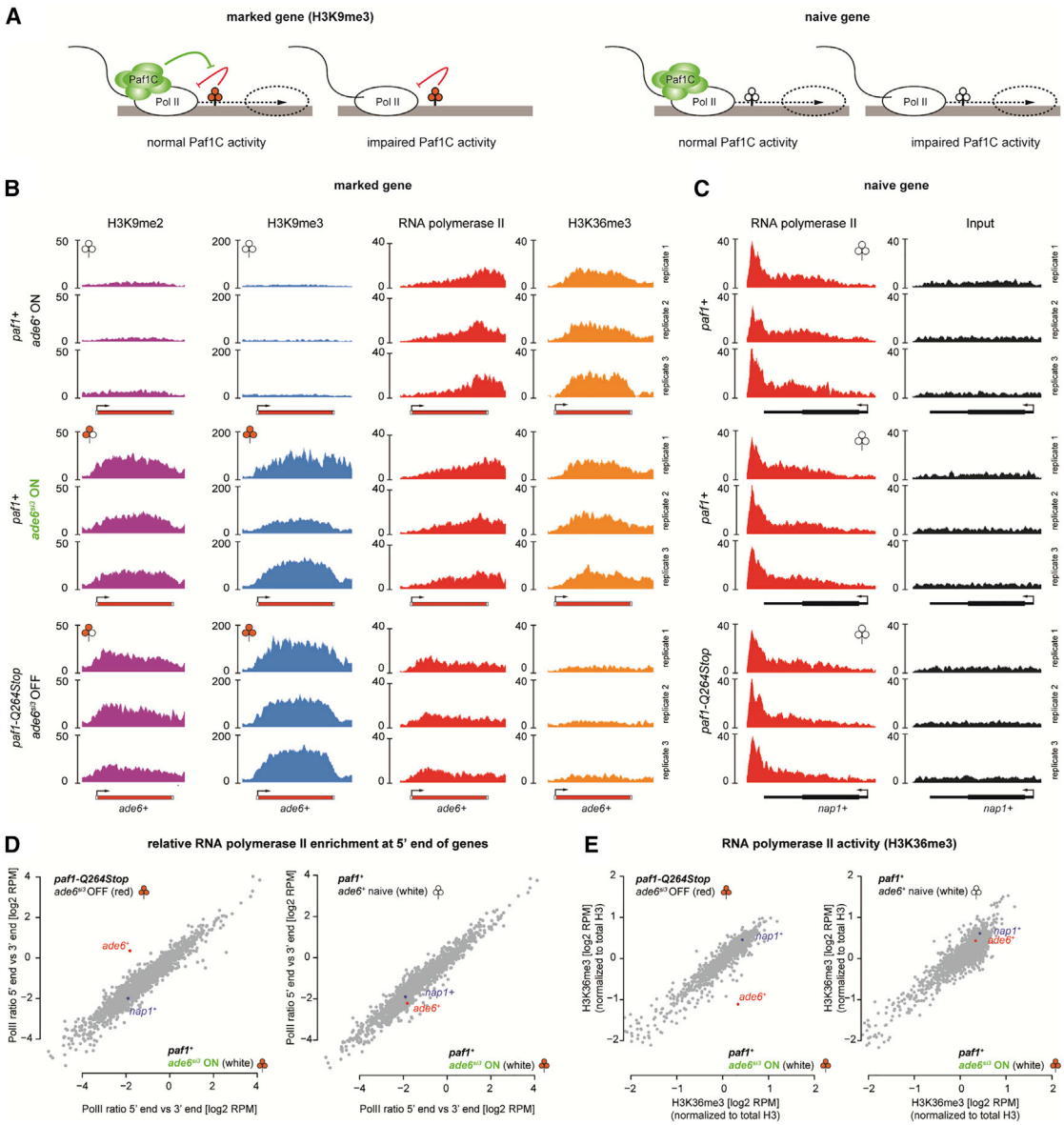

Figure 5. Paf1C Sustains Transcription when RNA Polymerase II Encounters H3K9me3 Marked Nucleosomes

(A) Schematic illustrating that Paf1C has an important role in sustaining transcription when RNA polymerase II encounters H3K9me3 marked nucleosomes.

(B) UCSC genome browser shots of naive and marked *ade6*$^{+}$ genes. ChIP-seq profiles for H3K9me2, H3K9me3, RNA polymerase II, and H3K36me3 for wild-type and *paf1-Q264Stop* cells were normalized to library size.

(C) UCSC genome browser shots of an unrelated euchromatic gene *nap1*$^{+}$. ChIP-seq profiles for RNA polymerase II for wild-type and *paf1-Q264Stop* cells were normalized to library size.

(D) Scatterplot quantifying RNA polymerase II (Pol II) redistribution between the 5′ end and the 3′ end of all expressed genes (n = 1,860; see STAR Methods). Shown are the log2 values of the ratio of read counts within the first 500 bp versus the last 500 bp of every gene. *ade6*$^{+}$ (red) and *nap1*$^{+}$ (blue) are highlighted. The left plot compares marked versus silenced cells, and the right plot compares marked with naive cells.

(E) Scatterplot comparing the levels of H3K36me3 over all genes. Shown are reads per million (RPM) values for each expressed gene (same gene list as in D). The left plot compares marked versus silenced cells, and the right plot compares marked with naive cells.

by mutating W41 to G (Schalch et al., 2009). In contrast to Chp1-F61A, the mark was lost and the silencing phenotype could not be re-established. This also occurred with the complete H3K9me3 binding mutant Clr4-W31G (Figure 4I). Therefore, maximal binding affinity of the Clr4, but not the Chp1, chromodomain to H3K9me3 is required for the inheritance of the marked *ade6*^{si3} epiallele. These results support a model in which Clr4 recognizes H3K9me3, which had been deposited during the initial primary siRNA-mediated silencing episode, and catalyzes the same modification on newly deposited histones. This

positive feedback loop is not self-sufficient but further depends on RITS binding to methylated H3K9 and subsequent amplification of secondary siRNAs, which promote further recruitment of Clr4 activity to the marked locus (Figure 4J).

RNA Polymerase II Accumulates at the Beginning of an H3K9 Methylated Gene if Paf1C Activity Is Impaired

Our results reveal that such coupling of siRNA- and H3K9me3-positive feedback regulation is still not sufficient to silence transcription of a protein-coding gene in *paf1*$^{+}$ cells. This attributes an important activity to Paf1C that facilitates transcription through H3K9me3 marked nucleosomes (Figure 5A). Supporting this, we observed a buildup of RNA polymerase II at the 5′ end of the marked *ade6*^{si3} OFF, but not on other genes in *paf1-Q264Stop* cells (Figures 5B–5D). Because H3K36 on *ade6*^{si3} OFF is not methylated (Figures 5B and 5E), we conclude that RNA polymerase II frequently stalls on H3K9 methylated nucleosomes if Paf1C activity is impaired. This implies that Paf1C's established function in promoting transcription elongation (Vos et al., 2018) is particularly important within difficult-to-transcribe chromatin. This is different from its less well-understood function in RNA 3′ end formation (Van Oss et al., 2017), which is important to prevent *de novo* deposition of H3K9 methyl marks (Kowalik et al., 2015). Thus, persistent impairment of Paf1C activity is required for manifestation of a silencing phenotype, but not for sustainable coupling of RNAi and H3K9me3 once initiated.

DISCUSSION

Our findings demonstrate that fission yeast has the ability to remember gene-silencing episodes that have occurred in previous generations. Unlike other examples of heritable epimutations (Baulcombe and Dean, 2014; Heard and Martienssen, 2014; Iwasaki and Paszkowski, 2014; Klosin and Lehner, 2016; Luteijn and Ketting, 2013; Yu et al., 2018), the phenomenon described here is unique in that the phenotypic change only manifests under the same conditions that had enabled acquisition of the epiallele. This shows that *S. pombe* cells can acquire a new trait that is plastic and can be passed down to its offspring. In *C. elegans*, environmental stresses give rise to changes in heritable small RNAs, which have been proposed to silence specific genes that could in turn improve the progeny's chance to cope with similar stresses (Rechavi and Lev, 2017). Because initiation of epigenetic gene silencing has only been observed in the presence of an enabling genetic mutation in *S. pombe* (Flury et al., 2017; Kowalik et al., 2015; Yu et al., 2018), modulation of repressors, such as Paf1C, is imperative for such an RNAe response to occur in the wild. Importantly, we noticed impaired recovery of spores after tetrad dissection of homozygous *paf1-Q264Stop* crosses (Figures S1C and S1E). This shows that functional Paf1C is vital for the reproductive success of *S. pombe*, and hence, RNAe-enabling mutations in Paf1C subunits are unlikely to become fixed during evolution. Yet our results raise the intriguing hypothesis that external factors, such as chemicals or metabolites present in the yeast's immediate environment, could transiently impair Paf1C activity and thereby enable the acquisition of a si3-marked epiallele. In light of this, we find it interesting that impaired Paf1C activity leads to seemingly stochastic production of siRNAs using endogenous mRNAs as templates (Kowalik et al., 2015), which continue to be amplified also in subsequent generations (Figure S5). Because these siRNAs have no homology to constitutive heterochromatin, they are not expected to trigger silencing that remains in wild-type cells (Yu et al., 2018) but rather leave, as we show here, a phenotypically neutral molecular mark. Therefore, transient inactivation of Paf1C could trigger random marking of protein-coding genes, some of which, or combinations thereof, may lead to an increased population fitness under adverse conditions. Such an epigenetic bet-hedging strategy would be ideal for a unicellular fungus to survive in a dynamic environment and could explain why this extremely potent form of cellular memory has evolved in this organism. Although challenging, it will be an exciting task to discover natural conditions that would lead to such a response.

STAR★METHODS

Detailed methods are provided in the online version of this paper and include the following:

- KEY RESOURCES TABLE
- CONTACT FOR REAGENT AND RESOURCE SHARING
- EXPERIMENTAL MODEL AND SUBJECT DETAILS
- METHOD DETAILS
  - Strains and plasmids
  - Mating and spore analysis
  - Analysis of epigenetic inheritance
  - Small RNA sequencing and analysis
  - Chromatin immunoprecipitation
  - ChIP-seq analysis
- QUANTIFICATION AND STATISTICAL ANALYSIS
- DATA AND SOFTWARE AVAILABILITY

SUPPLEMENTAL INFORMATION

Supplemental Information can be found with this article online at https://doi.org/10.1016/j.molcel.2019.02.009.

ACKNOWLEDGMENTS

We thank members of the Bühler lab for discussions, L. Kaaji for comments on the manuscript, and H. Pickersgill (Life Science Editors) for editing services. We thank N. Laschet for technical assistance and K. Hirschfeld and S. Smallwood for library construction and next-generation sequencing. This work has received funding from the European Research Council (ERC) under the European Union's Horizon 2020 research and innovation programme (grant agreement no. 681213 - REpiReg) and the Novartis Research Foundation.

AUTHOR CONTRIBUTIONS

L.D. and M.B. conceived ideas, designed and performed experiments, analyzed data, generated yeast strains, prepared figures, and wrote the manuscript. Y.S., S.L., A.A., and D.O. performed experiments and generated strains. F.M. and L.D. performed computational analyses. M.B. supervised the study and secured funding. All authors discussed results and commented on the manuscript.

DECLARATION OF INTERESTS

The Friedrich Miescher Institute for Biomedical Research (FMI) receives significant financial contributions from the Novartis Research Foundation.

Received: November 15, 2018
Revised: January 18, 2019
Accepted: February 6, 2019
Published: March 18, 2019

REFERENCES

Ashe, A., Sapetschnig, A., Weick, E.-M., Mitchell, J., Bagijn, M.P., Cording, A.C., Doebley, A.-L., Goldstein, L.D., Lehrbach, N.J., Le Pen, J., et al. (2012). piRNAs can trigger a multigenerational epigenetic memory in the germline of C. elegans. Cell *150*, 88–99.

Bähler, J., Wu, J.Q., Longtine, M.S., Shah, N.G., McKenzie, A., 3rd, Steever, A.B., Wach, A., Philippsen, P., and Pringle, J.R. (1998). Heterologous modules for efficient and versatile PCR-based gene targeting in Schizosaccharomyces pombe. Yeast *14*, 943–951.

Baulcombe, D.C., and Dean, C. (2014). Epigenetic regulation in plant responses to the environment. Cold Spring Harb. Perspect. Biol. *6*, a019471.

Chandler, V.L. (2007). Paramutation: from maize to mice. Cell *128*, 641–645.

Chandler, V.L. (2010). Paramutation's properties and puzzles. Science *330*, 628–629.

Dobin, A., Davis, C.A., Schlesinger, F., Drenkow, J., Zaleski, C., Jha, S., Batut, P., Chaisson, M., and Gingeras, T.R. (2013). STAR: ultrafast universal RNA-seq aligner. Bioinformatics *29*, 15–21.

Erhard, K.F., Jr., and Hollick, J.B. (2011). Paramutation: a process for acquiring trans-generational regulatory states. Curr. Opin. Plant Biol. *14*, 210–216.

Flury, V., Georgescu, P.R., Iesmantavicius, V., Shimada, Y., Kuzdere, T., Braun, S., and Bühler, M. (2017). The histone acetyltransferase Mst2 protects active chromatin from epigenetic silencing by acetylating the ubiquitin ligase Brl1. Mol. Cell *67*, 294–307.e9.

Forsburg, S.L., and Rhind, N. (2006). Basic methods for fission yeast. Yeast *23*, 173–183.

Gaidatzis, D., Lerch, A., Hahne, F., and Stadler, M.B. (2015). QuasR: quantification and annotation of short reads in R. Bioinformatics. *31*, 1130–1132.

Grentzinger, T., Armenise, C., Brun, C., Mugat, B., Serrano, V., Pelisson, A., and Chambeyron, S. (2012). piRNA-mediated transgenerational inheritance of an acquired trait. Genome Res. *22*, 1877–1888.

Heard, E., and Martienssen, R.A. (2014). Transgenerational epigenetic inheritance: myths and mechanisms. Cell *157*, 95–109.

Iwasaki, M., and Paszkowski, J. (2014). Epigenetic memory in plants. EMBO J. *33*, 1987–1998.

Jih, G., Iglesias, N., Currie, M.A., Bhanu, N.V., Paulo, J.A., Gygi, S.P., Garcia, B.A., and Moazed, D. (2017). Unique roles for histone H3K9me states in RNAi and heritable silencing of transcription. Nature *547*, 463–467.

Kent, W.J., Zweig, A.S., Barber, G., Hinrichs, A.S., and Karolchik, D. (2010). BigWig and BigBed: enabling browsing of large distributed datasets. Bioinformatics *26*, 2204–2207.

Klosin, A., and Lehner, B. (2016). Mechanisms, timescales and principles of trans-generational epigenetic inheritance in animals. Curr. Opin. Genet. Dev. *36*, 41–49.

Kowalik, K.M., Shimada, Y., Flury, V., Stadler, M.B., Batki, J., and Bühler, M. (2015). The Paf1 complex represses small-RNA-mediated epigenetic gene silencing. Nature *520*, 248–252.

Langmead, B., Trapnell, C., Pop, M., and Salzberg, S.L. (2009). Ultrafast and memory-efficient alignment of short DNA sequences to the human genome. Genome Biol. *10*, R25.

Luteijn, M.J., and Ketting, R.F. (2013). PIWI-interacting RNAs: from generation to transgenerational epigenetics. Nat. Rev. Genet. *14*, 523–534.

Luteijn, M.J., van Bergeijk, P., Kaaij, L.J.T., Almeida, M.V., Roovers, E.F., Berezikov, E., and Ketting, R.F. (2012). Extremely stable Piwi-induced gene silencing in Caenorhabditis elegans. EMBO J. *31*, 3422–3430.

Martin, M. (2011). Cutadapt removes adapter sequences from high-throughput sequencing reads. EMBnet.journal *17*, 10–12.

Quinlan, A.R. (2014). BEDTools: the swiss-army tool for genome feature analysis. Curr. Protoc. Bioinformatics *47*, 11.12.1–11.12.34.

Rechavi, O., and Lev, I. (2017). Principles of transgenerational small RNA inheritance in Caenorhabditis elegans. Curr. Biol. *27*, R720–R730.

Schalch, T., Job, G., Noffsinger, V.J., Shanker, S., Kuscu, C., Joshua-Tor, L., and Partridge, J.F. (2009). High-affinity binding of Chp1 chromodomain to K9 methylated histone H3 is required to establish centromeric heterochromatin. Mol. Cell *34*, 36–46.

Shirayama, M., Seth, M., Lee, H.-C., Gu, W., Ishidate, T., Conte, D., Jr., and Mello, C.C. (2012). piRNAs initiate an epigenetic memory of nonself RNA in the C. elegans germline. Cell *150*, 65–77.

Team, R.C. (2014). R: a language and environment for statistical computing. http://www.R-project.org/

Van Oss, S.B., Cucinotta, C.E., and Arndt, K.M. (2017). Emerging insights into the roles of the Paf1 complex in gene regulation. Trends Biochem. Sci. *42*, 788–798.

Verdel, A., Jia, S., Gerber, S., Sugiyama, T., Gygi, S., Grewal, S.I.S., and Moazed, D. (2004). RNAi-mediated targeting of heterochromatin by the RITS complex. Science *303*, 672–676.

Vos, S.M., Farnung, L., Boehning, M., Wigge, C., Linden, A., Urlaub, H., and Cramer, P. (2018). Structure of activated transcription complex Pol II-DSIF-PAF-SPT6. Nature *560*, 607–612.

Yu, R., Wang, X., and Moazed, D. (2018). Epigenetic inheritance mediated by coupling of RNAi and histone H3K9 methylation. Nature *558*, 615–619.

STAR★METHODS

KEY RESOURCES TABLE

REAGENT or RESOURCE	SOURCE	IDENTIFIER
Antibodies		
anti-H3, rabbit polyclonal	Abcam	Cat# ab1791, RRID:AB_302613
anti-H3K9me2, mouse monoclonal	MBL International	Cat# MABI0307, RRID:AB_11124951
anti-H3K9me3, rabbit polyclonal	Active Motif	Cat# 39161, RRID:AB_2532132
anti-H3K14ac, rabbit monoclonal	Novus	Cat# NB110-57051, RRID:AB_843953
anti-H3K36me3, rabbit polyclonal	Abcam	Cat# ab9050, RRID:AB_306966
anti-RNA polymerase II, mouse monoclonal	Covance Research Products Inc	Cat# MMS-126R, RRID:AB_10013665
Chemicals, Peptides, and Recombinant Proteins		
Glusulase	PerkinElmer	NEE154001EA
nourseothricin dihydrogen sulfate (NAT)	Fisher or WERNER BioAgents GmbH	Cat# 5029426 or Cat# 5.0
G418 sulfate (Geneticin)	Roche or Invitrogen/Life Technologies	Cat# 04727878001-2 or Cat# 10131027
Hygromycin	Sigma or Invitrogen/Life Technologies	Cat# H7772 or Cat# 10687010
NEBNext High-Fidelity 2X PCR Master Mix	NEB	Cat# M0541S
PrimeScript RT Master Mix	Takara	Cat# RR036A
Formaldehyde	Sigma	Cat# F8775
Tween 20	Sigma	Cat# P9416
PMSF	Sigma	Cat# P7626
cOmplete Protease Inhibitor Cocktail, EDTA-free	Roche	Cat# 05056489001
Dynabeads M-280 Sheep anti-Mouse IgG	Thermo Fisher	Cat# 11202D
Dynabeads M-280 Sheep anti-Rabbit IgG	Thermo Fisher	Cat# 11203D
Proteinase K	Roche	Cat# 3115879001
RNase A	Roche	Cat# 10109169001
AMPure XP Beads	Beckman Coulter	Cat# A63881
5-Fluoroorotic Acid (FOA)	US biological, Thermo Fisher	Cat# 207291-8-4
Critical Commercial Assays		
MasterPure Yeast RNA Purification Kit	Epicenter	Cat# MCR85102
Protein Assay Dye Reagent Concentrate	Bio-Rad	Cat# 500-0006
QIAseq miRNA Library Kit	QIAGEN	Cat# 331505
SsoAdvanced Universal SYBR Green Supermix	Bio-Rad	Cat# 172-5274
NEBNext Ultra II DNA Library Prep Kit for Illumina	NEB	Cat# E7645L
NEBNext Multiplex Oligos for Illumina	NEB	Cat# E7600S
Deposited Data		
smallRNA and ChIP-seq data	This paper	GEO: GSE120352
Experimental Models: Organisms/Strains		
S. pombe: Strain background: 972, see Table S1	This paper	N/A
Oligonucleotides		
Primers, see Table S2	This paper	N/A
Recombinant DNA		
pJET1.2 - clr4-F449Y	This paper	pMB1858
pJET1.2 - clr4-W31G::hph	This paper	pMB1928
pJET1.2 - clr4-W41G::hph	This paper	pMB1929
pJET1.2 - chp1-V24R::hph	This paper	pMB1931
pJET1.2 - chp1-F61A::hph	This paper	pMB1932

(*Continued on next page*)

Continued

REAGENT or RESOURCE	SOURCE	IDENTIFIER
Software and Algorithms		
Plugin Cell Counter 2.2.2	Fiji	https://imagej.nih.gov/ij/plugins/cell-counter.html
bcl2fastq2 v2.17	Illumina	https://support.illumina.com/sequencing/sequencing_software/bcl2fastq-conversion-software.html
STAR	Dobin et al., 2013	https://github.com/alexdobin/STAR
bedtools (version 2.26.0)	Quinlan, 2014	https://github.com/arq5x/bedtools2/
bedGraphToBigWig (from UCSC binary utilities)	Kent et al., 2010	http://genome.ucsc.edu/
R	Team, 2014	https://www.r-project.org/
QuasR	Gaidatzis et al., 2015	https://bioconductor.org/packages/release/bioc/html/QuasR.html
Other		
Illumina HiSeq2500	Illumina	N/A
Agilent 1100 system	Agilent	N/A
MSM System 400	Singer Instruments	Serial number 686-400-43911
Bioruptor Plus sonication device	Diagenode	N/A

CONTACT FOR REAGENT AND RESOURCE SHARING

Published research reagents from the FMI are shared with the academic community under a Material Transfer Agreement (MTA) having terms and conditions corresponding to those of the UBMTA (Uniform Biological Material Transfer Agreement). All custom codes used to analyze data and generate figures are available upon reasonable request. Genome-wide datasets are deposited at GEO under the accession number GSE120352. Further information and requests for resources and reagents should be directed to and will be fulfilled by the Lead Contact, Marc Bühler (marc.buehler@fmi.ch).

EXPERIMENTAL MODEL AND SUBJECT DETAILS

Schizosaccharomyces pombe strains used in this study are derivates of the standard laboratory strain 972 and are listed in Table S1. Strains were grown at 30°C either in liquid YES media (160rpm) or on solid agarose plates (YE or YES plates).

METHOD DETAILS

Strains and plasmids

S. pombe strains were generated by genetic crossing or by homologous recombination with transformed DNA (Bähler et al., 1998; Forsburg and Rhind, 2006). For the generation of the point mutants *clr4-F449Y*, *clr4-W31G*, *clr4-W41G*, *chp1-V24R*, *chp1-F61A*, first the entire *clr4* ORF or the first 90bp of *chp1* were deleted with URA3 from Candida albicans and then replaced by the mutated ORF at the same locus by FOA counter selection. *ago1Δ*, *clr4Δ*, *dcr1Δ* and *rdp1Δ* mutants were generated by deletion of the entire ORF with a hphMX or natMX cassette. All strains used in this study are listed in Table S1.

Mating and spore analysis

For a genetic cross, cells of opposite mating type were mixed in 10 μL H_2O, plated on SPAS plates (Forsburg and Rhind, 2006) and incubated at room temperature for 2-3 days. Cells were suspended in 1 mL H_2O and asci formation was assessed by microscopy. For random spore analysis (RSA), 2 μL glusulase were added and incubated either at 30°C for 8 hours or at room temperature overnight to kill vegetative cells. Different dilutions were plated to receive 20-500 colonies/plate. For tetrad dissection (Figures 1D, S1C, and S1E), 10 μL of a 1:100 tetrad asci dilution were dispersed on a yeast extract (YE) plate (Forsburg and Rhind, 2006) and tetrads were separated with a Singer Instruments MSM System. After 6 hours at room temperature, spores were dissected and plates were incubated at 30°C to allow colony formation (4-5 days).

Analysis of epigenetic inheritance

Inheritance of the marked ade6⁺ epiallele

F10 *h- paf1-Q264Stop ade6^{si3}* OFF cells (SPB3850) were crossed with *h+ paf1⁺ ade6⁺* ON cells (SPB3728). After 2 days, RSA was performed and spores were plated on YE plates. After 4-5 days colonies were genotyped. *h- paf1⁺* colonies were selected and grown in 55ml YES (Forsburg and Rhind, 2006). Cells were harvested at OD = 1 for ChIP, small RNA sequencing, and further

mating. F11 *h- paf1*$^{+}$ were crossed to *h+ paf1-Q264Stop::kanR ade6*$^{+}$ ON (SPB2063). After 2 days, RSA was performed and cells were plated on YE + geneticin (100ug/ml) plates to select for *paf1-Q264Stop::kanR* cells. After 5-7 days, images were acquired and the phenotype of the F12 *paf1-Q264Stop* colonies was manually quantified with the Fiji plugin Cell Counter.

Mitotic stability of the marked ade6^{+} *epiallele*

For Figures 3A and 3B, F10 *h- paf1-Q264Stop ade6*^{si3} OFF cells (SPB3850) were crossed with *h+ paf1*$^{+}$ *ade6*$^{+}$ ON cells (SPB3728). After 2 days, RSA was performed. 4 days later, F11 *h- paf1*$^{+}$ *ade6*^{si3} ON colonies were transferred to YES media and grown at 30°C at 200 rpm. The liquid cultures were kept in an exponential growth phase by diluting with YES media twice a day. Every 72 hours (30-40 mitotic cell divisions) a sample was crossed to *h+ paf1-Q264Stop::kanR ade6*$^{+}$ ON cells (SPB2063). After 2 days, RSA was performed and cells were plated on YE geneticin (100ug/ml) plates. 5-7 days later images were acquired and the phenotype of the F12 *paf1-Q264Stop* colonies was quantified.

Meiotic stability of the marked ade6^{+} *epiallele*

For Figures 3C and 3D, F10 *h- paf1-Q264Stop ade6*^{si3} OFF cells (SPB3850) were crossed to *h+ paf1*$^{+}$ *ade6*$^{+}$ ON cells (SPB3728). After 2 days, RSA was performed. After 4 days F11 *h- paf+ ade6*^{si3} ON colonies were crossed to *h+ paf+ ade6*$^{+}$ ON cells. After 2 days, F12 tetrad asci were inoculated in 1ml H_2O + 2 μL glusulase and incubated at 30°C for 10 hours with occasional vortexing. Spore pellets were resuspended in YES media and incubated at 30°C for 3 days for recovery. Then cells were crossed with *h+ paf1-Q264Stop::kanR ade6*$^{+}$ ON cells (SPB2063). After 2 days, RSA was performed and cells were plated on YE geneticin (100ug/ml) plates. 5-7 days later images were acquired and the phenotype of the F12 *paf1-Q264Stop* colonies was determined.

Small RNA sequencing and analysis

Total RNA from exponentially growing cultures was extracted with the MasterPure Yeast RNA Purification Kit (Epicenter). Small RNA libraries were prepared with the QIAseq miRNA Library Kit (QIAGEN) according to manufacturer's instructions and sequenced with an Illumina HiSeq2500. 3′ adaptor sequences were removed from the raw reads using Cutadapt (Cutadapt –a ''adapter''–discard-untrimmed -m 18) (Martin, 2011). Reads < 18 nt and untrimmed reads were removed. Trimmed reads were aligned to the *S. pombe* genome (ASM294 version 2.24) using Bowtie (bowtie -f -M 10000 -v 0 -S–best–strata) (Langmead et al., 2009). All analysis was done with uniquely mapping reads, which were extracted using mapping quality (mapq = 255) since bowtie assigns multi-mapping reads mapq = 0.

Chromatin immunoprecipitation

50 mL of exponentially growing cells were cross-linked at OD = 1/1.2 with 0.9% Formaldehyde for 15 min at room temperature. The crosslinking reaction was quenched with 2.6 mL Glycine (2.5 M) for 5 min at room temperature. After 2 washing steps with ice cold PBS Tween 20 (0.02%), cell pellets were lysed in ChIP lysis buffer (50 mM HEPES KOH pH 7.5, 140 mM NaCl, 1 mM EDTA, 1% Triton X-100, 0.1% Na-deoxycholate, 1 mM PMSF, 1x Roche cOMPLETE protease inhibitor cocktail) using a bead-beater (three times 1 min). Lysates were sonicated with a Bioruptor three times 10 × 30 s (30 s off) with 5 min pause in between. After centrifugation for 1x 5 min and 1x 15min, the protein concentration of the supernatant was determined using the Bio-Rad Assay. Equal protein amounts (1ug-2ug) were incubated with antibody overnight (12-16 hr) at 4°C (2.5 μL histone H3-specific antibody, 2.5 μL histone H3K9me2-specific antibody, 3 μL histone H3K9me3-specific antibody, 2.5 μL H3K36me3-specific antibody, and 2.5 μL RNA polymerase II antibody). Then supernatant + antibody were incubated with 30/40 μL Dynabeads. Washes were performed three times with lysis buffer, once with wash buffer (10 mM Tris/HCl pH 8, 250 mM LiCl, 0.5% NP40, 0.5% sodium deoxycholate and 1 mM EDTA) and once with TE buffer. Eluates were de-crosslinked in TE and 1% SDS over night at 65°C and subsequently treated with RNase A (0.2 mg/mL) for 1 hr at 37°C and 0.1 mg protease K for 1 hr at 65°C. DNA was purified using AMPure XP Beads and eluted in 20 μL 10mM Tris/HCl pH 8.

For ChIP-qPCR, SsoAdvanced Universal SYBR Green Supermix (Bio-Rad) was used. Enrichment was calculated by normalization to the *adh1*+ or *act1*+ locus over *clr4Δ*, which lacks H3K9me2 and H3K9me3. Primers used in this study are listed in Table S2.

For multiplex ChIP sequencing, samples were prepared with NEBNext Ultra II DNA Library Prep Kit for Illumina (NEB) and NEBNext Multiplex Oligos for Illumina (NEB).

ChIP-seq analysis

ChIP libraries were sequenced 50bp single-end on an Illumina HiSeq 2500 instrument. Raw data were demultiplexed and converted to fastq format using bcl2fastq2 v1.17 and mapped using STAR with the following parameters: –alignIntronMax 1–alignEndsType EndToEnd–outFilterType Normal–seedSearchStartLmax 30–outFilterMultimapNmax 10000–outSAMattributes NH HI NM MD AS nM–outMultimapperOrder Random–outSAMmultNmax 1–outSAMunmapped Within. For bigwig track generation by bedtools (version 2.26.0) and bedGraphToBigWig (from UCSC binary utilities), non-aligned reads and muli-mapping reads were discarded and read coverage was normalized to 1 million genome mapping reads (RPM).

H3K36me3 and RNA Pol II quantification was performed as follows: Overlapping genes, genes smaller than 1 kb and genes having another gene closer than 10 bp were excluded to avoid wrong assignment of reads. Then analysis was restricted to expressed genes only (i.e., genes with an RPM > 15), which yielded a final list of 1860 non-overlapping and expressed genes that could be unambiguously quantified. For H3K36me3, RPM values per gene were displayed as a scatterplot. For RNA polymerase II, we quantified the relocalization of Pol II relative to the gene ends. This was done by calculating the ratio of reads mapping to the first 500bp of every

gene divided by the number of reads mapping to the last 500bp of the same gene. The log2 values of this ratio (log2(read count5′end / read count 3′end)) were then plotted as scatterplot. Due to the insertion of a resistance cassette after the *paf1-Q264Stop* allele, we removed this gene from the analysis as the modification of the genomic locus gave rise to ChIP and mapping artifacts that precluded quantification.

QUANTIFICATION AND STATISTICAL ANALYSIS

The number of n biological replicates is given in each figure legend. p values were calculated using two-tailed Student's t tests with two-sample assuming unequal variances. The error bars in the plots denote SD, the center values denote the mean. No data or subjects were excluded.

DATA AND SOFTWARE AVAILABILITY

Genome-wide datasets are deposited at GEO under the accession number GEO: GSE120352 or were previously described in Kowalik et al., 2015 (GEO: GSE59170). All custom codes used to analyze data and generate figures are available upon reasonable request.

Molecular Cell, Volume *74*

Supplemental Information

Inheritance of a Phenotypically Neutral Epimutation Evokes Gene Silencing in Later Generations

Lea Duempelmann, Fabio Mohn, Yukiko Shimada, Daniele Oberti, Aude Andriollo, Silke Lochs, and Marc Bühler

SUPPLEMENTARY FIGURE LEGENDS

Figure S1. Transgenerational inheritance of an RNAi-directed gene silencing phenotype in the absence of the original siRNA trigger, Related to Figure 1

A, Schematic diagram depicting euchromatic origin (green) and target (red) of synthetic *ade6-hp* siRNAs. Gene silencing is not initiated in the presence of wild type Paf1C (Kowalik et al., 2015; Yu et al., 2018). **B**, Genotypes of strains used to assess transgenerational inheritance of gene silencing in *paf1-Q264Stop* cells. **C**, Representative pedigree illustrating spore viability and inheritance of the red silencing phenotype over 18 generations. Red *paf1-Q264Stop* (*ade6*$^{+}$ OFF) colonies were repeatedly crossed with white *paf1-Q264Stop* (*ade6*$^{+}$ ON) cells and tetrads were dissected on YE plates. Note that the ade6-hairpin, which initiated silencing in the parental strain (F0), was no longer present from F1 onwards. Each row represents the four spores that were micro-dissected from one tetrad. Grey dotted circles indicate spores that were dissected but failed to form a mitotically growing colony. Yellow box highlights F10 spores that gave rise to cells that were analyzed in Figure 1. **D**, Quantification of spore viability, as well as inheritance and mitotic stability (maintenance) of the *ade6*$^{+}$ silencing phenotype for five generations of three independent pedigrees. **E**, Representative photograph of a spore dissection experiment on YE plates. Left picture shows generation F8 of pedigree 2 as illustrated in c (homozygous *paf1-Q264Stop* cross). Right picture shows a heterozygous cross of red *paf1-Q264Stop* (F7) and white *paf1*$^{+}$ cells. The + symbol denotes those spores that inherited the wild type *paf1*+ allele. Note that the spore viability phenotype observed in homozygous crosses was largely rescued in the heterozygous crosses.

Figure S2. Secondary *ade6*$^{+}$ siRNAs persist in wild type progeny if they were present in the previous *paf1*$^{+}$ mutant generation, Related to Figure 2

A and B, Cells originating from four independent white (A, *ade6*$^{+}$ ON) and red (B, *ade6*^{si3} OFF) *paf1-Q264Stop* spores of generation 10 were crossed with wild type cells. *paf1*$^{+}$ progeny was subjected to sRNA sequencing. sRNA profiles over the *ade6*$^{+}$ gene of cells carrying either *ade6*$^{+}$ ON (A) or *ade6*^{si3} ON (B) alleles are shown. **C**, Length distribution and 5' U bias of small RNAs shown in B, which are characteristic of siRNAs. A-C, Read counts were normalized to library size.

Figure S3. The *ade6*$^{+}$ silencing phenotype is lost in wild type cells, but is re-established by repeated Paf1C impairment, Related to Figures 2 and 3

A, Crossing scheme for testing the inheritance of the marked *ade6*^{si3} epiallele in wild type cells and re-establishment of the silencing phenotype upon repeated Paf1C impairment. **B**, Representative images of a typical experiment performed to follow the *ade6*$^{+}$ silencing phenotype across generations (*paf1-Q264Stop* to *paf1*$^{+}$ to *paf1-Q264Stop*). RSA, random spore analysis. **C**, Recurrence frequency of the *ade6*$^{+}$ silencing phenotype (red color) in *paf1-Q264Stop* progeny whose parents were phenotypically normal (white). n=23 different crosses over 3 generations as depicted in a. At least 500 colonies (spores) per cross were scored for the silencing phenotype. Centre values denote the mean; error bars denote s.d.; P values were calculated with two-tailed Student's t-test **D,** Mitotic stability of the silent state that was re-established upon repeated *paf1*$^{+}$ mutation. 3 red *paf1-Q264Stop* F12 colonies for each of the 4 crosses analyzed in c were investigated (n=12). At least 500 cells per F12 clone were plated at single cell density and inspected for the silencing phenotype after mitotic propagation. The silencing phenotype was never observed if the original F10 colony was white (n>1500 colonies per plating). Centre values denote the mean; error bars denote s.d.; P values were calculated

with two-tailed Student's t-test. **E**, UCSC genome browser shots showing the ChIP-seq profiles at *ade6*$^{+}$ for H3K36me3, total H3, and input for wild type (with and without marked *ade6*$^{+}$) and *paf1-Q264Stop* cells. Profiles were normalized to library size. n = 3 different crosses.

Figure S4. H3K9 tri-methylation activity of Clr4 is required for continuous *ade6*$^{+}$ siRNA generation, Related to Figure 4

A, Red *paf1-Q264Stop* colonies (F10) were crossed with *paf1*$^{+}$ cells either lacking key RNAi factors (Ago1, Dcr1, or Rdp1) or the H3K9 methyltransferase Clr4, or expressing a mutant Clr4 that is deficient in catalyzing H3K9me3 (Clr4-F449Y). 3 spores for each combination of *paf1*$^{+}$ with one of the RNAi, Clr4 mutant alleles or wild type (*ade6*^{si3}) were expanded and subjected to small RNA sequencing. **B and C**, siRNA profiles over *ade6*$^{+}$ and the *dg* and *dh* repeats of *otrIR* are shown. Counts were normalized to library size.

Figure S5. Impaired Paf1C activity leads to the production of endogenous siRNAs that are complementary to protein-coding genes, Related to Figure 1

A, Wild type and different Paf1C mutant cells were subjected to small RNA sequencing. (A-C) All three *S. pombe* chromosomes are shown. siRNA peaks mapping to protein-coding genes are indicated by the black or green dots. Only small RNA reads with a length distribution and 5' U bias characteristic of siRNAs were considered. Gene names are indicated on top. **B**, Parental *paf1-Q264Stop* cells (indicated by a red line in A) were crossed and their descendants of the fourth generation were subjected to small RNA sequencing. Two independent crosses were analyzed (pedigree 1 and 2). Black dots denote siRNA peaks that arose newly over the four generations. Green dots denote siRNA peaks that were already present in the parental cells. **C**, F1 spores of another cross (pedigree 4) of the same parental cells as in B (indicated by a red line in A). Green dots denote siRNA peaks that were already present in the parental

cells. Blue dots denote siRNAs that were absent in parental cells but arose also in other pedigrees.

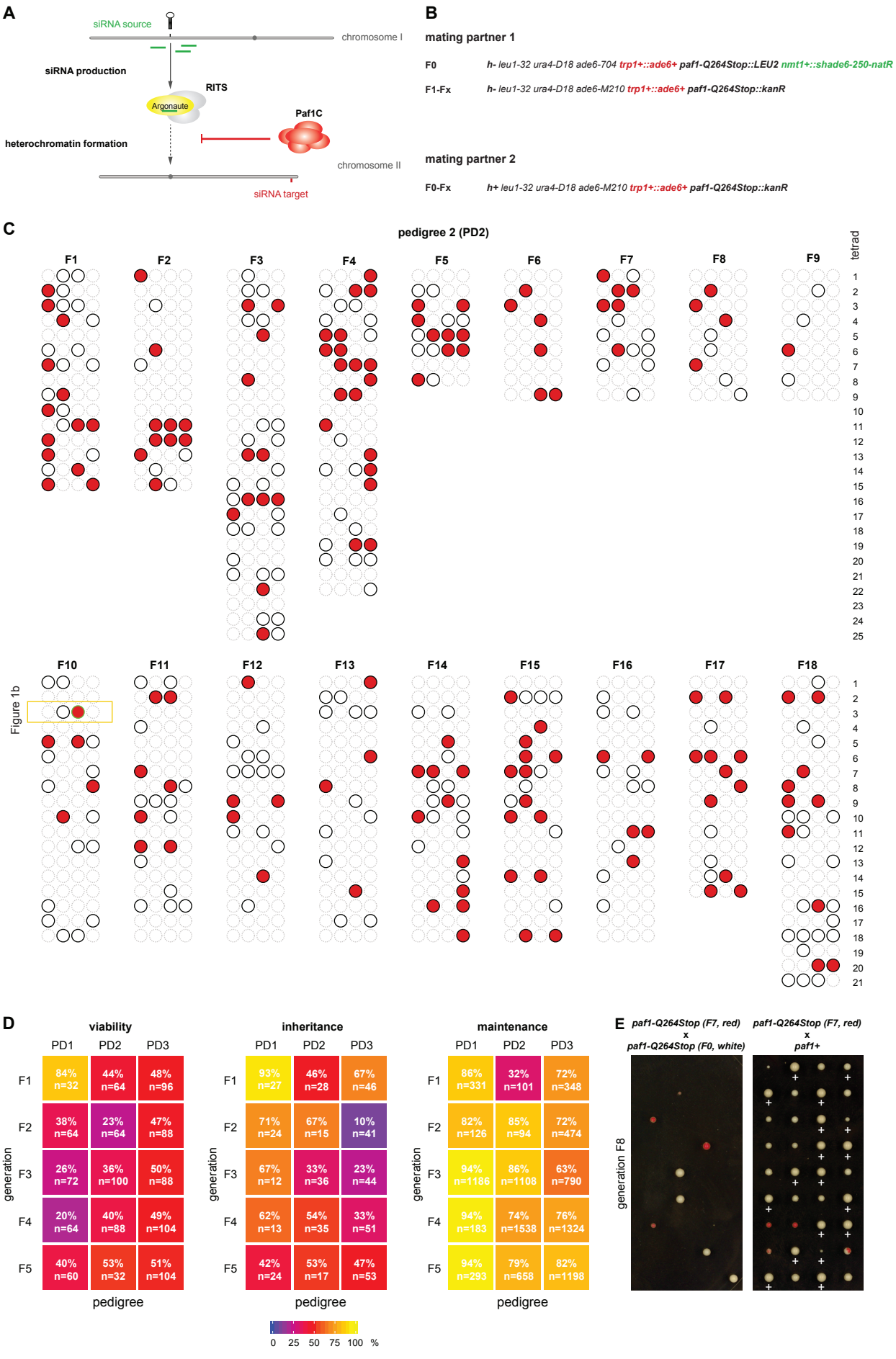

Dümpelmann *et al*, Figure S1

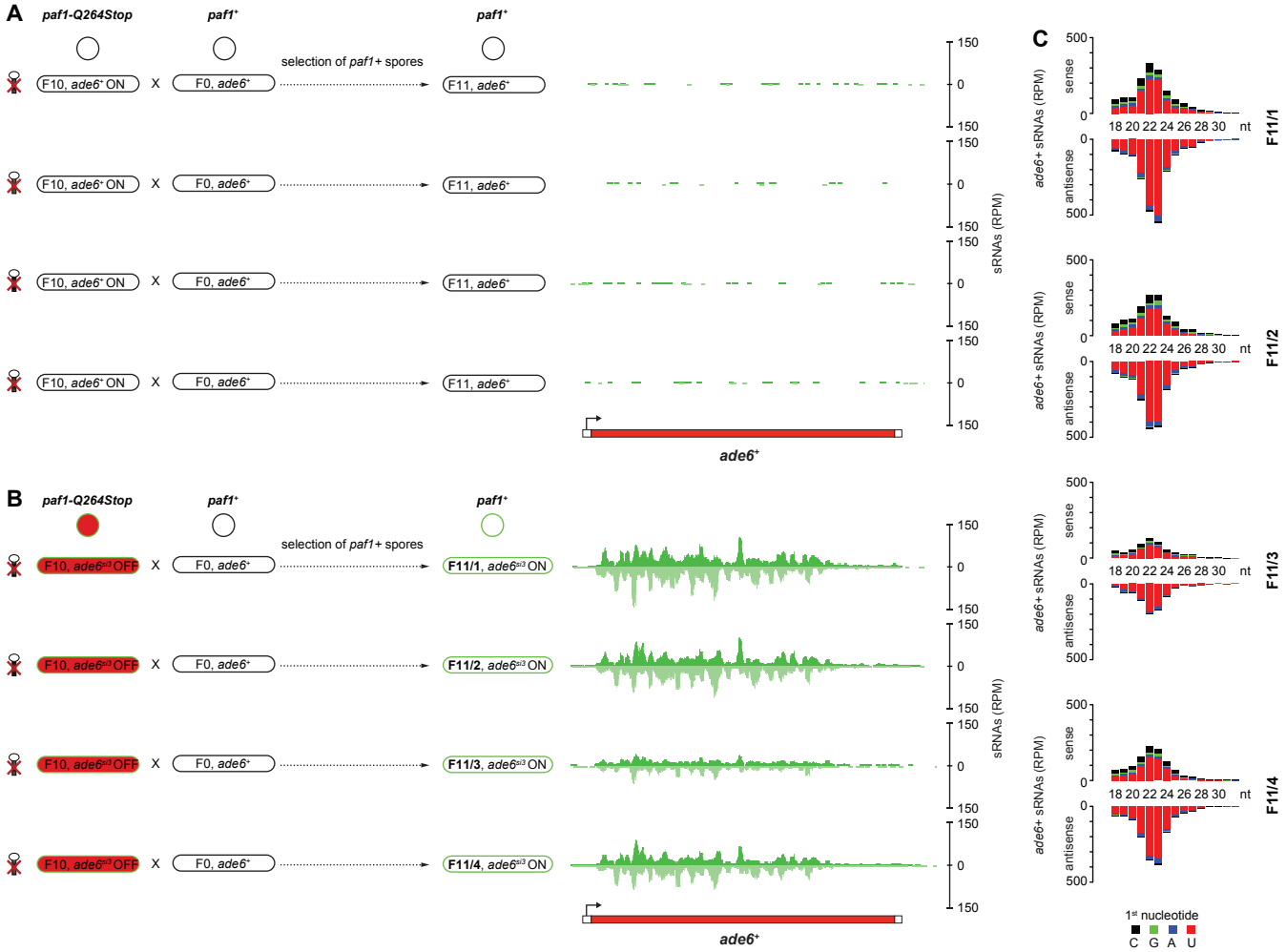

Dümpelmann *et al*, Figure S2

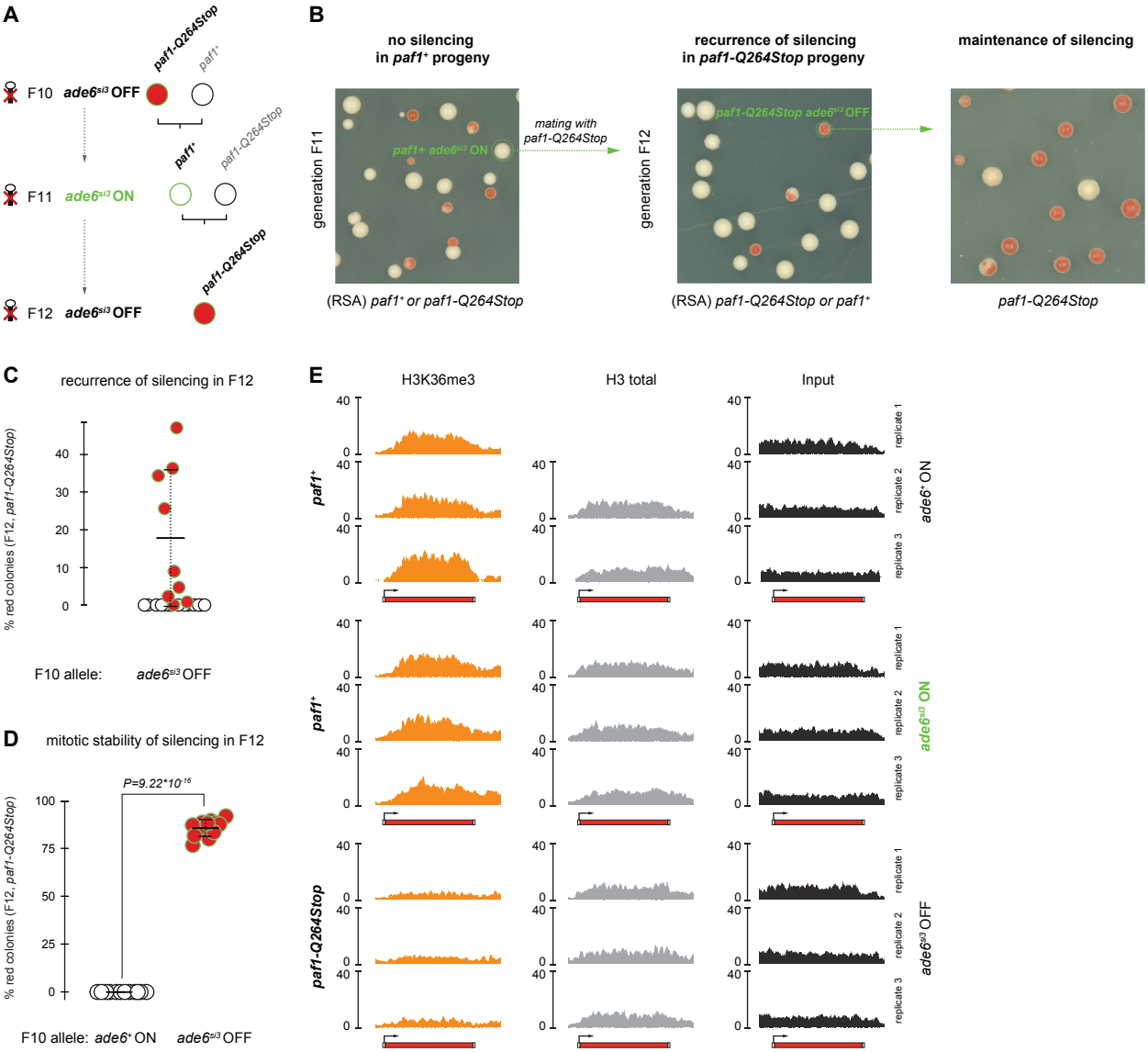

Dümpelmann *et al*, Figure S3

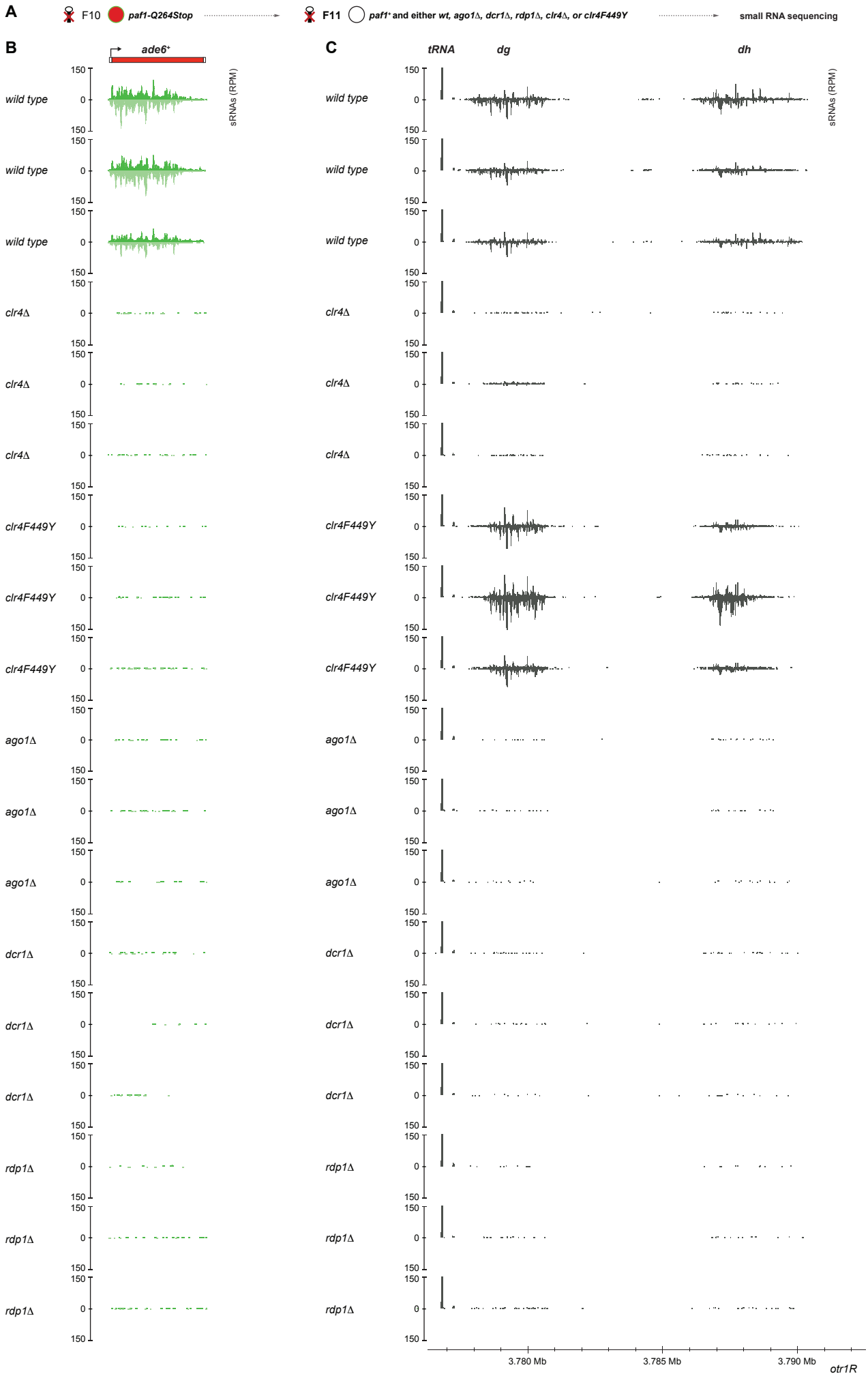

Dümpelmann *et al*, Figure S4

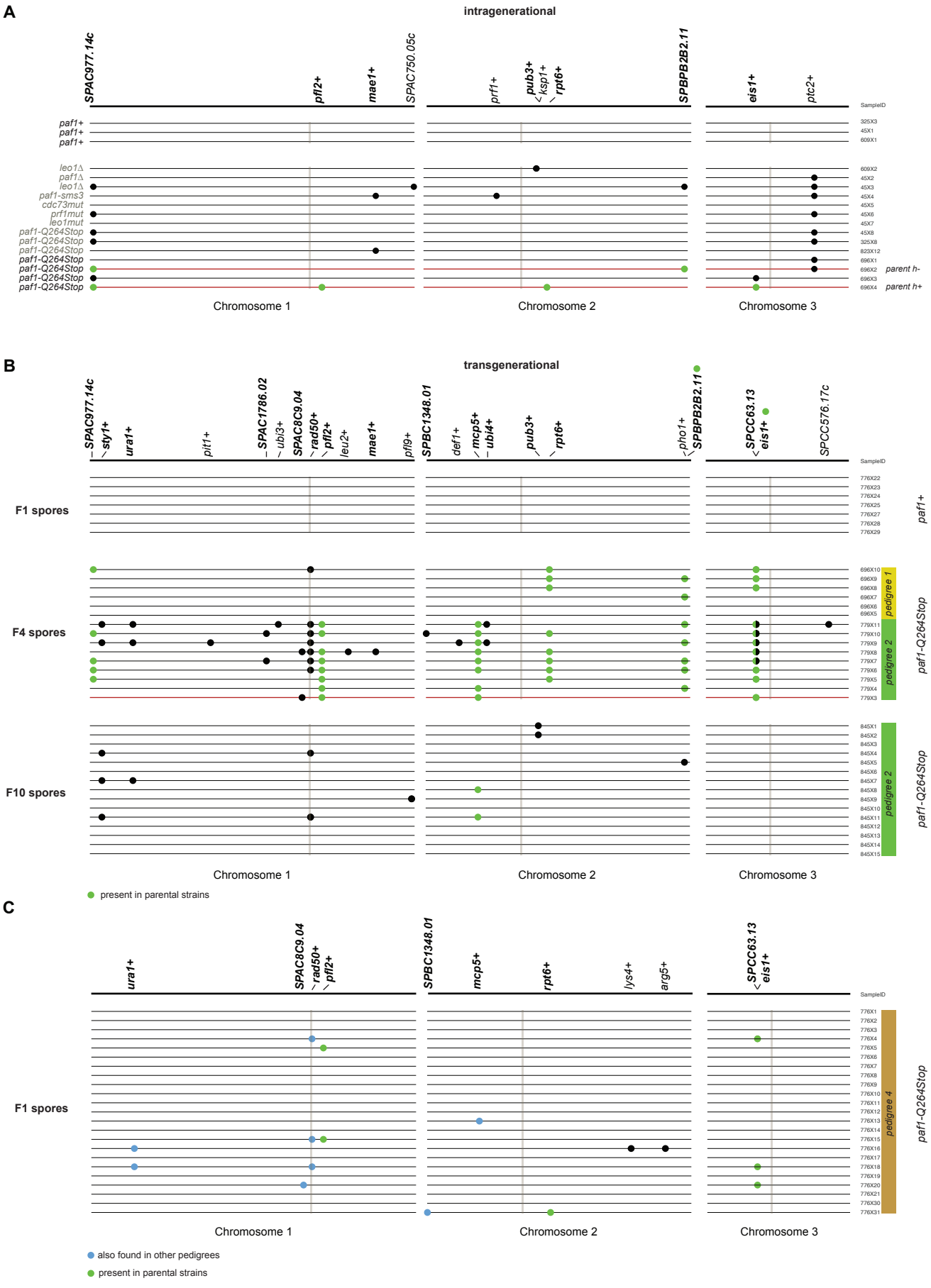

Dümpelmann *et al*, Figure S5

© 2020. Published by The Company of Biologists Ltd | Biology Open (2020) 9, bio052936. doi:10.1242/bio.052936

METHODS & TECHNIQUES

A fully automated deep learning pipeline for high-throughput colony segmentation and classification

Sarah H. Carl[1,2,*], Lea Duempelmann[1,3], Yukiko Shimada[1] and Marc Bühler[1,3,*]

ABSTRACT

Adenine auxotrophy is a commonly used non-selective genetic marker in yeast research. It allows investigators to easily visualize and quantify various genetic and epigenetic events by simply reading out colony color. However, manual counting of large numbers of colonies is extremely time-consuming, difficult to reproduce and possibly inaccurate. Using cutting-edge neural networks, we have developed a fully automated pipeline for colony segmentation and classification, which speeds up white/red colony quantification 100-fold over manual counting by an experienced researcher. Our approach uses readily available training data and can be smoothly integrated into existing protocols, vastly speeding up screening assays and increasing the statistical power of experiments that employ adenine auxotrophy.

KEY WORDS: Deep learning, Neural networks, Adenine auxotrophy, Yeast, Growth assay

INTRODUCTION

Auxotrophy is the inability of an organism to synthesize a particular organic compound required for its growth. For example, yeasts with mutations in the adenine biosynthetic pathway cannot grow on media lacking adenine. When grown under adenine-limiting conditions, adenine auxotrophs grow but accumulate a cell-limited red pigment in their vacuoles, whereas wild-type cells grow white. This red/white colony color assay has been widely used over the last few decades for the investigation of many biological processes, such as recombination, copy number, chromosome loss, plasmid stability, prion propagation, or epigenetic gene regulation in both budding and fission yeasts. However, adapting this assay to quantitative high-throughput applications has proven challenging, as it requires extensive scoring of colony phenotypes by eye. In addition to being time-consuming and tedious, manual colony scoring may suffer from inaccuracy and irreproducibility. Nonetheless, up to now manual scoring is a common practice in the yeast community. Modern machine-learning techniques such as deep learning have made huge strides in automated image classification in recent years and are beginning to be applied to previously intractable problems in the biomedical imaging domain. We set out to leverage these recent developments to build a computational pipeline that would enable fully automated high-throughput adenine auxotrophy-based screening and quantification.

Typically, red/white colony color assays start with plating individual yeast cells on limiting adenine indicator plates and allowing them to grow until they form colonies large enough to be inspected by eye. Each plate may represent an independent condition or genotype, the penetrance of which can be assessed by quantifying the percentage of non-white colonies per plate. In order to create a pipeline that would fit into existing protocols as seamlessly as possible, we considered our input to be images of plates and our desired output to be percentages of white and non-white colonies per plate. Two major tasks are required to generate this output: separating the colonies from the plate background and classifying them individually as white or non-white.

These two tasks could conceivably be completed either in one step, as with a single-shot detector (Liu et al., 2016) or RetinaNet (Lin et al., 2017), or in two separate steps, such as with a semantic segmentation, where each pixel is assigned a label such as 'foreground' or 'background', followed by classification of cropped images. While a single-step approach may be preferable from the perspective of algorithmic efficiency and speed (Huang et al., 2016), the training data annotations are more complex, requiring both manually assigned labels and matched bounding boxes identifying the location of each colony on a plate. As insufficient training data is a common problem hampering efforts to apply deep learning in many biological domains (Hughes et al., 2018), we opted to use a pragmatic approach, treating the segmentation and classification steps as separate problems (Fig. 1A). This allowed us to use simpler and, when available, pre-existing annotations for training data: for the segmentation task, we used masks generated previously using the Ilastik image-processing toolkit (Sommer et al., 2011), while for the classification task, we relied on manual labels assigned by experienced biologists to cropped images of single colonies. All of our training data consisted of *Schizosaccharomyces pombe* colonies, with red pigment resulting from heterochromatin-mediated silencing of the *ade6*$^{+}$ gene.

RESULTS

Implementation of the pipeline

All analyses were performed in Python v. 3.6.5 inside a conda virtual environment (v. 4.5.4). Deep learning models were built and trained using the fast.ai library (https://github.com/fastai/fastai) (Howard and others, 2018). Image processing steps were performed using the scikit-image library (v. 0.13.1) (https://scikit-image.org) (van der Walt, 2014). Model training and prediction was run on a GeForce GTX 1080 GPU with CUDA v. 9.0 and CUDNN v. 7.1.2.

Image segmentation

A modified U-net architecture using a Resnet-34 network pre-trained on ImageNet as the encoder was used as the network

[1]Friedrich Miescher Institute for Biomedical Research, Maulbeerstrasse 66, 4058 Basel, Switzerland. [2]SIB Swiss Institute of Bioinformatics Quartier Sorge - Batiment Amphipole 1015, Lausanne, Switzerland. [3]University of Basel, Petersplatz 10, 4003 Basel, Switzerland.

*Authors for correspondence (marc.buehler@fmi.ch, sarahhcarl@gmail.com)

S.H.C., 0000-0003-3927-2559; L.D., 0000-0002-5775-5186; M.B., 0000-0001-6661-9795

Received 15 April 2020; Accepted 14 May 2020

Biology Open (2020) 9, bio052936. doi:10.1242/bio.052936

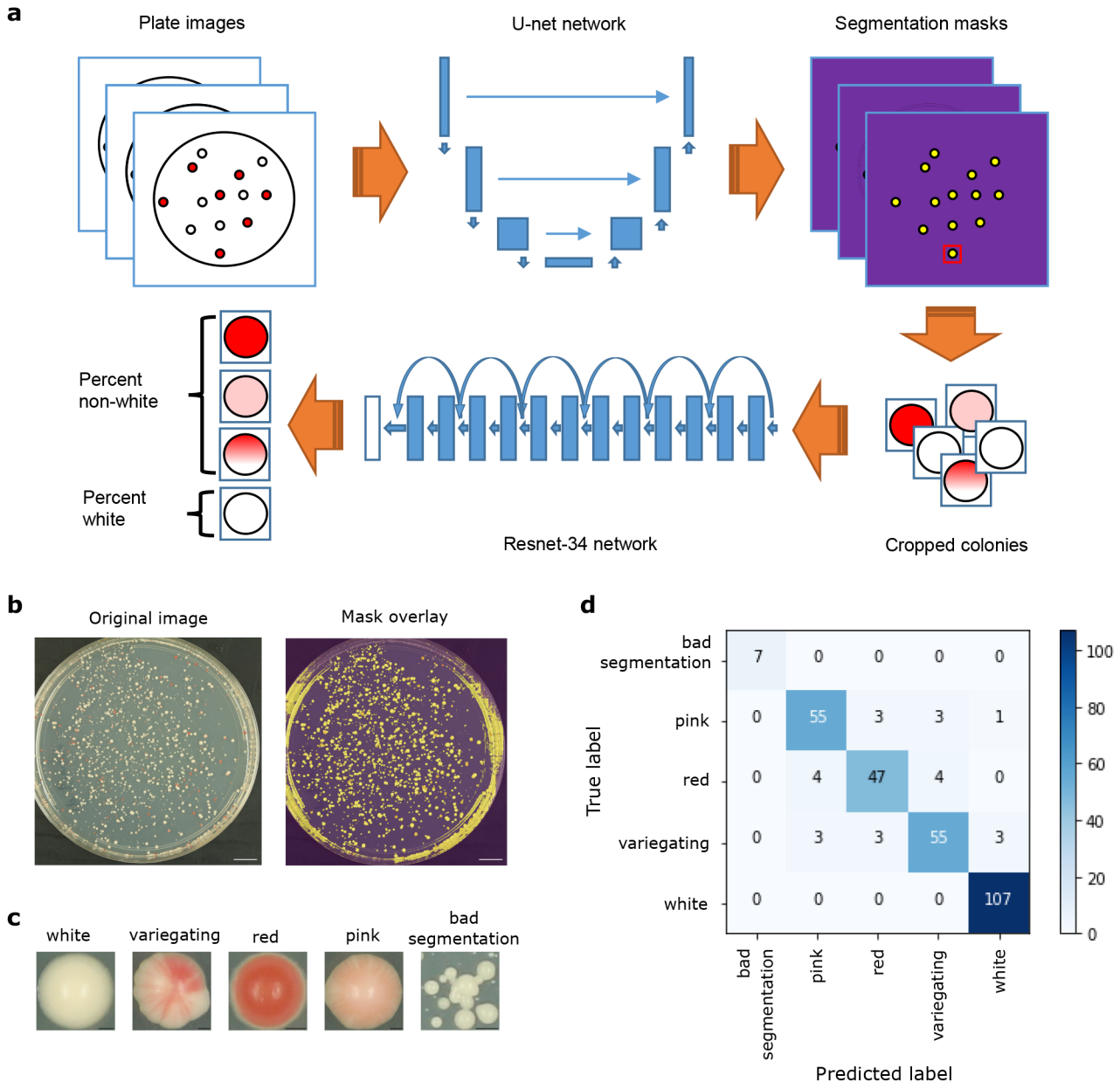

Fig. 1. Overview of deep learning setup and results. (A) Schematic of the entire automated colony classification pipeline. Plate images are given as input, then pass through a U-net network for segmentation prediction, resulting in cropped colony images. These are then fed into a Resnet-34 network for classification, followed by plate-level aggregation into white and non-white percentages. (B) An example input plate image (left), and the same image overlaid with the predicted segmentation mask (right). Scale bars: 1 cm. (C) Examples of cropped colonies classified into each of the five possible classes. Scale bars: 0.3 mm. (D) Confusion matrix showing the results of the classification step (Resnet-34 network) on the validation data. Numbers in each square indicate the number of colonies with each true (y-axis) and predicted (x-axis) label.

architecture for the plate image segmentation task (He et al., 2016; Ronneberger et al., 2015). A total of 492 pairs of plate images and corresponding segmentation masks generated by Ilastik were used as training data, with approximately 20% (95 pairs) set aside for validation. Binary cross-entropy with logits ('BCEWithLogitsLoss') was used as a loss function, and the dice coefficient was used as an evaluation metric. Data augmentation was applied to the training images with the following transformations: random rotation up to 4°, random horizontal flip, random adjustment of brightness and contrast. The same transformations, except for adjustment of brightness and contrast, were applied to the training masks.

The network was first trained with center-cropped masks and images resized to 512×512 pixels, with a batch size of 4. A weight decay parameter of 1e-7 was used for all training. First, only the last layer was trained using stochastic gradient descent with restarts (SGDR) for 1 cycle of 8 epochs, using a circular learning rate scheduler with a maximum learning rate of 4e-2, a minimum learning rate of 8e-3, 1 epoch of increasing learning rate, and 7 epochs of decreasing learning rate (Huang et al., 2017; Smith, 2015). Next, all layers were trained using SGDR for 1 cycle of 20 epochs. Differential learning rates were applied across layers, with the first third of layers having a maximum learning rate of 1e-4, the middle third having a maximum learning rate of 1e-3, and the last

Biology Open (2020) 9, bio052936. doi:10.1242/bio.052936

third having a maximum learning rate of 1e-2. A circular learning rate scheduler was again used, with minimum learning rates of one-twentieth of respective maximum learning rates, 2 epochs of increasing learning rates, and 18 epochs of decreasing learning rates. The resulting weights were then saved and used as a starting point to train the network with larger, 1024×1024 images.

Training images and masks were scaled up to 1024×1024 pixels and the network was further trained. First, only the last layer was trained using SGDR for one cycle of 2 epochs, using a circular learning rate scheduler with a maximum learning rate of 4e-2, a minimum learning rate of 8e-3, 0.5 epochs of increasing learning rate, and 1.5 epochs of decreasing learning rate. Next, all layers were trained using SGDR for 20 cycles of 20 epochs. Differential learning rates were applied across layers, with the first third of layers having a maximum learning rate of 4e-5, the middle third having a maximum learning rate of 2e-4, and the last third having a maximum learning rate of 4e-3. A circular learning rate scheduler was again used, with minimum learning rates of one-twentieth of respective maximum learning rates, 2.5 epochs of increasing learning rates per cycle, and 17.5 epochs of decreasing learning rates per cycle. The resulting weights were saved and used for prediction.

Colony classification

A Resnet-34 network that had been pre-trained on ImageNet was used as the network architecture for the colony classification task. The final output layer was replaced with a layer predicting five classes (‘white’, ‘red’, ‘pink’, ‘variegating’ and ‘bad segmentation’). A total of 1476 manually labeled, cropped images of individual colonies were used as training data, with approximately 20% (295 images) set aside for validation. Out of the total pool of images, 537 were labeled as white, 273 as red, 310 as pink, 318 as variegating, and 38 as bad segmentation. Validation images were chosen so as to have the same proportions among the five classes as in the total pool. For training, images were resized to 50×50 pixels and a batch size of 128 was used. Stochastic gradient descent (SGD) with a Momentum of 0.9 was used as an optimization algorithm. Categorical cross-entropy was used as a loss function, and both log loss and accuracy were used as evaluation metrics. Data augmentation was applied to the training images with the following transformations: random rotation up to 10°, random rotation or reflection of dihedral group 8, random adjustment of brightness and contrast, random zoom up to 1.1×.

The last layer of the network was first trained without data augmentation for 1 epoch using a learning rate of 1e-2. Data augmentation was then added, and it was trained with SGDR for three cycles of 1 epoch each using cosine annealing, with an initial learning rate of 1e-2. Next, all layers were trained for 17 sets of three cycles of increasing length (1 epoch, followed by 2 epochs, followed by 4 epochs), for a total of 51 cycles and 119 epochs. Differential learning rates were applied across layers, with the first third of layers having a maximum learning rate of 1.1e-4, the middle third having a maximum learning rate of 3.3e-4, and the last third having a maximum learning rate of 1e-3. Training was stopped when over-fitting was observed, and the resulting weights were saved and used for prediction.

Mask prediction, post-processing and colony class prediction

The full prediction pipeline is implemented as follows: first, plate images are center-cropped and resized to 1024×1024 pixels. Segmentation masks are predicted using the trained U-net network, then resized to match the dimensions of the original (center-cropped) images. Border clearing and morphological opening are applied to the masks, reducing plate edge artefacts. Individual colonies are then labelled and a bounding box is drawn around each one, defining a region. Finally, colonies are selected if they have a regional eccentricity <=0.6 and a regional area >=400 pixels. Selected colonies are cropped and saved as individual .jpg images, retaining information about which plate each colony came from.

Classes are then predicted for individual colonies using the trained Resnet-34 network with test-time augmentation. This applies the same data augmentation transforms as were used during training to the test images, creating four randomly transformed versions of each image, then takes the average prediction for all four plus the original. The five colony class predictions are then aggregated per plate, and the percentage of non-white colonies is defined as the sum of predicted red, pink and variegating colonies divided by the sum of all properly segmented colonies (excluding those in the bad segmentation class). Segmentation and colony class prediction can also be performed separately, allowing for classification of previously-segmented images.

Performance of the pipeline

To perform the segmentation task, we chose a U-net-like architecture implemented in the fast.ai library (Howard and others, 2018). U-net was developed specifically for semantic segmentation and has been successfully applied to complex biomedical images such as electron microscopy of neuronal structures and MRI or ultrasound images in breast cancer screening (Ronneberger et al., 2015; Kumar et al., 2018; Dalmış et al., 2017). We trained the U-net network using 492 plate images and corresponding Ilastik-generated masks, with 20% kept aside for validation (see Image segmentation for full training parameters). After training, visual inspection of predicted masks revealed an accurate segmentation of colonies from background, although some errors remained around plate edges (Fig. 1B). This was not unexpected, considering that the Ilastik-generated masks also often contained artefacts at the edges. In order to circumvent this problem, we applied post-processing on the predicted masks, which effectively removed artefacts. The vast majority of resulting cropped regions contained a single colony; however, a few regions still contained multiple small, overlapping colonies. To reduce possible bias that might result from counting multiple colonies as one, we filtered these out during the classification stage.

For the classification task, we fine-tuned a Resnet-34 architecture that was pre-trained on ImageNet (http://www.image-net.org/) (He et al., 2016; Deng et al., 2009), also implemented in the fast.ai library (Howard and others, 2018). We trained the network using 1476 images of individually cropped colonies, which were split into five manually-labeled classes: white, red, pink, variegating and multiple colonies. Again, 20% of colony images were kept aside for validation. After training, we achieved a validation accuracy of 91.8% across the five classes (Fig. 1D, Table 1). Further, aggregating the three classes of non-white colonies together (red, pink and variegating) yielded a much higher validation accuracy of 98.6%. This higher pooled accuracy was encouraging, considering our desired output of percentages of white and non-white colonies per plate. It also demonstrates that most classification errors occur within non-white classes rather than between white and non-white classes, an expected result given that the non-white classes often do not have clear distinctions and can be difficult to define even by eye.

Biology Open (2020) 9, bio052936. doi:10.1242/bio.052936

Table 1. Detailed performance metrics for colony classification in validation dataset

Class	Sensitivity	Specificity	F1-score
White	1.0	0.98	0.99
Non-white	0.98	1.0	0.99
Pink	0.89	0.97	0.93
Red	0.86	0.97	0.91
Variegating	0.86	0.97	0.91

Class labels were predicted for *n*=295 colonies and compared against manual annotations. Metrics are shown for individual class labels (white, pink, red and variegating), as well as for the aggregated non-white class, which includes pink, red and variegating colonies. For each class, true positives (TP) are considered to be colonies that were predicted to have a given label and also manually annotated with that label. False positives (FP) are considered to be colonies that were predicted to have a given label, but manually annotated with a different label. True negatives (TN) are considered to be colonies that were predicted to have any label besides a given label and also manually annotated to have any label besides that label. False negatives (FN) are considered to be colonies that were predicted to have any label besides a given label, but manually annotated with that label. Sensitivity was calculated as TP/(TP+FN). Specificity was calculated as TN/(TN+FP). The F1-score represents the harmonic mean of sensitivity and specificity and was calculated as 2*(sensitivity * specificity)/(sensitivity+specificity).

While we were encouraged by our high validation accuracy, we wanted to test the pipeline's performance against manual counting in a real-world, experimental context. To this end, we took data from two published experiments testing trans-generational inheritance of *ade6*$^{+}$ silencing in *Schizosaccharomyces pombe* (Duempelmann et al., 2019). In these experiments, *ade6*$^{+}$ silencing was first induced by expression of small interfering RNAs (siRNAs) that are complementary to the *ade6*$^{+}$ gene in a *paf1-Q264Stop* nonsense-mutant background, leading to red colonies. Paf1 is a subunit of the Paf1 complex (Paf1C), which represses siRNA-induced heterochromatin formation in *S. pombe* (Kowalik et al., 2015). In the presence of the *paf1-Q264Stop* allele, the silenced (red) phenotype was inherited through meiosis, even in the absence of the original siRNAs that have triggered *ade6*$^{+}$ repression. This was not the case if the progeny inherited a *paf1*$^{+}$ wild-type allele, i.e. the red silencing phenotype was lost. However, these white *paf1*$^{+}$ cells inherited a marked *ade6*$^{+}$ epiallele (*ade6*^{si3}), which reinstated silencing when cells became mutant for Paf1 again in subsequent generations (Duempelmann et al., 2019). The following experiments were performed to quantify different aspects of this phenomenon.

In the first experiment, *paf1-Q264Stop* cells that inherited the *ade6*^{si3} allele and re-established the red silencing phenotype were plated on limiting adenine indicator plates to quantify the maintenance of this re-established silencing through mitosis. Out of 59 plates derived from a red progenitor colony, our automated pipeline predicted a mean of 84.7% non-white colonies, indicating a high degree of maintenance of *ade6*$^{+}$ silencing. Ten of these plates were manually counted, and the mean difference in the percent of counted and predicted non-white colonies was 2.1 percentage points. In comparison, many red colonies (43%) were falsely classified as white when using the popular open-source software *CellProfiler* (github.com/CellProfiler/CellProfiler/tree/v3.1.9) (Fig. 2A). As a control, colonies derived from cells of white *paf1-Q264Stop* progenitor colonies were also quantified by both methods. Our automated pipeline predicted a mean of 0.57% non-white colonies across 60 plates, while manual counting of colonies on 12 plates detected 0 non-white colonies. Also, here the predictions made with *CellProfiler* were less accurate and misclassified 14.66% of the white colonies as non-white (Fig. 2B).

The second experiment was performed to assess mitotic stability of the *ade6*^{si3} epiallele. White *paf1*$^{+}$ cells with an *ade6*^{si3} epiallele were grown exponentially and a sample was crossed to white *paf1-Q264Stop* cells every 3 days (30–40 mitotic divisions) over 19 days total. Progeny of these crosses were also observed to re-establish silencing; however, the frequency of re-establishment declined with the number of mitotic divisions the cells had gone through. The percentage of non-white colonies on plates resulting from crosses at each time point was both counted manually (66,000 colonies total) and predicted using the automated pipeline. Both methods showed a near-exponential decrease in non-white colonies over time; the mean difference in the percent of non-white colonies between the two methods ranged from 0.26 to 5.1 percentage points (Fig. 2C).

DISCUSSION

Here we introduce a novel computational pipeline for colony segmentation and classification. It allows us to achieve accuracy comparable to human performance, which was difficult to achieve with existing colony segmentation and classification programs. For example, many red colonies were falsely classified as white when analyzing our data with *CellProfiler* (Fig. 2 and data not shown). *CellProfiler* also cannot distinguish variegating, pink and red colonies.

We observed several factors that contributed to the accuracy of the automated pipeline predictions versus manual counting. In general, the pipeline performed with very high accuracy on plates with a low (<5%) percentage of non-white colonies; however, on some plates that had been grown for over 2 weeks, white colonies formed an irregular ring-like morphology and tended to be mis-classified as pink. The accuracy of the pipeline was also decreased for plates with very dense, small colonies. This may be partly due to the difficulty in segmenting individual colonies when they are touching one another, leading to many colonies being excluded from the analysis. Very small colonies are also more likely to be mistakenly filtered out during post-processing. Since cells with a silenced *ade6*$^{+}$ gene tend to grow more slowly, this may lead to bias, as very small colonies are more likely to be non-white. However, plating cells at a controlled density and imaging the plates after an appropriate amount of time can counteract this potential bias. We have posted a full suggested protocol describing plating and imaging for most accurate prediction on Protocol Exchange (https://protocolexchange.researchsquare.com/article/nprot-7305/v1).

Our pipeline generates as output the numbers of predicted colonies per plate for both the aggregated non-white versus white categories as well as for the more granular classes of red, pink and variegating colonies. As detailed in Table 1, we observed a higher overall performance for white versus non-white predictions; however, in some cases researchers may prefer to use the more granular predictions despite their lower accuracy. This decrease in accuracy is largely due to reduced sensitivity for individual class predictions, while a high level of specificity is maintained.

Our fully automated pipeline can be run on a CUDA-enabled CPU or GPU. On a GeForce GTX 1080 GPU, it took approximately 45 minutes to process 245 plate images, representing an 80–100x speedup over manual counting by an experienced biologist. In addition to saving time and manual labor, the pipeline has the potential to increase reproducibility by removing variations between individual researchers or computer monitors. Our pragmatic approach, combining transfer learning with readily available annotations, allows us to achieve accuracy comparable to human performance with relatively little training data. Our work should

Biology Open (2020) 9, bio052936. doi:10.1242/bio.052936

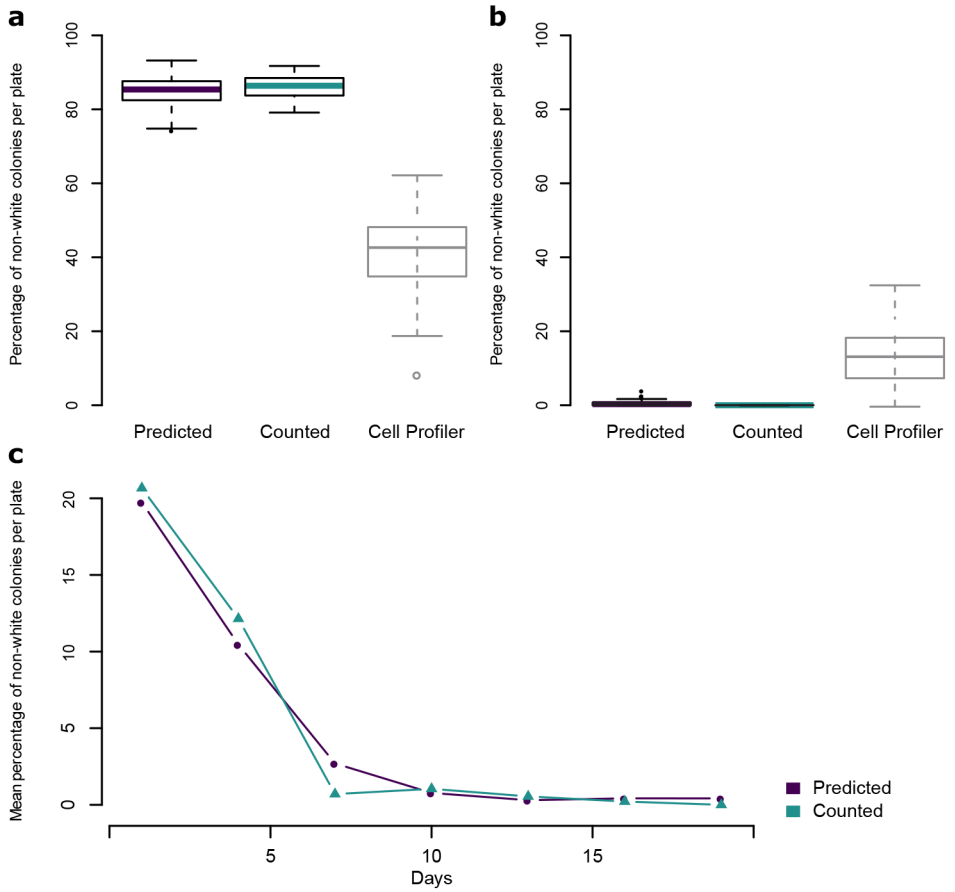

Fig. 2. Comparison of automated colony classification and manual counting on experimental data. (A) Boxplots showing the predicted or manually counted percentage of non-white colonies per plate on plates resulting from red *paf1-Q264Stop; ade6^{si3}* cells. *n*=59 (predicted) or *n*=10 (counted). For comparison, percentage of non-white colonies per plate were also predicted with *CellProfiler*, with a threshold value of 0.055 (*n*=59). (B) Boxplots showing the predicted or manually counted percentage of non-white colonies per plate on plates resulting from white *paf1-Q264Stop* cells. *n*=60 (predicted) or *n*=12 (counted). For comparison, percentage of non-white colonies per plate were also predicted with *CellProfiler*, with a threshold value of 0.055 (*n*=60). For boxplots, center line is median, bottom and top hinges are first and third quartiles, whiskers show the most extreme points within 1.5 times the interquartile range, and more extreme values are plotted as individual points. (C) Mean predicted or manually counted percentages of non-white colonies per plate across a time course of mitotically dividing white *paf1^{+} ade6^{si3}* cells crossed to white *paf1-Q264Stop* cells every 3 days. The time course was repeated with 11 independent biological replicates, and six plates per replicate per timepoint were quantified by automated prediction (*n*=66 per time point). The mean of all 66 plates is reported for each timepoint. For manual counting, one plate per replicate per timepoint was counted (*n*=11 per time point); the mean of 11 plates is reported for each timepoint.

thus enable larger-scale experiments and higher statistical power, unlocking a true quantitative use of the red/white color assay in yeast research. We have made the code and trained network weights freely available to the community at https://github.com/fmi-basel/buehler-colonyclassification.

MATERIALS AND METHODS

Protocol for plating and imaging of yeast

We have posted a full suggested protocol describing plating and imaging for most accurate prediction on Protocol Exchange (https://protocolexchange.researchsquare.com/article/nprot-7305/v1).

Pipeline requirements
Operating system(s): Platform independent
Programming language: Python
Other requirements: Python 3.6 or higher, fastai library v. 0.7
License: GNU GPL v3.0
Any restrictions to use by non-academics: None

Predictions with CellProfiler

Analyses with CellProfiler were performed as described previously (Bray et al., 2015) with few changes. The step 'Align' was removed due to inaccurate alignment, therefore individual PlateTemplate.png files were made for each image. Because of the high memory usage and memory leaks we reduced the image resolution from 5184×3456 pixels to 1728×1152 pixels. The range of typical diameter of objects was set to 6–33 pixel units and the threshold value which separates white from non-white colonies was optimized to 0.055.

Acknowledgements

We thank M. Rempfler for discussions and for suggesting ideas for the automated segmentation, and K. Volkmann and S. van Eeden for help with image acquisition and processing.

Competing interests

The Friedrich Miescher Institute for Biomedical Research (FMI) receives significant financial contributions from the Novartis Research Foundation. Published research reagents from the FMI are shared with the academic community under a Material Transfer Agreement (MTA) having terms and conditions corresponding to those of the UBMTA (Uniform Biological Material Transfer Agreement).

Author contributions

Conceptualization: L.D., S.H.C.; Methodology: L.D., S.H.C., Y.S.; Software: S.H.C.; Validation: L.D., S.H.C., Y.S.; Formal analysis: L.D., S.H.C.; Resources: M.B.; Data curation: L.D., S.H.C.; Writing - original draft: S.H.C.; Writing - review & editing: L.D., S.H.C., M.B.; Visualization: L.D., S.H.C., M.B.; Supervision: M.B.; Project administration: M.B.; Funding acquisition: M.B.

Funding
The Schweizerischer Nationalfonds zur Förderung der Wissenschaftlichen Forschung NCCR RNA & Disease [grant no. 141735], the European Research Council [ERC-CoG-REpiReg-681213], and the Friedrich Miescher Institute for Biomedical Research, which is supported by the Novartis Stiftung für Medizinisch-Biologische Forschung, provided funds to cover salary and infrastructure costs. Design of the study and collection, analysis, and interpretation of data and writing of the manuscript was not influenced by the funding bodies.

Data availability
Code and trained network weights are freely available to the community at https://github.com/fmi-basel/buehler-colonyclassification. Raw images of plates with yeast colonies used in Fig. 2 are available from the Zenodo data archive (https://zenodo.org/). DOI: 10.5281/zenodo.3779863.

References
Bray, M.-A., Vokes, M. S. and Carpenter, A. E. (2015). Using CellProfiler for automatic identification and measurement of biological objects in images. *Curr. Protoc. Mol. Biol* **109**, 14.17.1-14.17.13. doi:10.1002/0471142727.mb1417s109
Dalmış, M. U., Litjens, G., Holland, K., Setio, A., Mann, R., Karssemeijer, N. and Gubern-Mérida, A. (2017). Using deep learning to segment breast and fibroglandular tissue in MRI volumes. *Med. Phys.* **44**, 533-546. doi:10.1002/mp.12079
Deng, J., Dong, W., Socher, R., Li, L.-J., Kai Li, R., Li Fei-Fei, N. (2009). Image*N*et: a large-scale hierarchical image database. *IEEE Computer Vision and Pattern Recognition (CVPR)*, pp. 248-255. doi:10.1109/CVPR.2009.5206848
Duempelmann, L., Mohn, F., Shimada, Y., Oberti, D., Andriollo, A., Lochs, S. and Bühler, M. (2019). Inheritance of a phenotypically neutral epimutation evokes gene silencing in later generations. *Mol. Cell* **74**, 534-541.e4. doi:10.1016/j.molcel.2019.02.009
He, K., Zhang, X., Ren, S. and Sun, J. (2016). Deep Residual Learning for Image Recognition. 2016 IEEE Conference on Computer Vision and Pattern Recognition (CVPR), Las Vegas, NV, 770-778, doi:10.1109/CVPR.2016.90
Howard, J. and **others**. (2018). *fastai*. GitHub.
Huang, J., Rathod, V., Sun, C., Zhu, M., Korattikara, A., Fathi, A., Fischer, I., Wojna, Z., Song, Y., Guadarrama, S. et al. (2016). Speed/Accuracy Trade-Offs for Modern Convolutional Object Detectors. 2017 IEEE Conference on Computer Vision and Pattern Recognition (CVPR), Honolulu, HI, 3296-3297. doi:10.1109/CVPR.2017.351
Huang, G., Li, Y., Pleiss, G., Liu, Z., Hopcroft, J. E. and Weinburger, K. Q. (2017). Snapshot Ensembles: Train 1, get M for free. arXiv:1704.00109v1 [cs.LG].
Hughes, A. J., Mornin, J. D., Biswas, S. K., Beck, L. E., Bauer, D. P., Raj, A., Bianco, S. and Gartner, Z. J. (2018). Quanti.us: a tool for rapid, flexible, crowd-based annotation of images. *Nat. Methods* **15**, 587-590. doi:10.1038/s41592-018-0069-0
Kowalik, K. M., Shimada, Y., Flury, V., Stadler, M. B., Batki, J. and Bühler, M. (2015). The Paf1 complex represses small-RNA-mediated epigenetic gene silencing. *Nature*. doi:10.1038/nature14337
Kumar, V., Webb, J. M., Gregory, A., Denis, M., Meixner, D. D., Bayat, M., Whaley, D. H., Fatemi, M. and Alizad, A. (2018). Automated and real-time segmentation of suspicious breast masses using convolutional neural network. *PLoS ONE* **13**, e0195816. doi:10.1371/journal.pone.0195816
Lin, T.-Y., Goyal, P., Girshick, R., He, K. and Dollár, P. (2017). IEEE International Conference on Computer Vision (ICCV), Venice, 2999-3007, doi:10.1109/ICCV.2017.324
Liu, W., Anguelov, D., Erhan, D., Szegedy, C., Reed, S., Fu, C-Y. and Berg, A. C. (2016). SSD: Single Shot MultiBox Detector. In: Leibe B., Matas J., Sebe N., Welling M. (eds) Computer Vision - ECCV 2016. ECCV 2016. Lecture Notes in Computer Science, vol 9905. Springer, Cham. doi:10.1007/978-3-319-46448-0_2
Ronneberger, O., Fischer, P. and Brox, T. (2015). U-Net: Convolutional Networks for Biomedical Image Segmentation. In: Navab N., Hornegger J., Wells W., Frangi A. (eds) Medical Image Computing and Computer-Assisted Intervention - MICCAI 2015. MICCAI 2015. Lecture Notes in Computer Science, vol 9351. Springer, Cham. doi:10.1007/978-3-319-24574-4_28
Smith, L. N. (2015). Cyclical Learning Rates for Training Neural Networks. arXiv:1506.01186 [cs.CV].
Sommer, C., Straehle, C., Köthe, U. and Hamprecht, F. A. (2011). Ilastik: Interactive learning and segmentation toolkit. in 2011 IEEE International Symposium on Biomedical Imaging: From Nano to Macro 230–233. doi:10.1109/ISBI.2011.5872394
Van Der Walt, S., Schönberger, J. L., Nunez-Iglesias, J., Boulogne, F., Warner, J. D., Yager, N., Gouillart, E. and Yu, T. (2014). Scikit-image: image processing in Python. *PeerJ* **2**, e453. doi:10.7717/peerj.453

Trends in Genetics

CellPress
REVIEWS

Review

Small RNAs in the Transgenerational Inheritance of Epigenetic Information

Lea Duempelmann,[1,2,5] Merle Skribbe,[1,3,5] and Marc Bühler [1,2,4,*,@]

In recent years it has become evident that RNA interference-related mechanisms can mediate the deposition and transgenerational inheritance of specific chromatin modifications in a truly epigenetic fashion. Rapid progress has been made in identifying the RNAi effector proteins and how they work together to confer long-lasting epigenetic responses, and initial studies hint at potential physiological relevance of such regulation. In this review, we highlight mechanistic studies in model organisms that advance our understanding of how small RNAs trigger long-lasting epigenetic changes in gene expression and we discuss observations that lend support for the idea that small RNAs might participate in mechanisms that trigger epigenetic gene expression changes in response to environmental cues and the effects these could have on population adaptation.

Highlights

Small RNAs have long been known to be involved in specifying and stabilizing distinct chromatin states. Only recently has it become evident that small RNAs have the capacity to trigger epigenetic gene silencing.

Once initiated by primary small RNAs, the repressed states can be propagated across multiple generations in different model organisms, commonly through the amplification of secondary small RNAs in stable feedback loops, while the primary small RNAs become dispensable.

Small RNAs have also been demonstrated to direct the deposition of phenotypically plastic epigenetic marks, which mediate repression under specific conditions only.

These observations lend support to the hypothesis that small RNAs might be involved in sensing environmental conditions and triggering epigenetic gene expression changes that may lead to increased population fitness of an organism that lives in a dynamic habitat.

Epigenetics as a Driver of Phenotypic Variation

Closely related members of a species can sometimes exhibit substantial phenotypic variation and yet share essentially identical DNA sequences [1]. Examples include the epigenetic recombinant inbred lines of the flowering plant *Arabidopsis thaliana*, which show phenotypic differences while being almost isogenic [2,3]. Phenotypic variation is not determined by DNA sequence alone and epigenetic changes are known to affect development and influence complex traits. **Epigenetics** (see Glossary) was initially defined as any heritable change in gene expression patterns without changes in the DNA sequence [4,5]. Now, epigenetic phenomena are often characterized as 'gene expression changes that are mutation independent and heritable in the absence of the triggering event' [5], a definition we will follow in this review. We note that this definition can be expanded to include protein only-based inheritance mechanisms that do not necessarily cause changes in gene expression. For example, prions are infectious proteinaceous agents that can transmit their distinct conformation to their native counterparts, causing structural and functional changes that are inherited across generations (reviewed in [6]). In this review, we will pay special attention to heritability through meiosis and highlight mechanisms that rely on noncoding RNAs and post-translational modifications of histones.

The heritability of epigenetic changes can vary significantly, even within the same population, and generally does not follow Mendelian rules. Striking examples of non-Mendelian inheritance are prions and paramutation where any of the offspring can potentially inherit the epigenetic state of one parent. Paramutation has been best studied in maize and describes a trans-interaction between two alleles where one imposes its silent chromatin state on the other, causing heritable gene expression changes [7]. While it is still unclear exactly how the alleles interact, one model proposes that the modifications are communicated by small RNAs.

Small RNAs are the common denominator of **RNA interference (RNAi)**-related pathways [8], which function both in the cytoplasm of eukaryotic cells and in the nucleus where they often correlate with changes in chromatin modifications. Early work in *Caenorhabditis elegans* revealed stable transgene silencing that was maintained under selection for over 80 generations after only

[1]Friedrich Miescher Institute for Biomedical Research, 4058 Basel, Switzerland
[2]University of Basel, 4003 Basel, Switzerland
[3]Heidelberg University, 69117 Heidelberg, Germany
[4]www.fmi.ch/buehler.m
[5]These authors contributed equally to this work.

*Correspondence: marc.buehler@fmi.ch (M. Bühler).
@Twitter: @MarcBhler4

a single exposure to double-stranded RNA (dsRNA) to trigger RNAi [9]. Mechanistic dissection of such RNA-mediated epigenetic silencing phenomena has gained momentum recently and their complexity is becoming apparent. In this review we will discuss recent advances in understanding small RNA-mediated epigenetic phenomena and their potential physiological relevance on the basis of studies in *Schizosaccharomyces pombe, C. elegans*, and *A. thaliana*.

Nuclear Small RNA-Directed Gene Silencing Pathways

Small RNAs mediate canonical RNAi responses in the cytoplasm and are also intimately linked to chromatin-regulatory processes. These latter pathways have been extensively studied in yeasts, nematodes, plants, and fruit flies (reviewed in [10–12]). Mechanistically, they differ substantially between organisms, but they share important key features, suggesting that general concepts are conserved. At the core of each pathway is a small-RNA-bound Argonaute complex that targets nascent RNA via complementary base-pairing. Although base-pairing with DNA would in principle be possible, work in yeast and plants has shown that this is unlikely [13,14]. Target specificity is influenced by how tolerant the system is in allowing base-pairing mismatches. Upon nascent transcript binding, the small RNA-Argonaute complex recruits additional effector complexes that can induce changes in chromatin states and/or inhibit elongation of the RNA polymerase. A characteristic feature of such small RNA-mediated nuclear gene silencing pathways is that maintenance of the silent state requires the continuous amplification of the small RNA pool. Yeasts, plants, and nematodes rely on RNA-dependent RNA polymerases (RdRPs) for small RNA amplification. Organisms without RdRPs have evolved other strategies to amplify the pool of small RNAs that can function in the nucleus, as, for example, amplification of PIWI-interacting RNAs (piRNAs) by the ping-pong cycle in flies (reviewed in [11]).

Nuclear small RNA-directed gene silencing has been studied intensively in *S. pombe*, *C. elegans*, and *A. thaliana* (Figure 1). In *S. pombe*, a functional RNAi pathway is necessary to maintain centromeric repeats in their constitutive heterochromatic state (reviewed in [15–17]). The Argonaute subunit (Ago1) of the RNA-induced transcriptional silencing (RITS) complex associates with an siRNA to target nascent RNAs transcribed from the pericentromeric repeats by RNA polymerase II (RNA Pol II). The RITS complex recruits the RNA-dependent RNA polymerase complex (RDRC). RDRC uses the nascent transcript as a template to generate dsRNA that is further processed into mature siRNAs by the physically associated Dicer homolog, Dcr1. These siRNAs are assembled by a chaperone complex into a new RITS complex. RITS also interacts with the cryptic loci regulator complex (CLRC). The Clr4 subunit of CLRC is the only known H3K9 methyltransferase in *S. pombe.* It can deposit mono-, di-, and tri-methylation marks on H3K9. Once methylated, H3K9 (H3K9me2/3) serves as a binding site for chromodomain-containing proteins such as Clr4 itself or the RITS subunit Chp1, thus establishing self-enforcing, positive feedback loops (Figure 1A).

In *A. thaliana*, small RNAs are implicated in silencing transposable elements by the RNA-directed DNA methylation (RdDM) pathway (reviewed in [12,18,19]). This pathway involves two specialized, RNA Pol II-related polymerases, RNA Pol IV and V, and specifies DNA methylation in the context of CG, CHG, or CHH (H = A, T, or C) nucleotides. Similar to the fission yeast pathway, RdDM relies on siRNA-guided Argonaute complexes that assemble effector proteins on an RNA scaffold and facilitate chromatin modifications. However, in contrast to fission yeast, the siRNA source and the RNA scaffold originate from two different transcripts. RNA Pol IV transcribes a single-stranded siRNA precursor from which the RNA-DEPENDENT RNA POLYMERASE 2 (RDR2) synthesizes dsRNA that is further processed by DICER-LIKE 3 (DCL3) and HEN1 into mature, 3′-methylated 24-nt siRNAs. The mature siRNAs are loaded onto the Argonaute protein AGO4 and target Pol V-transcribed nascent RNA via complementary base-

Glossary

Epigenetics: epigenetics is widely referred to as heritable changes in gene expression that do not originate from DNA mutations. Although known epigenetic phenomena are commonly linked to changes in DNA or chromatin modifications, other mechanisms are likely to exist and gene expression must not necessarily be different. For example, prions transmit their distinct conformation to their native counterparts, which can cause structural and functional changes of such proteins without changing expression of their cognate genes. In this review we put special emphasis on epigenetic phenomena in which DNA sequence-independent gene expression changes are heritable even after the triggering event ceases [5].

Epimutant: the term epimutation is derived from the expression 'epigenetic mutation' and describes heritable changes in chromatin states that control gene activity [80]. A well-known example is that of the epigenetic recombinant inbred lines (epiRILs) of the flowering plant *A. thaliana*, which were generated to study the impact of different DNA methylation patterns on the plant's phenotype [2]. In these mostly isogenic lines, epigenetic changes were associated with heritable variations in complex traits, such as flowering time and drought tolerance.

RNA interference (RNAi): classical RNAi describes a post-transcriptional mRNA silencing pathway that is induced by double-stranded RNA (dsRNA) in the cytoplasm. Components of the RNAi pathway are widely conserved across all kingdoms. The dsRNA is initially processed by the endonuclease Dicer into small RNAs that can guide Argonaute effector complexes to complementary mRNAs and promote mRNA degradation or repression of translation (reviewed in [8,79]). In some organisms, RNAi also functions in the nucleus to regulate gene expression, which is the focus of this review [10].

Transgenerational inheritance: it is important to distinguish between transgenerational and intergenerational inheritance when studying the impact of epigenetic changes on subsequent generations. In viviparous animals, exposure of a pregnant animal to a stimulus that triggers an epigenetic change in gene expression can potentially affect mother, fetus, and the

pairing. Following the physical association of the siRNA-AGO4 complex with the RNA, and with the elongation factor KTF1 and RNA Pol V itself, the *de novo* DNA methyltransferase DRM2 is recruited. DNA methylation is closely linked to histone modification and either modification can recruit the RdDM machinery, thereby reinforcing chromatin compaction and gene repression in a positive feedback loop (Figure 1C).

Small RNAs also mediate gene silencing in the nuclei of *C. elegans* cells. *C. elegans* encodes 27 distinct Argonaute proteins, which associate with several different classes of small RNAs generated through various biogenesis pathways (reviewed in [11,20,21]). In our discussion below, we emphasize that primary endogenous and exogenous small RNAs trigger the biogenesis of distinct classes of secondary small RNAs in *C. elegans*. For example, 21U RNAs, which constitute piRNAs in the worm, guide the Argonaute family protein PRG-1 to target transcripts via base-pairing interactions that usually display a preference for perfect seed-region binding [11,22]. Upon engagement with the target RNA, the 21U-PRG-1 complex triggers the generation of secondary siRNAs, requiring the RdRPs EGO-1 and RRF-1 and components of perinuclear foci [23–25]. In contrast to small RNAs in yeast and plants, the secondary siRNAs in worms are distinct from the primary 21U RNAs, being 22-nt long and displaying a 5′ guanine bias (22G RNAs) [23,26,27]. The 22G RNAs are sorted into different worm-specific Argonaute proteins (WAGOs), which

fetus's developing germline, simultaneously. Thus, epigenetic changes would be considered intergenerational up to F2 (grandchildren) and transgenerational from F3. However, in oviparous animals, which lay eggs, an epigenetic change may be considered transgenerational from F2 onwards (reviewed in [1]).

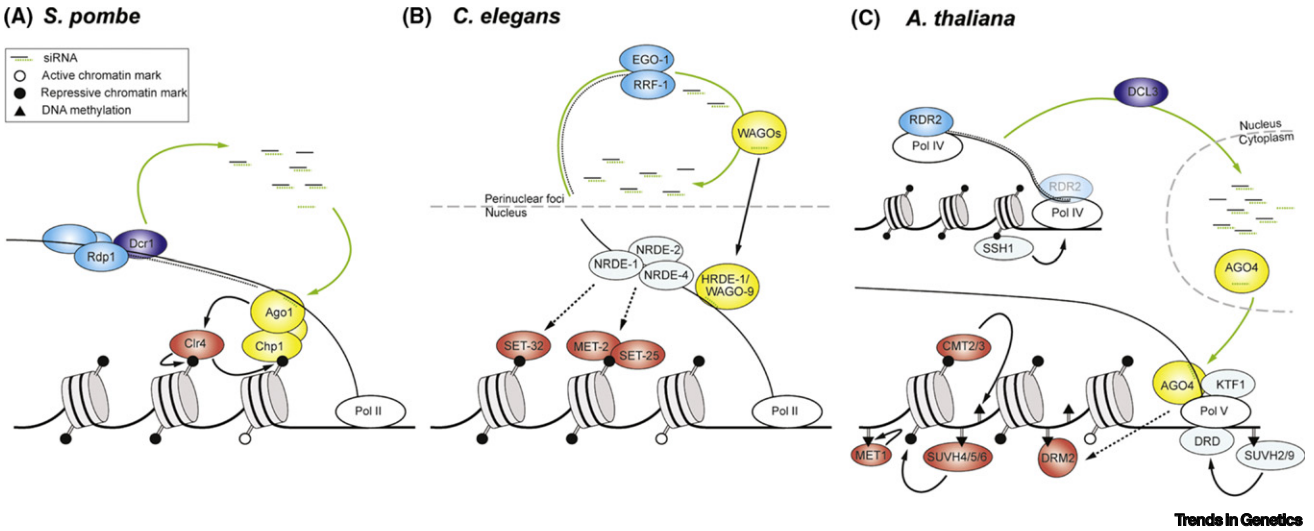

Figure 1. Positive Feedback Loops Maintain Chromatin Modifications. Similarities of the small RNA silencing pathways in *Schizosaccharomyces pombe* (A), *Caenorhabditis elegans* (B), and *Arabidopsis thaliana* (C) are highlighted by identical coloring of conserved effector proteins. (A) The *S. pombe* RNA-induced transcriptional silencing (RITS) complex (yellow) is guided to the nascent transcript by its small RNA-bound Ago1 subunit. Chp1 binds to methylated chromatin and RITS recruits the cryptic loci regulator complex CLRC (red) and the RNA-dependent RNA polymerase (RdRP) complex RDRC (light blue). The CLRC subunit Clr4 mediates H3K9me2/3 and the Rdp1 subunit of RDRC synthesizes double-stranded RNA (dsRNA) from the nascent transcript: dsRNA is processed by Dcr1 (dark blue) into secondary siRNAs channeled into new RITS complexes, creating a self-reinforcing feedback loop that stabilizes H3K9me2/3 heterochromatin. Clr4 creates a positive feedback loop by binding methylated histones through its chromo-domain and methylation of neighboring histones. (B) In *C. elegans*, 22G RNAs (siRNAs) are continuously amplified in perinuclear foci, which requires the RdRPs EGO-1 and RRF-1 (light blue). Mature 22G RNAs associate with different worm-specific Argonaute proteins (WAGOs), such as HRDE-1 (WAGO-9). The 22G RNA-HRDE-1 complex (yellow) re-enters the nucleus and targets nascent RNA Pol II transcripts. This interaction and the association with the NRDE factors NRDE-1/-2/-4 likely recruits H3K9 histone methyltransferases SET-25, SET-35, and MET-2, which ultimately repress transcription. (C) The RNA-dependent DNA methylation (RdDM) pathway in *A. thaliana* requires DNA-dependent RNA polymerases Pol IV and V. Pol IV produces short transcripts that are channeled into the associated RdRP RDR2 (light blue) [81]. RDR2-synthesized dsRNA serves as substrate for DCL-3 (dark blue), which generates 24-nt siRNAs that load onto AGO4 (yellow). The siRNA-AGO4 complex then binds the nascent transcript of Pol V, Pol V itself, and the elongation factor KTF1. These interactions are thought to promote the recruitment of DRM2, which mediates *de novo* DNA methylation. Subsequently, histone methyltransferases (SUVH4/5/6) deposit H3K9me2. The repressive chromatin modifications are maintained via positive feedback loops, including DNA and H3K9 methyltransferases (red) [18,19]. Both modifications further promote positive feedback as H3K9me2-bound SHH1 recruits Pol IV, and DNA methylation-bound SUVH2 and SUVH9 recruit Pol V through the DRD complex [19]. Filled arrows indicate confirmed interactions, dashed arrows indicate putative recruitment of chromatin modifiers.

facilitate either post-transcriptional or transcriptional gene silencing (reviewed in [21]). For example, HRDE-1 (WAGO-9) binds, with HRDE-2, to 22G RNAs in the cytoplasm and then translocates to the nucleus to trigger transcriptional silencing of complementary target genes [28]. Transcription is also suppressed by the WAGO protein NRDE-3, which associates with both endogenous and exogenous small RNAs [29,30]. Akin to fission yeast and plants, NRDE-3 and HRDE-1 are thought to base-pair with RNA Pol II-transcribed nascent transcripts, followed by the recruitment of histone methyltransferases, such as MET-2, SET-25, and SET-32, resulting in H3K9 methylation (Figure 1B) [29,31–34]. A feature of small RNA-mediated silencing responses in *C. elegans* is that they are heritable across generations in the germline of the worms. For example, a silencing response initiated by the 21U-PRG-1 complex can be independently maintained by 22G RNAs through a positive feedback loop involving the RdRP activity of EGO-1 and RRF-1 [33,35,36] (Figure 2). As this is consistent with the definition of 'epigenetics', this phenomenon has been dubbed 'RNA-induced epigenetic silencing' (RNAe).

Transcription-Associated Factors Counteract RNAe

Whether siRNAs in *S. pombe* could also induce epigenetic gene silencing phenomena, as seen in *C. elegans*, has been unclear. Because of the repetitive nature of *S. pombe* centromeric heterochromatin, it is not possible to identify and delete a putative locus that may encode primary siRNAs that initiate an epigenetic silencing response. Similarly, although expression of synthetic siRNAs was shown to promote H3K9 methylation in *trans* at a small number of loci, it is inefficient, locus dependent, and the silent state is highly unstable [37–40]. However, recent research has shown that synthetic siRNAs are able to initiate robust silencing responses in yeast strains with mutations in genes encoding subunits of the RNA Polymerase-associated factor 1 complex (Paf1C), mRNA export factors Mlo3 and Dss1, transcription termination factors Ctf1 and Res2, and the acetyltransferase Mst2 [41–46]. Once initiated, silencing is maintained across generations independently of the synthetic siRNA source in such mutants [41,42]. Thus, in the presence of an 'enabling' mutation, primary siRNAs can trigger an RNAe response in *S. pombe* (Figure 2). Secondary siRNA amplification is required for **transgenerational inheritance** [41,43], as in *C. elegans*.

The mechanisms by which these transcription-associated factors counteract RNAe in *S. pombe* remain elusive. Two non-mutually exclusive models have been put forward for Paf1C (Figure 3). Model 1 suggests that reduced histone H3 exchange rates in Paf1C mutants [45] may reduce

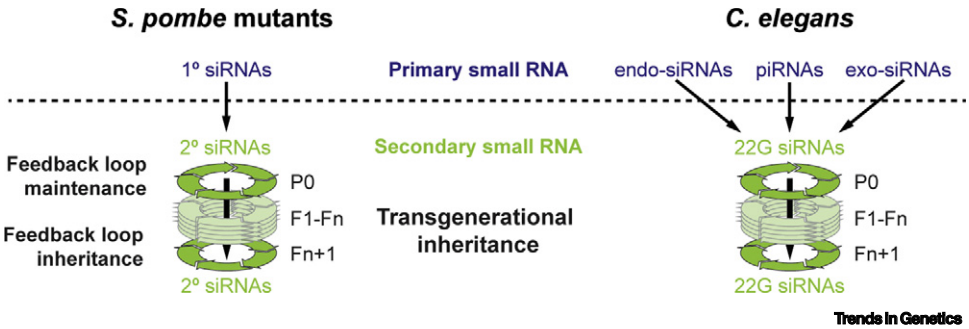

Figure 2. Primary siRNAs Initiate Silencing, Secondary siRNAs Maintain Silencing. In *Schizosaccharomyces pombe* cells that harbor RNAi-enabling mutations, transcriptional gene silencing can be initiated by *trans*-acting primary (1°) siRNAs that derive from RNA hairpins [42] or centromeric heterochromatin [41]. Deposition of H3K9me3 leads to the production of secondary (2°) siRNAs, which re-enforce methylation of H3K9, creating a positive feedback loop sustained across generations independently of the triggering 1° siRNAs [41,43]. In *Caenorhabditis elegans*, 1° small RNAs, like endo-siRNAs, piRNAs, and exo-siRNAs, initiate the biogenesis of 2° 22G RNAs, which can be inherited over multiple generations. The piRNA-bound PIWI protein PRG-1 is required for initiation, but not maintenance of the silent state in subsequent generations.

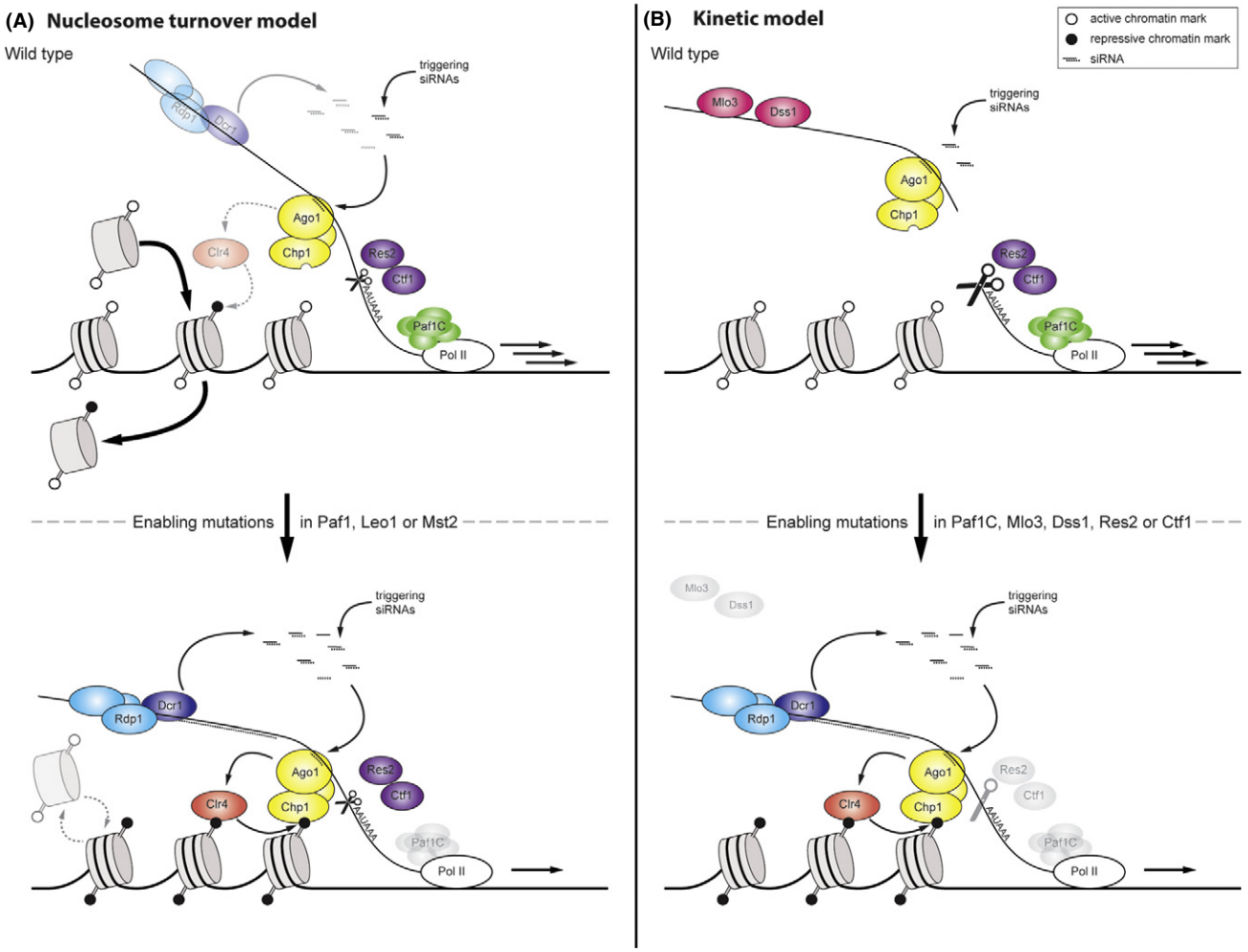

Figure 3. Enabling Mutations in Fission Yeast and Their Potential Modes of Action. (A) Nucleosome turnover model (model 1). Under wild type conditions (upper panel), triggering 1° siRNAs lead to the deposition of H3K9me2/3 marks at the complementary target locus. Because methylated nucleosomes are constantly exchanged, no stable heterochromatin can be established, weakening the feedback loop and preventing transcriptional gene silencing. Upon loss of the Paf1-Leo1 subcomplex (lower panel), nucleosome turnover rates are reduced and the persistence of methylated H3K9 promotes the RNAi feedback loop to form stable heterochromatin and reduce transcription at the target locus. (B) Kinetic model (model 2). Following transcription elongation, wild type cells rapidly terminate and release the siRNA target RNA from the site of transcription (upper panel). Kinetics of these processes are reduced when Paf1C, or termination and processing factors like Res2 and Ctf1, or RNA export factors such as Mlo3 and Dss1 are mutated. As a result, the nascent RNA transcript is maintained close to its site of transcription, allowing sufficient time for establishment of stable heterochromatin. Proteins with enabling mutations are depicted as transparent grey where their function is lost. Scissors depict the cleavage site for the transcript release. The polyadenylation signal is represented by the consensus motif AAUAAA.

dilution of K9 methylated H3 (Figure 3A). In line with this, the acetyltransferase Mst2 has been proposed to promote histone turnover [44,47]. This model would predict that regions with low nucleosome turnover rates, such as lowly expressed genes, are more prone to RNAe, a hypothesis that remains to be tested. Model 2 suggests that reducing the kinetics of nascent transcript release from chromatin in Paf1C mutants allows sufficient time for RITS to recruit CLRC and methylate H3K9 (Figure 3B) [42] and is supported by observations that mutating nascent transcript processing signals in the target RNA enable siRNA-directed H3K9 methylation [48]. Moreover, ribozyme-mediated cleavage of the nascent transcript abolished initiation of silencing in Paf1C mutant cells [42]. Model 2 would also explain why centromeric repeats are not under the

control of Paf1C, as repeat transcripts do not contain strong cleavage and polyadenylation signals [48].

Inducing repression of protein-coding genes at the transcriptional level using siRNAs has been challenging in most organisms. This suggests that the mechanisms that antagonize silencing of euchromatic genes might be conserved. In accordance with this idea, Paf1C has been recently implicated in counteracting PIWI-dependent silencing in piRNA-targeted reporter assays in *Drosophila melanogaster* [49]. Furthermore, defects in RNA 3′-end processing complexes in *A. thaliana* have been shown to enhance the silencing phenotype [50], lending support to model 2. Thus, RNAe-related phenomena might be much more prevalent, but only unveiled under specific conditions.

Propagation of the Repressed State across Generations

Gene silencing can persist over multiple generations in the germline of *C. elegans*. Gene repression is typically maintained without the initial trigger for three to seven generations [51] and occasionally for tens of generations [9,33,35,36]. In contrast, silencing of somatically expressed genes mostly affects only the subsequent generation through nonepigenetic parental effects, with rare exceptions [51,52]. Following the discovery of stably inherited silencing in the germline, forward genetic screens have identified various factors required for the propagation of the repressed state across generations.

The nuclear Argonaute HRDE-1, which is dispensable for the initial silencing response, is essential for transgenerational inheritance [23,32,33,35,36], as are NRDE-1/-2/-4 and the heterochromatin protein 1 (HP1) homolog HPL-2 [51,53]. 22G RNAs are strictly required to propagate silencing across generations: RNAe responses cease if 22G RNAs are not continuously generated, which occurs in dedicated cellular compartments [20,24,28,54,55]. There is evidence that 22G RNAs are paramutagenic: HRDE-1-22G-RNA complexes can be inherited and induce silencing of the homologous zygotic allele without transmission of the silenced locus and its chromatin marks [56]. Further, the in *trans* silenced second allele remains silenced over tens of generations, even after the first allele is lost [56]. Thus, it is tempting to speculate that RNAe in *C. elegans* could be propagated over multiple generations through transmissible HRDE-1-bound 22G RNAs. What role histone modifications play in propagation of a *C. elegans* RNAe response remains unclear. Although histone methyltransferases SET-25 and SET-32 are recruited to methylate H3K9, it is debated whether they are essential for the propagation of the silent state [28,33,34,52,57]. Thus, more work is required to elucidate the crosstalk between RNA silencing and chromatin in worms.

Although feedback loops could in principle lead to infinite silencing responses, the duration of epigenetically inherited silencing is typically restricted to a few generations in wild type worms. Genetic screens designed to discover modifiers of RNAe revealed several factors that influence the duration of RNAe. Mutations in the heritable enhancer of RNAi (*heri-1*) gene prolong RNAe heritability by more than 20 generations [58], probably by abolishing allosteric inhibition of nuclear RNAi at the silenced locus. The duration of RNAe responses can also be modulated by shifting the balance between different small RNA pathways [59]. Many RNA silencing factors are shared between pathways and defects in one pathway enhance parallel pathways as effector availability increases [60–62]. Finally, endo-siRNAs against RNAi factor genes have been proposed to autoinhibit RNAi and thereby also limit the duration of an RNAe response [59].

RNAe responses in *S. pombe* depend strictly on the continuous generation of secondary siRNAs, as in *C. elegans*. In contrast to *C. elegans*, amplification of siRNAs by the RNAi machinery and

H3K9 methylation are mutually dependent processes and the tri-methylated state of H3K9 is necessary for transgenerational inheritance [43]. Thus, RNAe in fission yeast is not possible without the coupling of the RNAi pathway and H3K9 methylation [41].

The Role of H3K9me3 in RNAe

Until recently, small RNA-directed H3K9me3 deposition had always been associated with persistent gene silencing [10,53]. Whether mechanisms exist that allow transgenerational inheritance of H3K9me3 without the associated repressed state, as a form of 'silencing memory', was unknown. However, that this is possible in principle was recently demonstrated in *S. pombe*. In the presence of an enabling Paf1 mutation, hairpin-derived siRNAs induced epigenetic gene silencing at a target locus that persisted for at least 18 generations. As soon as the Paf1 allele was reverted to wild type, the repressed state was lost. However, H3K9me3 and the generation of secondary siRNAs from the target locus remained unaffected and were still transmitted across generations, implying that H3K9me3 is not repressive *per se* but can function as an epigenetic mark that retains information of a previous gene-silencing event. If Paf1 was mutated again in cells with this mark, the repressed state was re-established (Figure 4, Box 1) [43].

This observation in fission yeast gives rise to the idea that H3K9me3 is only repressive under specific conditions, such as impaired Paf1C activity. Consistent with such model, the transcription factor Moonshiner enables transcription within the heterochromatic, H3K9me3-enriched piRNA clusters in *Drosophila* [63]. For some fly genes H3K9 methylation is a prerequisite for efficient expression [64,65]. Transcription of H3K9 methylated protein-coding genes has also been observed in mammalian cells [66–68]. Thus, H3K9 methylation may be an epigenetic mark that is not repressive *per se*, which may explain some apparently conflicting observations in *C. elegans*. RNAe has generally been considered to correlate with H3K9me3 enrichment at the target locus and to depend on H3K9 methyltransferases [28,33,35,36]. However, recent observations reveal that histone methyltransferases are required for gene silencing of somatic, but not germline genes [52]. There may also be gene specific requirements, as, for example, repression of the *oma-1* gene was shown to be inherited in the absence of H3K9me3 [34], and another study showed that initiation, but not maintenance of silencing of a gene depended on H3K9me3 [57].

Physiological Relevance of RNAe

While substantial progress has been made in studying RNAe responses that can be triggered experimentally, insights into potential physiological roles of this phenomenon are only just emerging. Recent studies in *C. elegans* suggest that RNAe may facilitate sensing and reacting to a dynamic environment, potentially allowing adaptation to harsh conditions and transmitting the acquired epigenetic changes in gene expression to subsequent generations. For example, starvation was reported to induce expression of endogenous small RNAs that can potentially repress genes linked to nutrition. Because some small RNAs were still present in subsequent generations grown in nutritionally rich conditions, it is possible these animals might inherit information on how to cope with starvation. Indeed, the F3 progeny of starved ancestors had a significantly increased life span and were more resistant to starvation [69].

These worms also had an increased resistance to heat stress, suggesting that starvation might lead to epigenetic inheritance of general stress resistance [70]. However, the mechanism of cross-stress resistance and the functional relationship between the inherited small RNAs and lifespan requires further study [69,70]. Temperature has been shown to change the abundance of small RNA populations, resulting in gene expression changes that lasted for several generations, independent of the temperature that triggered the change [71–73]. Heat stress in *hrde-1* mutant

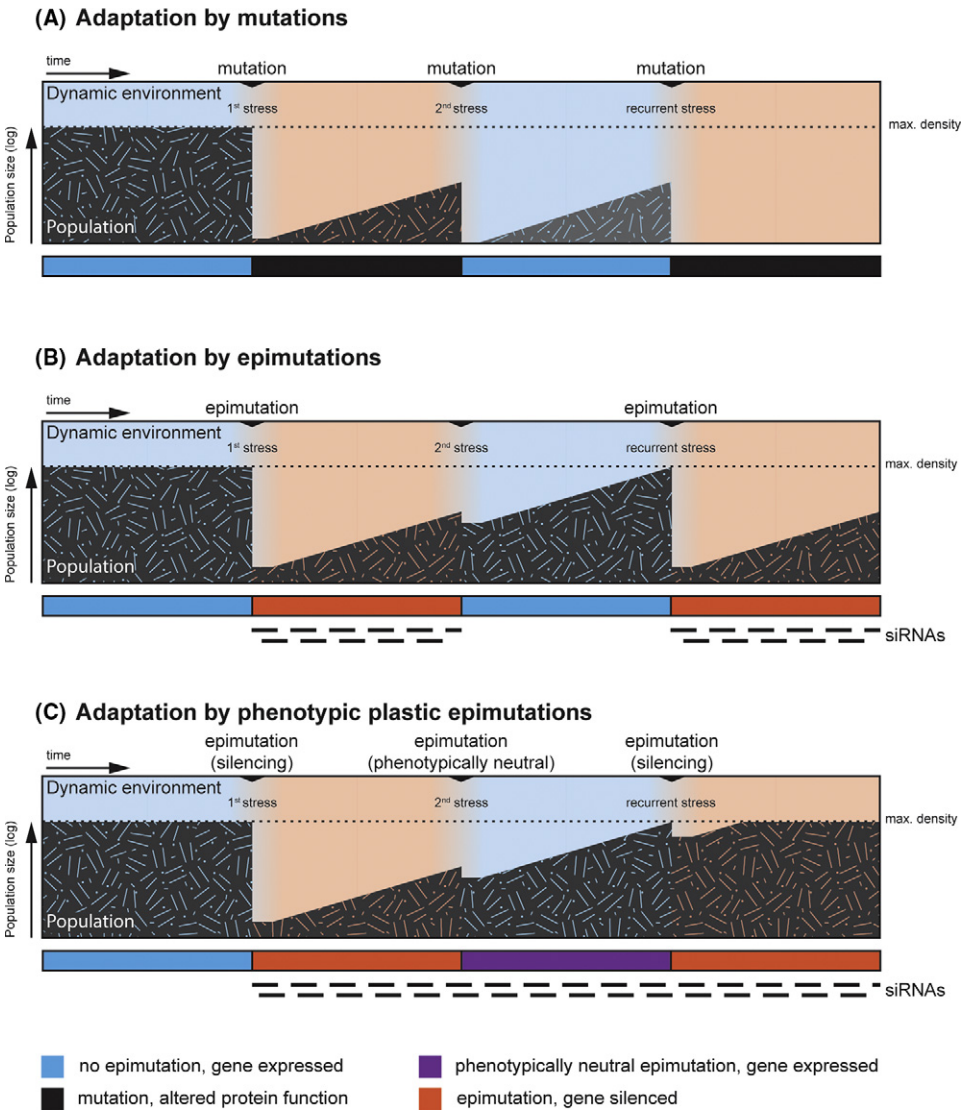

Figure 4. Population Adaptation Strategies to a Dynamic Two-State (Blue and Red) Environment. (A) A well-adapted population (grey) is at its maximal density (dotted line) in a given niche until an environmental change (1st stress) creates a bottleneck. Only few individuals can adapt through mutations and repopulate the niche. After the environment changes back to the initial blue state, only individuals that acquire rare counteracting mutations survive, often leading to extinction of the population. (B) Individuals of a population in the red state can gain beneficial epimutations through siRNAs and repopulate the niche. When exposed again to the blue state, the epimutations can be quickly reversed and the population rapidly reaches maximal density. After recurrence of the red state, organisms establish *de novo* epimutations with the same low frequency as when they first encountered this state. (C) In contrast, organisms that can maintain the memory of a beneficial silencing event can quickly re-establish beneficial epimutations and grow to full density. Such memory can be maintained by phenotypically neutral epimutations, marked by the continuously high production of siRNAs without substantial reductions in the expression of a gene. Thus, a population that can adapt through phenotypically plastic epimutations is predicted to have a maximal fitness advantage in a dynamic environment.

animals resulted in the upregulation of a large number of genes (>280). In wild type worms these genes are H3K9 methylated and produce abundant HRDE-1-associated siRNAs, suggesting that RNAe can also act to dampen heat-induced transcriptional gene activation [72].

Box 1. Conceptual Framework of Adaptation to a Dynamic Environment

The fitness of a population in a dynamic environment strongly depends on the ability of individuals to adapt to the new condition as well as to remember, inherit, and forget such adaptation. In this conceptual model we compare the fitness of populations that adapt with different survival strategies: mutations, epimutations, or phenotypically plastic epimutations. For simplicity, we presume a dynamic environment consisting of two alternating states (Figure 4) where the transition between states creates a bottleneck. Consequently, individuals adapted to one state require mutations or epimutations to adapt to and propagate in the other state.

Individuals of a population can adapt by acquiring beneficial mutations (Figure 4A), leading to changes in protein function or gene expression (e.g., [76]). Such mutations mainly occur randomly and often affect only one gene directly. Adaptive mutations must originate in the germline to be inherited and have full penetrance. Consequently, mutations beneficial in the red environment cannot be lost and re-adaptation through another mutation is required should the environment change back to blue. However, the probability of a mutated gene regaining its original function/expression is low, leading to loss of the maladaptable population.

In contrast, epimutations (Figure 4B) tend to occur in hot spots (e.g., in stress-related or nutritional pathway genes [69,82]) and can potentially silence several homologous genes simultaneously [77]. As small RNAs from the soma can be amplified in the germline [75], and epimutations can be paramutagenic [56], they can increase the population fitness faster than a recessive mutation. Incomplete penetrance of a beneficial epimutation by stochastic loss of siRNAs [59] can result in loss of adaptation in a given environment (red state), but can be beneficial if the previous blue state is re-established. Consequently, the population can quickly revive to full density. However, when the environment changes back to the red state, epimutations must initiate *de novo*, at the same low frequency as when the population first encountered this state.

This is different for populations that can maintain a small RNA-mediated memory of previously beneficial silencing events without displaying the repressed state itself. This phenomenon, termed phenotypically neutral epimutation (Figure 4C), allows high-frequency re-establishment of the epimutant phenotype in a pedigree founded by ancestors that have acquired the respective epimutation [43]. Consequently, individuals that adapt through epimutations and maintain the memory in a phenotypically neutral state are predicted to have greatest fitness advantages in a dynamic environment.

Most recently, small RNAs have been implicated in the heritability of learned behavior in *C. elegans* [74,75]. In its natural habitat, *C. elegans* is surrounded by both nutritious and pathogenic food sources. Worms quickly learn to avoid pathogenic *Pseudomonas*. Descendants inheriting the avoidance behavior escape faster from the same pathogen and thereby have an adaptive survival advantage. This behavior was found to depend on the expression change of the neuronal expressed, HRDE-1-targeted gene *daf-7*. It also required nuclear RNAi factors (*mut-7*, *rrf-1*, *set-25*, and *hpl-2*) as well as germline expressed PRG-1 [74], suggesting that learned behavior is inherited by RNAe and that RNAe is involved in adaptive responses in nematodes.

In contrast to *C. elegans*, evidence for naturally occurring RNAe-related phenomena in other animals is scarce and we thus should be cautious about inferring RNAe as a widely conserved phenomenon. Even if not widely conserved, current literature suggests that a thorough understanding of RNAe may be of significant biomedical relevance. *Mucor circinelloides* is one of the major agents of mucormycosis, a deadly fungal infection. *Mucor* can acquire resistance against antifungal agents either through mutation, or by small RNA-mediated epigenetic silencing of the gene that encodes the respective drug target (Figure 4, Box 1) [76,77]. Upon several passages of growth in drug-free medium, previously drug-resistant **epimutants** lose their endogenous small RNAs, restore target gene mRNA levels, and revert to being drug-sensitive, similar to the parental wild type. It remains to be tested whether drug resistance is stable through meiosis. The acquisition rate of small RNA-induced epimutations in wild type *Mucor* (20%–30%) can be enhanced to 80%–100% by impairing the other RNAi-related pathways of *Mucor* [60,76], reminiscent of enhanced RNAi in *C. elegans* [59,61]. Virulent isolates of *Mucor* from human and other mammals have an enhanced ability to develop drug resistance through epimutations (76%–96%). It seems worth exploring if the resistance of those *Mucor* isolates is higher because of acquired genetic mutations in its other RNAi-related pathways or by RNAe-enabling mutations

such as those described in *S. pombe*. Given the phenotypically neutral inheritance of H3K9me3 in *S. pombe* [43], it will be interesting to investigate whether past exposure to antifungal drugs increases development of drug resistance in later generations (Figure 4, Box 1).

Concluding Remarks and Future Perspectives

The extent to which epigenetic changes are heritable varies significantly, even within the same population, and understanding the determinants that drive initiation and inheritance is an ongoing challenge. Similarly, to what extent the environment can lead to heritable changes in gene expression patterns and to what degree this may increase population fitness remains largely hypothetical (see Outstanding Questions) [1]. Yet, we might be at a turning point, as genetically tractable model organisms now enable us to address these outstanding problems through cleverly designed and well controlled experiments.

It has become increasingly clear over the past few years that RNA-mediated epigenetic responses could contribute to adaptation, although evidence for causation remains sparse. An attractive hypothesis is that RNAe-related phenomena have been difficult to detect because they are under strong negative control. Even though RNAe may yield significant adaptive advantages, a high induction frequency could cause silencing of multiple essential genes and therefore be detrimental. Hence, it is plausible that mechanisms would have coevolved that counteract silencing of euchromatic regions, potentially to limit the initiation of RNAe [28,42,44,59,78]. Similarly, if constituting a bet-hedging strategy to cope with ever-changing environments, permanent fixation of an acquired silencing response would not constitute a selective advantage [74] and mechanisms that modify and limit the duration of RNAe would be predicted [28,59]. Thus, the better we understand modulators of RNAe and how they could be potentially regulated, the more we might learn about its relevance for an organism to adjust to its natural habitat.

Outstanding Questions

What is the physiological relevance of RNA-induced epigenetic silencing (RNAe)?

Are RNAe-like mechanisms conserved in mammals?

Are epimutations in organisms other than fission yeast also phenotypically plastic?

Do metabolites or stressful conditions block RNAe counteracting mechanisms?

Can H3K9me3 confer memory of a previous silencing episode in *C. elegans*?

What are the factors involved in regulating transgenerational inheritance?

Could RNAe be involved in adaptation to changing environmental conditions?

Acknowledgments

We apologize to colleagues whose work was not cited due to length restrictions. The authors' work related to the topic of this review is supported by funds from the European Research Council (ERC-CoG-REpiReg-681213) and the Novartis Research Foundation. We thank members of the Bühler lab for discussions and G. Riddihough (Life Science Editors) for editing the manuscript.

References

1. Heard, E. and Martienssen, R.A. (2014) Transgenerational epigenetic inheritance: myths and mechanisms. *Cell* 157, 95–109
2. Johannes, F. *et al.* (2009) Assessing the impact of transgenerational epigenetic variation on complex traits. *PLoS Genet.* 5, e1000530
3. Liegard, B. *et al.* (2019) Quantitative resistance to clubroot infection mediated by transgenerational epigenetic variation in *Arabidopsis*. *New Phytol.* 222, 468–479
4. Noble, D. (2015) Conrad Waddington and the origin of epigenetics. *J. Exp. Biol.* 218, 816–818
5. Ptashne, M. (2013) Epigenetics: core misconcept. *Proc. Natl. Acad. Sci. U. S. A.* 110, 7101–7103
6. Halfmann, R. and Lindquist, S. (2010) Epigenetics in the extreme: prions and the inheritance of environmentally acquired traits. *Science* 330, 629–632
7. Arteaga-Vazquez, M.A. and Chandler, V.L. (2010) Paramutation in maize: RNA mediated trans-generational gene silencing. *Curr. Opin. Genet. Dev.* 20, 156–163
8. Conte Jr., D. and Mello, C.C. (2003) RNA interference in *Caenorhabditis elegans*. *Curr. Protoc. Mol. Biol.* 109, 26.3.1–26.3.30
9. Vastenhouw, N.L. *et al.* (2006) Long-term gene silencing by RNAi. *Nature* 442, 882
10. Holoch, D. and Moazed, D. (2015) RNA-mediated epigenetic regulation of gene expression. *Nat. Rev. Genet.* 16, 71–84
11. Luteijn, M.J. and Ketting, R.F. (2013) PIWI-interacting RNAs: from generation to transgenerational epigenetics. *Nat. Rev. Genet.* 14, 523–534
12. Matzke, M.A. and Mosher, R.A. (2014) RNA-directed DNA methylation: an epigenetic pathway of increasing complexity. *Nat. Rev. Genet.* 15, 394–408
13. Shimada, Y. *et al.* (2016) The RNA-induced transcriptional silencing complex targets chromatin exclusively via interacting with nascent transcripts. *Genes Dev.* 30, 2571–2580
14. Wierzbicki, A.T. *et al.* (2008) Noncoding transcription by RNA polymerase Pol IVb/Pol V mediates transcriptional silencing of overlapping and adjacent genes. *Cell* 135, 635–648
15. Martienssen, R. and Moazed, D. (2015) RNAi and heterochromatin assembly. *Cold Spring Harb. Perspect. Biol.* 7, a019323
16. Allshire, R.C. and Madhani, H.D. (2018) Ten principles of heterochromatin formation and function. *Nat. Rev. Mol. Cell Biol.* 19, 229–244
17. Grewal, S.I. (2010) RNAi-dependent formation of heterochromatin and its diverse functions. *Curr. Opin. Genet. Dev.* 20, 134–141
18. Law, J.A. and Jacobsen, S.E. (2010) Establishing, maintaining and modifying DNA methylation patterns in plants and animals. *Nat. Rev. Genet.* 11, 204–220
19. Wendte, J.M. and Pikaard, C.S. (2017) The RNAs of RNA-directed DNA methylation. *Biochim. Biophys. Acta Gene Regul. Mech.* 1860, 140–148

20. Weiser, N.E. and Kim, J.K. (2019) Multigenerational regulation of the *Caenorhabditis elegans* chromatin landscape by germline small RNAs. *Annu. Rev. Genet.* 53, 289–311
21. Almeida, M.V. *et al.* (2019) Function and evolution of nematode RNAi pathways. *Noncoding RNA* 5, E8
22. Zhang, D. *et al.* (2018) The piRNA targeting rules and the resistance to piRNA silencing in endogenous genes. *Science* 359, 587–592
23. Bagijn, M.P. *et al.* (2012) Function, targets, and evolution of *Caenorhabditis elegans* piRNAs. *Science* 337, 574–578
24. Uebel, C.J. *et al.* (2018) Distinct regions of the intrinsically disordered protein MUT-16 mediate assembly of a small RNA amplification complex and promote phase separation of Mutator foci. *PLoS Genet.* 14, e1007542
25. Phillips, C.M. *et al.* (2012) MUT-16 promotes formation of perinuclear mutator foci required for RNA silencing in the *C. elegans* germline. *Genes Dev.* 26, 1433–1444
26. Pak, J. and Fire, A. (2007) Distinct populations of primary and secondary effectors during RNAi in *C. elegans*. *Science* 315, 241–244
27. Sijen, T. *et al.* (2007) Secondary siRNAs result from unprimed RNA synthesis and form a distinct class. *Science* 315, 244–247
28. Spracklin, G. *et al.* (2017) The RNAi inheritance machinery of *Caenorhabditis elegans*. *Genetics* 206, 1403–1416
29. Guang, S. *et al.* (2008) An Argonaute transports siRNAs from the cytoplasm to the nucleus. *Science* 321, 537–541
30. Guang, S. *et al.* (2010) Small regulatory RNAs inhibit RNA polymerase II during the elongation phase of transcription. *Nature* 465, 1097–1101
31. Burkhart, K.B. *et al.* (2011) A pre-mRNA-associating factor links endogenous siRNAs to chromatin regulation. *PLoS Genet.* 7, e1002249
32. Buckley, B.A. *et al.* (2012) A nuclear Argonaute promotes multigenerational epigenetic inheritance and germline immortality. *Nature* 489, 447–451
33. Ashe, A. *et al.* (2012) PiRNAs can trigger a multigenerational epigenetic memory in the germline of *C. elegans*. *Cell* 150, 88–99
34. Kalinava, N. *et al.* (2017) Decoupling the downstream effects of germline nuclear RNAi reveals that H3K9me3 is dispensable for heritable RNAi and the maintenance of endogenous siRNA-mediated transcriptional silencing in *Caenorhabditis elegans*. *Epigenetics Chromatin* 10, 6
35. Luteijn, M.J. *et al.* (2012) Extremely stable Piwi-induced gene silencing in *Caenorhabditis elegans*. *EMBO J.* 31, 3422–3430
36. Shirayama, M. *et al.* (2012) piRNAs initiate an epigenetic memory of nonself RNA in the *C. elegans* germline. *Cell* 150, 65–77
37. Iida, T. *et al.* (2008) siRNA-mediated heterochromatin establishment requires HP1 and is associated with antisense transcription. *Mol. Cell* 31, 178–189
38. Simmer, F. *et al.* (2010) Hairpin RNA induces secondary small interfering RNA synthesis and silencing in trans in fission yeast. *EMBO Rep.* 11, 112–118
39. Buhler, M. *et al.* (2006) Tethering RITS to a nascent transcript initiates RNAi- and heterochromatin-dependent gene silencing. *Cell* 125, 873–886
40. Sigova, A. *et al.* (2004) A single Argonaute protein mediates both transcriptional and posttranscriptional silencing in *Schizosaccharomyces pombe*. *Genes Dev.* 18, 2359–2367
41. Yu, R. *et al.* (2018) Epigenetic inheritance mediated by coupling of RNAi and histone H3K9 methylation. *Nature* 558, 615–619
42. Kowalik, K.M. *et al.* (2015) The Paf1 complex represses small-RNA-mediated epigenetic gene silencing. *Nature* 520, 248–252
43. Duempelmann, L. *et al.* (2019) Inheritance of a phenotypically neutral epimutation evokes gene silencing in later generations. *Mol. Cell* 74, 534–541
44. Flury, V. *et al.* (2017) The histone acetyltransferase Mst2 protects active chromatin from epigenetic silencing by acetylating the ubiquitin ligase Brl1. *Mol. Cell* 67, 294–307
45. Sadeghi, L. *et al.* (2015) The Paf1 complex factors Leo1 and Paf1 promote local histone turnover to modulate chromatin states in fission yeast. *EMBO Rep.* 16, 1673–1687
46. Verrier, L. *et al.* (2015) Global regulation of heterochromatin spreading by Leo1. *Open Biol.* 5, 150045
47. Wang, J. *et al.* (2015) Rapid epigenetic adaptation to uncontrolled heterochromatin spreading. *Elife* 4, 06179
48. Yu, R. *et al.* (2014) Determinants of heterochromatic siRNA biogenesis and function. *Mol. Cell* 53, 262–276
49. Clark, J.P. *et al.* (2017) *Drosophila* PAF1 modulates PIWI/piRNA silencing capacity. *Curr. Biol.* 27, 2718–2726
50. Herr, A.J. *et al.* (2006) Defective RNA processing enhances RNA silencing and influences flowering of *Arabidopsis*. *Proc. Natl. Acad. Sci. U. S. A.* 103, 14994–15001
51. Minkina, O. and Hunter, C.P. (2018) Intergenerational transmission of gene regulatory information in *Caenorhabditis elegans*. *Trends Genet.* 34, 54–64
52. Minkina, O. and Hunter, C.P. (2017) Stable heritable germline silencing directs somatic silencing at an endogenous locus. *Mol. Cell* 65, 659–670
53. Rechavi, O. and Lev, I. (2017) Principles of transgenerational small RNA inheritance in *Caenorhabditis elegans*. *Curr. Biol.* 27, R720–R730
54. Wan, G. *et al.* (2018) Spatiotemporal regulation of liquid-like condensates in epigenetic inheritance. *Nature* 557, 679–683
55. Xu, F. *et al.* (2018) A cytoplasmic Argonaute protein promotes the inheritance of RNAi. *Cell Rep.* 23, 2482–2494
56. Sapetschnig, A. *et al.* (2015) Tertiary siRNAs mediate paramutation in *C. elegans*. *PLoS Genet.* 11, e1005078
57. Woodhouse, R.M. *et al.* (2018) Chromatin modifiers SET-25 and SET-32 are required for establishment but not long-term maintenance of transgenerational epigenetic inheritance. *Cell Rep.* 25, 2259–2272
58. Perales, R. *et al.* (2018) Transgenerational epigenetic inheritance is negatively regulated by the HERI-1 chromodomain protein. *Genetics* 210, 1287–1299
59. Houri-Ze'evi, L. *et al.* (2016) A tunable mechanism determines the duration of the transgenerational small RNA inheritance in *C. elegans*. *Cell* 165, 88–99
60. Calo, S. *et al.* (2017) A non-canonical RNA degradation pathway suppresses RNAi-dependent epimutations in the human fungal pathogen *Mucor circinelloides*. *PLoS Genet.* 13, e1006686
61. Lev, I. *et al.* (2017) MET-2-dependent H3K9 methylation suppresses transgenerational small RNA inheritance. *Curr. Biol.* 27, 1138–1147
62. Duchaine, T.F. *et al.* (2006) Functional proteomics reveals the biochemical niche of *C. elegans* DCR-1 in multiple small-RNA-mediated pathways. *Cell* 124, 343–354
63. Andersen, P.R. *et al.* (2017) A heterochromatin-dependent transcription machinery drives piRNA expression. *Nature* 549, 54–59
64. Schultz, J. (1936) Variegation in *Drosophila* and the inert chromosome regions. *Proc. Natl. Acad. Sci. U. S. A.* 22, 27–33
65. Yasuhara, J.C. and Wakimoto, B.T. (2006) Oxymoron no more: the expanding world of heterochromatic genes. *Trends Genet.* 22, 330–338
66. Frietze, S. *et al.* (2010) ZNF274 recruits the histone methyltransferase SETDB1 to the 3′ ends of ZNF genes. *PLoS One* 5, e15082
67. Vogel, M.J. *et al.* (2006) Human heterochromatin proteins form large domains containing KRAB-ZNF genes. *Genome Res.* 16, 1493–1504
68. Vakoc, C.R. *et al.* (2005) Histone H3 lysine 9 methylation and HP1gamma are associated with transcription elongation through mammalian chromatin. *Mol. Cell* 19, 381–391
69. Rechavi, O. *et al.* (2014) Starvation-induced transgenerational inheritance of small RNAs in *C. elegans*. *Cell* 158, 277–287
70. Jobson, M.A. *et al.* (2015) Transgenerational effects of early life starvation on growth, reproduction, and stress resistance in *Caenorhabditis elegans*. *Genetics* 201, 201–212
71. Schott, D. *et al.* (2014) Natural RNA interference directs a heritable response to the environment. *Sci. Rep.* 4, 7387
72. Ni, J.Z. *et al.* (2016) A transgenerational role of the germline nuclear RNAi pathway in repressing heat stress-induced transcriptional activation in *C. elegans*. *Epigenetics Chromatin* 9, 3
73. Klosin, A. *et al.* (2017) Transgenerational transmission of environmental information in *C. elegans*. *Science* 356, 320–323

74. Moore, R.S. *et al.* (2019) Piwi/PRG-1 Argonaute and TGF-beta mediate transgenerational learned pathogenic avoidance. *Cell* 177, 1827–1841
75. Posner, R. *et al.* (2019) Neuronal small RNAs control behavior transgenerationally. *Cell* 177, 1814–1826
76. Calo, S. *et al.* (2014) Antifungal drug resistance evoked via RNAi-dependent epimutations. *Nature* 513, 555–558
77. Chang, Z. *et al.* (2019) Broad antifungal resistance mediated by RNAi-dependent epimutation in the basal human fungal pathogen *Mucor circinelloides*. *PLoS Genet.* 15, e1007957
78. Pisacane, P. and Halic, M. (2017) Tailing and degradation of Argonaute-bound small RNAs protect the genome from uncontrolled RNAi. *Nat. Commun.* 8, 15332
79. Wilson, R.C. and Doudna, J.A. (2013) Molecular mechanisms of RNA interference. *Annu. Rev. Biophys.* 42, 217–239
80. Oey, H. and Whitelaw, E. (2014) On the meaning of the word 'epimutation'. *Trends Genet.* 30, 519–520
81. Singh, J. *et al.* (2019) Reaction mechanisms of Pol IV, RDR2, and DCL3 drive RNA channeling in the siRNA-directed DNA methylation pathway. *Mol. Cell* 75, 576–589
82. Zheng, X. *et al.* (2017) Transgenerational epimutations induced by multi-generation drought imposition mediate rice plant's adaptation to drought condition. *Sci. Rep.* 7, 39843

LEA DÜMPELMANN - Curriculum Vitae

PhD – Molecular Biology

Passionate biomedical scientist and innovative thinker, highly skilled in problem solving, data analysis, teamwork and project management.

INTERNATIONAL AND NATIONAL RESEARCH EXPERIENCE

06/2016 - 05/2020 **PhD student** in Prof. Dr. Marc Bühler's group
Friedrich Miescher Institute (**FMI**), *Basel, Switzerland*

Mechanistic dissection and physiological relevance of RNAi-mediated gene silencing

- Worked on different projects on my own or in teams, resulting in publications
- For the first time in *S. pombe* we reported H3K9me3 to act as non-repressive epigenetic mark
- Established and performed a 15'000 compound screen in collaboration with Novartis
- Wrote a review together with a Master student and co-supervised another Master student and intern
- Data analysis of ChIP-seq, siRNA-seq and RNA-seq, and optimized SNP calling pipeline

11/2014 - 09/2015 **Scientific Associate II** in Andreas Bauer's hub
Novartis Institutes for BioMedical Research (**NIBR**), Basel, Switzerland

Set-up of screens to identify modulators of liver fibrosis

- Established human reporter cell lines for subsequent whole genome CRISPR-Cas9 and compound screen
- Validated reporter cell line by KO/KD with gRNAs & siRNAs and compound treatment

04/2013 - 03/2014 **Scientific Associate** in Prof. Dr. Knut Woltjen's group, director: Nobel Prize Laureate Prof. Yamanaka
Center for induced Pluripotent Stem Cell Research and Application (**CiRA**), *Kyoto, Japan*

Genetic engineering of stem cells (hESCs & iPSCs)

- Determined integration efficiency, location and expression level of transgenes and transposons

08/2011 - 01/2013 **Master student** in Prof. Dr. Rafal Ciosk's group
Friedrich Miescher Institute (**FMI**), *Basel, Switzerland*

Unravelling the role of dimerization for GLD-1, an RNA-binding major regulator of the C. elegans germ line

EDUCATION

2016 - 2020 **PhD in Genetics** (summa cum laude = excellent) at the University of Basel and FMI

2011 - 2013 **MSc in Molecular Biology** (grade: 5.5 = very good) at the University of Basel and FMI

2008 - 2011 **BSc in Molecular Biology** (grade: 5 = good) at the University of Basel

AWARDS

Best presentation & poster price from Marie-Curie Epigenetics course (2017)
Scholarship from the Kyoto University Foundation (for 3 months, 2013)

PAPERS

- **L. Duempelmann**, F. Mohn, Y. Shimada, D. Oberti, A. Andriollo, S. Lochs, M. Bühler, Inheritance of a phenotypically neutral epimutation evokes gene silencing in later generations, *Mol. Cell* 74(3), 534-541 (2019).

- S.H. Carl, **L. Duempelmann**, Y. Shimada, M. Bühler, A fully automated deep learning pipeline for high-throughput colony segmentation and classification, *Biol Open* (2020) 9 (6): bio052936.

- **L. Duempelmann***, M. Skribbe*, Marc Bühler, Small RNAs in the transgenerational inheritance of epigenetic information. *Trends in Genetics* 36 (3), 203-214 (2020). *equal contribution

CONFERENCES

Presentations Austrian Swiss RNA Meeting, Salzburg, Austria (2019)
Epigenetics & Quant. Biology Progress Report, FMI (2017, 2018, 2019)
DMP department Seminar, Novartis, Basel, Switzerland (2015)

Poster presentations International Pombe meeting, Barcelona, Spain (2019)
FMI annual meeting, Switzerland (2016, 2017, 2018, 2019)

SKILLS AND TECHNIQUES

Software

- R programming, Spotfire and familiar with Knime
- Shell scripting with bash (NGS data processing)
- Windows, MacOS and UNIX environments
- Adobe Illustrator CC and Adobe Photoshop CC for creating paper figures
- Image analysis with AxioVision, ImageJ and CL Quant

Laboratory

- Cultivation of cell culture (hESC/hiPSC/liver cells), as well as C. elegans and S. pombe
- Cell manipulation using CRISPR – Cas9 (KO/ KI), transposons, lentiviral transduction/ transfection (Nucleofection/Lipofection) of constructs, gRNAs & siRNAs and compound treatment
- Chromatin and Protein-RNA co-immunoprecipitation (ChIP, RIP)
- Library preparation for next generation sequencing (NGS) from ChIP, RNA and gDNA
- Flow cytometry, immunocytochemistry, confocal microscopy and IN Cell Analyzer

LANGUAGES

German native tongue
English working proficiency (working language at FMI and CiRA, 3-years residence in Australia)
French intermediate proficiency (7.5-years in school)
Japanese basic proficiency (1-year language course and residence)

INTERESTS

Intercultural exchange, underwater world (Dive Master), swimming, salsa, piano